UNIVERSITAT DE BARCELONA

Unveiling the biological role of stigmasterol biosynthesis in tomato plants

Laura Gutiérrez García

Unveiling the biological role of stigmasterol biosynthesis in tomato plants

Laura Gutierrez

PhD thesis
2019

UNIVERSITAT DE BARCELONA

FACULTAT DE FARMÀCIA I CIÈNCIES DE L'ALIMENTACIÓ

UNVEILING THE BIOLOGICAL ROLE OF STIGMASTEROL BIOSYNTHESIS IN TOMATO PLANTS

LAURA GUTIÉRREZ GARCÍA

2019

UNIVERSITAT DE BARCELONA

FACULTAT DE FARMÀCIA I CIÈNCIES DE L'ALIMENTACIÓ

PROGRAMA DE DOCTORAT: BIOTECNOLOGÍA

UNVEILING THE BIOLOGICAL ROLE OF STIGMASTEROL BIOSYNTHESIS IN TOMATO PLANTS

Memòria presentada per Laura Gutiérrez García per optar al títol de doctor per la universitat de Barcelona

Dr. Albert Boronat Margosa
Director

Dr. Albert Ferrer Prats
Director

Laura Gutiérrez García
Doctoranda

Dr. Albert Ferrer Prats
Tutor

LAURA GUTIÉRREZ GARCÍA
2019

Dedicada a mi madre.

“Por muy larga que sea la tormenta, el sol siempre vuelve a brillar entre las nubes”
Kahlil Gibran

AGRADECIMIENTOS

Si he sido capaz de llegar hasta aquí, ha sido gracias a la ayuda, apoyo y motivación de las personas que me rodean, y como bien dice el saber popular: "*Es de bien nacido el ser agradecido".*

En primer lugar, me gustaría agradecer a mi familia, que ha sido uno de los pilares principales en mi vida y sin los que jamás habría llegado a ser quien soy. GRACIAS a mis padres, por todo en general. Gracias por haber sido tan perseverantes en mi educación y mis estudios, por enseñarme el valor de la responsabilidad, por estar siempre ahí. GRACIAS infinitas a mi madre, por hacerme fuerte, por guiarme, incluso desde la ausencia. Gracias a la familia Fraguela-Bermúdez, por haberme acogido como a una más. Y GRACIAS a Miguel, mi marido, por TODO. Por haberme seguido en esta aventura, porque sin tu apoyo, nada habría sido igual. Por cuidarme, aguantarme, y sobre todo, por quererme. Nunca podré agradecértelo lo suficiente. Muchas gracias a Karmela y Lola, por acompañarme sin descanso en este largo camino.

GRACIAS a mis directores de tesis, Albert Boronat y Albert Ferrer, por darme la oportunidad de formar parte de vuestro laboratorio. Esta tesis doctoral no habría sido posible sin vuestro apoyo y dedicación. Gracias por haberme abierto las puertas al mundo de la ciencia. Igualmente agradezco a Montse y Teresa, que aunque no constan oficialmente como mis directoras, han desempeñado un papel muy importante en mi formación.

Al laboratorio 203 en su conjunto. En especial, a mis mexicanos favoritos, con los que he compartido la mayor parte del tiempo durante estos 4 años. Dra. Castillo (costó, pero finalmente lo lograste), muchas gracias por tu buen humor, por tu apoyo, tus consejos y enseñanzas. Has sido para mí como mi hermana científica, tanto dentro como fuera del laboratorio. Alma, Srta. Cara de Pizza, muchas gracias por las risas, por las *cheves*, y sobre todo, por ser la experta en GC-MS y ayudarnos constantemente. A ti, Ángel, te agradezco todos los buenos momentos que hemos pasado juntos, sé que me echarás de menos (y yo a ti también, a pesar de todo). Muchas gracias a Viqui, por enseñarme tantísimo en tan poco tiempo. Para mí, siempre serás parte del 203.

Muchas gracias al resto de amigos que he hecho en el CRAG, por hacer inolvidable esta etapa de mi vida, por haber conseguido que me sienta como en casa y haber hecho de Barcelona mi nuevo hogar: A “los Manolos” [Rosa (y por supuesto Veni), Briardo, Neto, Vicky, Miguelón, Salva, Miguelez…], por ser los vecinos perfectos, siempre dispuestos a tomar un café, prestar un poco de azúcar (o *Accuprime*…), y por estar siempre ahí en los momentos difíciles. Os agradezco tanto, que no tendría palabras para describirlo. Muchas gracias a Chiqui, por conseguir que los días tristes tuvieran una luz especial después de un abrazo. A mis gemelas favoritas, por vuestro cariño, por hacer del CRAG un sitio mucho más alegre y dulce. A mis compañeros de “chupito time”, por aguantarme en mis picos de estrés, por vuestro apoyo, preocupación y por cuidarme dentro y fuera del centro (nunca había tenido tantos GIF en el móvil). Isa, Andrés, Víctor, gracias por convertir las pizzas en tradición, por las risas, los datos curiosos y los buenos ratos que hemos compartido. Irma, muchas gracias por estar siempre dispuesta a ayudarme y aconsejarme cuando lo he necesitado, y por compartir conmigo tu afición por las manualidades. Gracias a Nadja, por conservar un trocito de Sur aquí en el Norte. Especial agradecimiento a María Coca, y cómo no, a Laia, por enseñarme todo lo que ahora sé de nuestros amados honguitos. Muchas gracias por vuestra generosa paciencia y amabilidad.

Muchas gracias en general a todo el personal del CRAG, porque todos me habéis ayudado en algún momento de este periodo. En especial a los servicios científicos, por hacerme mucho más fácil el trabajo experimental, sobre todo a Mercè, Pilar, Gloria, Montse Amenós y Joana, por estar siempre dispuestas a ayudar con una sonrisa.

No podría olvidarme de dar las gracias a las personas que la vida me ha ido regalando, desde Cádiz, donde conservo mis amigos de toda la vida; pasando por Sevilla, en donde conocí gente maravillosa cuando estudié la carrera; y Madrid, donde estudié el Máster y guardo grandes amistades. Gracias por confiar en mí, y animarme siempre a conseguir lo que quiero.

GRACIAS POR TODO Y MÁS

SUMMARY

In plants, the sterol biosynthetic pathway leads to the production of a complex mixture of end-products, among which β-sitosterol, stigmasterol, campesterol, and cholesterol are the most abundant ones. Stigmasterol, the end-product of the 24-ethyl sterol branch is synthesized from β-sitosterol by the action of sterol C22-desaturase (C22DES). Despite C22DES was identified about a decade ago, there is still a lack of knowledge about several relevant aspects related to the structure and function of this enzyme. Furthermore, several studies have reported the occurrence of changes in the stigmasterol to β-sitosterol ratio (STIG/SIT) during plant development and in their responses to environmental stimuli which have been related with the activity of C22DES. However, the biological relevance of the changes in stigmasterol levels is currently unknown.

Based on this, the main objective of present work has been the elucidation of the role of stigmasterol during plant growth and development as well as in its response to environmental challenges. Tomato (*Solanum lycopersicum* cv. MicroTom) was selected for these studies taking advantage that is one of the few plants in which C22DES is encoded by a single-copy gene. The goals of this thesis have been: (1) the functional and structural characterization of C22DES in terms of subcellular localization and mechanism of action, and (2) the evaluation of the role of stigmasterol biosynthesis in tomato plant growth, development and in responses to biotic and abiotic stresses. The results obtained in this thesis have confirmed that C22DES is targeted and retained in the endoplasmic reticulum (ER)-membrane. C22DES consists of two well-differentiated domains: a single N-terminal transmembrane-helix domain (TMH1), which is sufficient for the ER-membrane targeting and retention, and a globular domain that also contacts with the ER-membrane. The globular domain may also interact and be retained in the ER in the absence of TMH1, but it is enzymatically inactive, revealing the requirement of the N-terminal membrane domain for enzyme activity. The *in silico* analysis of the TMH1 region revealed several features that could be involved in substrate recognition and binding. Transgenic tomato plants with altered STIG/SIT ratios have been generated by overexpression, amiRNA-mediated silencing, and knock-out of the *C22DES* gene. The obtained results have shown that lack of stigmasterol is not lethal for the plant since the *C22des*$^{-}$ knock-out plants are able to complete their life cycle. However,

C22des^{-} knock-out mutant showed several phenotypic abnormalities related to growth and developmental processes. The *C22des*$^{-}$ knock-out plants also show increased susceptibility to *Botrytis cinerea* infection.

The data provided in this thesis contribute to expand the current knowledge on the mechanism of action of stigmasterol and C22DES in tomato plants and set the basis for further studies focused on unraveling the mechanisms involved in the regulation of C22DES activity. The *C22des*$^{-}$ knock-out mutant generated in this work also provides a unique and highly relevant tool to evaluate the role of stigmasterol in plants.

RESUMEN

En las plantas, la ruta de biosíntesis de los esteroles da lugar a la generación de una compleja mezcla de productos finales, entre los cuales, el β-sitosterol, estigmasterol, campesterol, colesterol son los más abundantes. El estigmasterol es el producto final en la rama de los 24-etil esteroles, y se sintetiza a partir del β-sitosterol por la acción de la enzima esterol C22-desaturasa (C22DES). A pesar de que C22DES fue identificada hace una década, aún hace falta mayor conocimiento acerca de algunos aspectos relevantes relacionados con la estructura y función de esta enzima. Además, algunos estudios han descrito la existencia de cambios en la relación estigmasterol a β-sitosterol (STIG/SIT) durante el desarrollo de la planta y su respuesta a estímulos ambientales, que se han relacionado con la actividad de C22DES. Sin embargo, aún se desconoce la relevancia biológica de los cambios en los niveles de estigmasterol.

Basándonos en esto, el objetivo principal del presente trabajo ha sido el esclarecimiento del papel del estigmasterol durante el crecimiento de la planta y el desarrollo, así como en su respuesta a desafíos ambientales. Para este estudio se seleccionó el tomate (*Solanum lycopersicum*) como planta modelo aprovechando que es una de las pocas especies vegetales en las que C22DES está codificada por un gen de copia única. Los objetivos de esta tesis han sido: (1) la caracterización funcional y estructural de C22DES en términos de localización subcelular y mecanismo de acción, y (2) la evaluación del papel de la biosíntesis de estigmasterol sobre el crecimiento, desarrollo y respuestas a estrés biótico y abiótico en plantas de tomate. Los resultados obtenidos en esta tesis han confirmado que C22DES se dirige y retiene en la membrana del retículo endoplásmico (RE). C22DES consiste en dos dominios bien diferenciados: un dominio hélice transmembrana en el extremo amino-terminal (TMH1), que es suficiente para su direccionamiento y retención en la membrana del RE, y un dominio globular que también mantiene zonas de contacto con la membrana del RE. El dominio globular también puede interaccionar y ser retenido en el RE en ausencia de TMH1, pero es enzimáticamente inactivo, lo que revela la necesidad del dominio transmembrana amino-terminal para la actividad enzimática. Los análisis *in silico* de la región TMH1 revelaron algunas características que pueden estar implicadas en el reconocimiento y unión de sustrato. Se generaron plantas transgénicas de tomate con relaciones STIG/SIT alteradas mediante la

sobreexpresión, silenciamiento mediado por amiRNA, y la eliminación del gen *C22DES*. Los resultados obtenidos mostraron que la ausencia de estigmasterol no es letal para la planta, ya que las plantas del genotipo mutante nulo *C22des*$^{-}$ son capaces de completar su ciclo de vida. Sin embargo, este mutante mostró algunas anormalidades fenotípicas relacionadas con procesos de crecimiento y desarrollo. Las plantas mutantes *C22des*$^{-}$ también mostraron aumentada su susceptibilidad a la infección por *Botrytis cinerea.*

Los datos proporcionados en esta tesis contribuyen a aumentar el conocimiento actual sobre los mecanismos de acción del estigmasterol y C22DES en plantas de tomate y sienta las bases para futuros estudios dedicados a desentrañar los mecanismos involucrados en la regulación de la actividad C22DES. El mutante *C22des*$^{-}$ generado en este trabajo también proporciona una herramienta única y de gran importancia para evaluar el papel del estigmasterol en las plantas.

Table of contents

Table of Figures

GENERAL INTRODUCTION

CHAPTER I

CHAPTER II

Table of figures

ABBREVIATIONS

ABBREVIATIONS

AACT – acetyl-CoA thiolase
ABA – Abscisic acid
AcAc-CoA – Acetoacyl-CoA
AEBSF – 4-(2-Aminoethyl)benzenesulfonyl fluoride hydrochloride
amiRNA – Artificial micro-RNA
AN – Anthesis
ASAT – Acyl-CoA-sterol acyltransferase
ASG – Acylated steryl glycosides
ATP – Adenosine triphosphate
BR – Breaker
BRs – Brassinosteroids
BSTFA – Bis(trimethylsilyl) trifluoroacetamide
C22DES – Sterol C22-desaturase
C22DESΔ2-27 - C22DES truncated protein with a 26 residues deletion of the N-terminal end
CARC – CRAC specular sequence
CAS – Cycloartenol synthase
CRAC – Cholesterol recognition/interaction amino acid consensus
CTAB – Cetyl Trimethyl Ammonium Bromide
CYP – Cytochrome P450
DMAPP – Dimethylallyl diphosphate
DOPC – dioleoyl-sn-glycero-3-phosphocholine
DPA – Days post anthesis
DPB – Days post-breaker
DPI – Days post-infection
DPS – Days post-sowing
DTT – Dithiothreitol
DW – Dry weight
EDTA – Ethylenediaminetetraacetic acid
EPCS – Endoplasmic reticulum-plasma membrane contact sites
ER – Endoplasmic reticulum
Erg11p - Lanosterol 14α-Demethylase
ERRP – Endoplasmic reticulum retention protein

FLA – Flagellin 22
FPP – Farnesyl pyrophosphate
FPS – Farnesyl pyrophosphate synthase
FRAP – Fluorescence recovery after photobleaching
FS – Free sterol
G3P – Glyceraldehyde-3-phosphate
GC-MS – Gas chromatography-mass spectrometry
GCS – Glucosylceramide synthase
GFP – Green fluorescent protein
GGPP – Geranylgeranyl pyrophosphate
GGPS – Geranylgeranyl pyrophosphate synthase
GPP – Geranyl pyrophosphate
GPS – Geranyl pyrophosphate synthase
GW – Gateway
HB – Homogenization buffer
HCPRO – HC-Pro silencing suppressor
HMG-CoA – 3-hydroxy3-methylglutaryl-CoA
HMGR – HMG reductase
HMGS – HMG synthase
IDI – Isopentenyl diphosphate isomerase
IG – Immature green
IPP – Isopentenyl diphosphate
Kan – Kanamycin
LDs – Lipid droplets
lo – liquid-ordered
MeJa – Methyl jasmonate
MEP – Methylerythritol phosphate
MF – Microsomal fraction of proteins
MG – Mature green
MOPS – 3-(-N-morpholino) propanesulfonic acid
MT – MicroTom
MVA – Mevalonic acid
MVD – MVA diphosphate decarboxylase
MVK – MVA kinase

MVP – 5-phosphomevalonate
MVPP – 5-diphosphomevalonate
OD600 – Optic density at 600 nm
OPM – Orientation of proteins in membranes
OR – Orange
OS – 2,3-oxidosqualene
PK – proline kink, proline-rich motif
PM – Plasma membrane
PMK – Phospho-MVA kinase
PMSF – Phenylmethanesulfonyl fluoride
PSAT – Phospholipid-sterol O-acyltransferase
Pst – Pseudomonas syringae
PVPP – Polyvinyl polypyrrolidone
RFLP – Restriction fragment length polymorphism
RFP – Red fluorescent protein
ROI – Region of interest
RR – Red ripe
SA – Salicylic acid
SD – Standard deviation
SDS-PAGE – Sodium Dodecyl Sulfate Polyacrylamide Gel Electrophoresis
SE – Steryl ester
SF – Soluble fraction of proteins
SG – Steryl glycosides
SGAT – Steryl-glycoside acyltransferase
SGT – UDP-glucose:sterol glycosyltransferase
SMT1/2/3 – Sterol methyltransferase 1/2/3
Sp – Streptomycin
SQS – Squalene synthase
SSR2 – Sterol side-chain reductase 2
STIG/SIT – Stigmasterol to β-sitosterol
TF – Total fraction of proteins
TGN – Trans-Golgi network
THF – Tetrahydrofuran
TLC – Thin layer chromatography

TMH1 – Transmembrane helix motif
TZ – Tetrazolium
VIGS – Virus-induced gene silencing
WT – Wild type

GENERAL INTRODUCTION

GENERAL INTRODUCTION

1. THE IMPORTANCE OF TOMATO AS AN AGRONOMICAL CROP AND AS A MODEL PLANT

Tomato (*Solanum lycopersicum*) is an important crop belonging to the genus *Solanum* within the family *Solanaceae* that consists of approximately 1500 species. The genus *Solanum* also includes other important crop plants such as tobacco (*Nicotiana tabacum*), potato (*Solanum tuberosum*) or eggplant (*Solanum melongena*).

The wild ancestors of cultivated tomato are native from western South America with its center of origin in Peru. Its domestication has been proposed to occur independently in Peru and Mexico (Peralta and Spooner, 2006), and Spaniards took it to Europe after their arrival to the American continent (Baranski *et al.*, 2016). In Europe, it became an important crop in the 1900s, especially after World War II. Nowadays, tomato is one of the most consumed plant crops due to its status as a basic ingredient in the majority of cultural diets, since it is a rich source of vitamins, minerals, fiber and antioxidants (Trivedi *et al.*, 2016; OECD, 2017). In 2017, over 182 million tons (Mt) of tomatoes were produced worldwide with an average yield of 37.800 kg per ha (FAOSTAT, 2017). The top producers were China (59.5 Mt), India (20.7 Mt), Turkey (12.7 Mt) and USA (10.9 Mt). Spain was also part of the top 10 producers (5.1 Mt).

Tomato is a model system for studies on fruit development and ripening because of its interesting features as a producer of fleshy fruit that differentiates it from other model plants such as *O. sativa* or *A. thaliana* (Kimura and Sinha, 2008; Klee and Giovannoni, 2011). As a fruit ripening model plant, tomato is the most manageable organism because it has a diploid genome and its life cycle is relatively short compared with other species. Moreover, the ripening phenotype is easy to distinguish and there is also an available collection of mutants affected in the ripening processes, such as *nor* and *rin* (Barry and Giovannoni, 2007).

Tomato plants produce a globular or ovoid fruit that exhibits all of the common characteristics of berries: a fleshy fruit derived from the ovary with enclosed seeds in the pulp (Barry and Giovannoni, 2007; OECD, 2017). The most external tissue,

called pericarp, comprises the rest of the fruit wall as well as the placenta, where the seeds are located. The seeds contain the embryo and surrounding it the endosperm, which is a nutrient supplying tissue. They are covered by a strong seed-coat, called the testa (Figure 1).

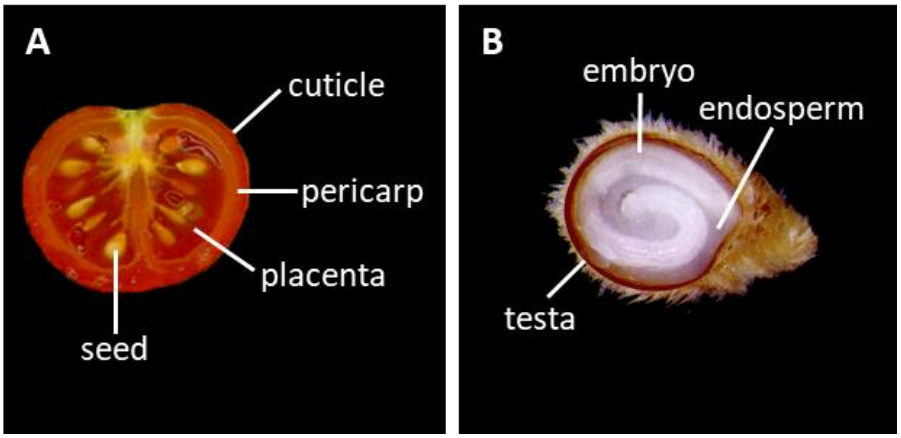

Figure 1 Tomato fruit and seed anatomy. The pictures show **(A)** a ripe tomato fruit and **(B)** a seed from the MicroTom (MT) variety. Different parts of each organ are indicated.

Fruit development and ripening take seven to nine weeks (from the time of anthesis to the end of ripening). The most well-defined pathway that mediates fruit ripening is controlled by ethylene. The ethylene-mediated ripening can be divided into two different phases or systems. During early development, while cell divisions and expansion are taking place to enlarge the final fruit size, system 1 acts as an autoinhibitory element of the ethylene mechanisms. This means that the exogenous ethylene inhibits its synthesis, and the inhibitory elements of ethylene action can increase ethylene production (Barry and Giovannoni, 2007). In these early stages, the production of sterols is highly active, since they are essential for rapid cell division and subsequent cell expansion (Gutensohn and Dudareva, 2016).

In contrast, system 2 acts during fruit ripening and it is stimulated by ethylene (McMurchie, B. and Eaks, 1972). At this stage, multiple phenotypic changes such as color, sugar metabolism, fruit softening and synthesis of volatiles will take place. Several changes in the distribution and metabolism of steryl lipids have also been shown during tomato fruit development and ripening, being the increase in stigmasterol levels one of the most remarkable events (Whitaker, 1988) (Figure 2).

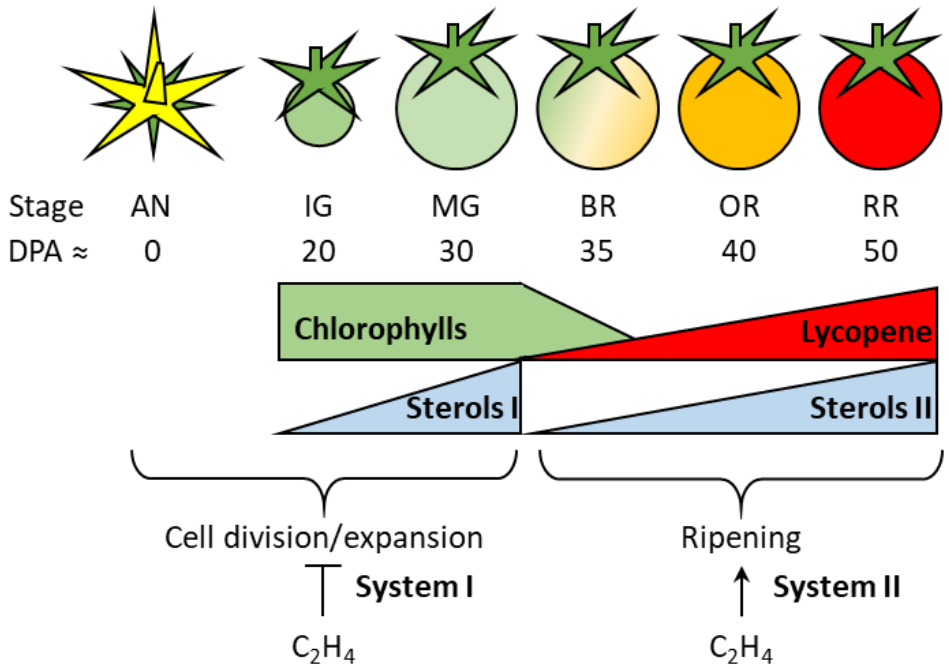

Figure 2 Tomato fruit development. Development of tomato fruit can be divided into two phases. The first one involves cell division and expansion events until the fruit gets its final size [approximately 30 days post-anthesis (DPA)]. The second phase involves fruit ripening and it is characterized by profound changes in the organoleptic properties of the fruit. By the beginning of this phase, chlorophylls are degraded and lycopene starts to accumulate. Sterol metabolism can also be divided into two different phases. The first one is active during cell division and expansion, and the second one during fruit ripening. MT fruits are typically ripe at 50 DPA. AN, anthesis; IG: Immature Green; MG: Mature Green; BR: Breaker; OR: Orange; and RR: Red Ripe.

2. ISOPRENOIDS: MULTIPLE METABOLITES, TWO BIOSYNTHETIC PATHWAYS

2.1 Diversity and biosynthesis of isoprenoids

Isoprenoids, also called terpenoids, are the most diverse family of metabolites. More than 50.000 isoprenoid compounds have been identified (approximately one-third of all known natural products) and although all free-living organisms synthesize them, their abundance and diversity are higher in bacteria and plants. (Hemmerlin, Harwood and Bach, 2012; Vickers *et al.*, 2014).

In plants, and depending on their function, the diverse types of isoprenoids are involved either in the primary or the secondary metabolism. Some isoprenoids are considered as primary metabolites because they play an essential role in normal cell function. In this group we find sterols, which participate in membrane architecture; most of the molecules involved in photosynthesis, such as chlorophylls or carotenoids; and several plant hormones involved in the regulation of growth and development, such as brassinosteroids (BRs) or gibberellins (Vickers *et al.*, 2014; Rodríguez-Concepción and Boronat, 2015). Most plant isoprenoids, however, are considered as secondary metabolites, as they are responsible for more specific and specialized functions that are not common for all species and do not involve essential mechanisms for plant life, but for the interaction of plants with their environment (Tholl, 2015). Some of them are involved in plant defense, biotic and abiotic stress responses, aroma and flavor (Hemmerlin, Harwood and Bach, 2012).

Despite the high number of molecules that comprises the isoprenoid family and their chemical and functional singularities, all of them are derived from the same five-carbon (C5) building blocks (known as isoprene units): isopentenyl diphosphate (IPP) and its allylic isomer dimethylallyl diphosphate (DMAPP). The IPP and DMAPP isomers are generated as products from two independent metabolic pathways which are confined in different cell compartments. In the cytosol, the mevalonic acid (MVA) pathway takes place while the methylerythritol phosphate (MEP) pathway is acting in the plastids (Rodríguez-Concepción and Boronat, 2002; Hemmerlin, Harwood and Bach, 2012). Despite their physical separation, there are some interactions between both at molecular and metabolic levels (Figure 3). Most organisms only have one of those pathways, while plants and some algae use both.

Apart from the different cellular locations, both pathways also differ in the preferred carbon source used as a substrate and also in terms of the generated products. The initial substrates for both pathways derive from central carbon metabolism: acetyl-CoA for the MVA pathway, and pyruvate and glyceraldehyde-3-phosphate (G3P) in the case of the MEP pathway. Regarding their products, the isoprene units are condensed to form farnesyl diphosphate (FPP) primarily in the cytosol, while geranyl diphosphate (GPP) and geranylgeranyl diphosphate (GGPP) are synthesized in the chloroplast. These prenyl diphosphate molecules ($C5_n$) are then used as precursors for isoprenoid biosynthesis (Rodríguez-Concepción and Boronat, 2015; Tholl, 2015).

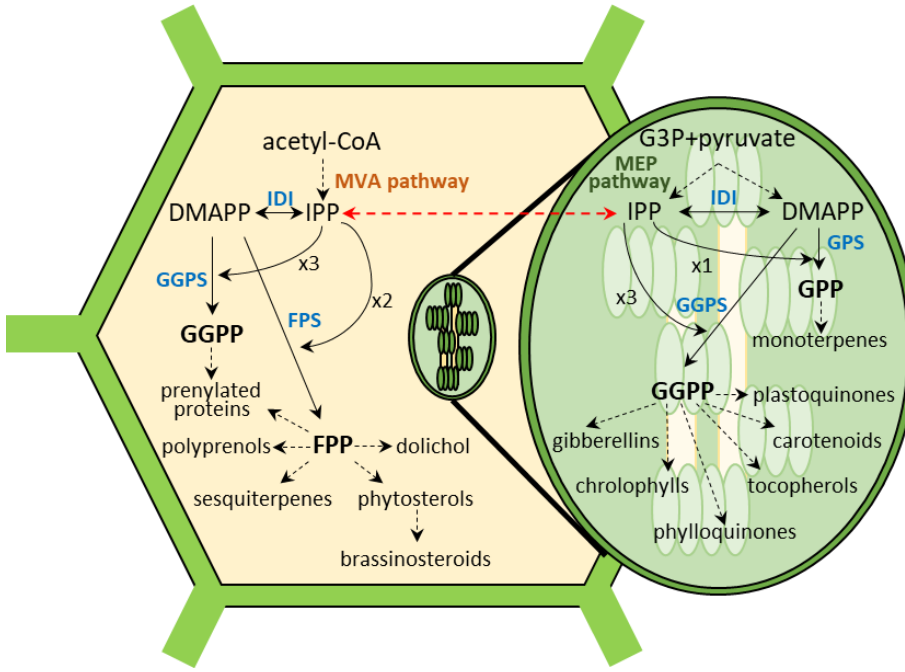

Figure 3 Isoprenoid biosynthetic pathways in plant cells. IPP and DMAPP, the precursors for isoprenoid biosynthesis, are produced via the MVA pathway in the cytosol and the MEP pathway in plastids. These precursors can be transported between subcellular compartments (indicated by a red dashed-arrow). While GPP synthesis takes place in plastids, FPP and GGPP can be produced in several cell locations. Short-chain prenyl diphosphates are in black capital letters and the involved enzymes in their synthesis are shown in blue capital letters. DMAPP, dimethylallyl diphosphate; FPP, farnesyl diphosphate; FPS, farnesyl diphosphate synthase; GGPP, geranylgeranyl diphosphate; GGPS, geranylgeranyl diphosphate synthase; GPP, geranyl diphosphate; GPS, geranyl diphosphate synthase; IDI, isopentenyl diphosphate isomerase; IPP, isopentenyl diphosphate. Solid arrows represent single enzymatic step and dotted arrows indicate multiple reactions.

By this way, the MVA pathway provides precursors for the production of sesquiterpenes, polyprenols, sterols, and BRs among others, whereas those for the synthesis of monoterpenes, diterpenes, carotenoids, gibberellins, chlorophylls, or tocopherols are primarily synthesized by the MEP pathway (Figure 3).

2.2 The MVA pathway provides the precursors for the synthesis of sterols

The MVA pathway represents an important metabolic process in the early steps of sterol biosynthesis, as it provides the isoprene units used as primary precursors. Although the MVA pathway is basically described as a cytosolic process, the different

enzymes involved are distributed in different subcellular compartments (Pulido, Perello and Rodriguez-Concepcion, 2012) (Figure 4).

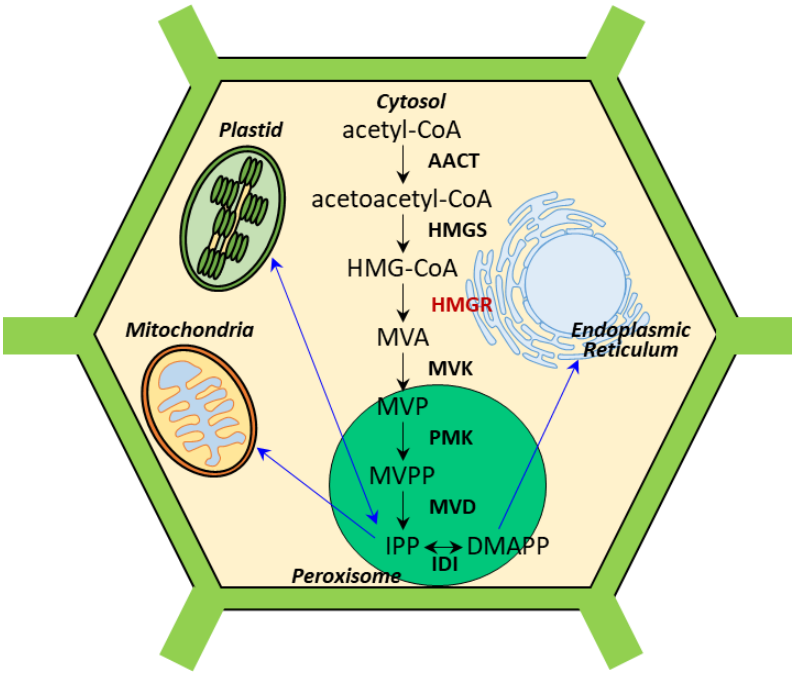

Figure 4 The MVA pathway in plant cells. The MVA pathway enzymes are shown in bold, and each enzymatic step is represented in the cell compartment where it takes place. The HMGR enzyme, which is known to have a relevant regulatory role over the metabolic flux through the MVA pathway is shown in red. Blue arrows represent the transport of metabolites between cell compartments. Metabolic intermediates: DMAPP, dimethylallyl diphosphate; HMG-CoA, 3-hydroxy3-methylglutaryl-CoA; IPP, isopentenyl diphosphate; MVA, mevalonic acid; MVP, 5-phosphomevalonate; MVPP, 5-diphosphomevalonate. Enzymes: AACT, acetyl-CoA thiolase; HMGR, 3-hydroxy3-methylglutaryl-CoA reductase; HMGS, HMG-CoA synthase; IDI, isopentenyl diphosphate isomerase; MVD, MVA diphosphate decarboxylase; MVK, MVA kinase; PMK, phospho-MVA kinase.

In plants, the MVA pathway involves six steps beginning with the condensation of two molecules of acetyl-CoA to form acetoacetyl-CoA catalyzed by acetyl-CoA thiolase (AACT). Then, this metabolic intermediate is combined with a third molecule of acetyl-CoA to produce 3-hydroxy-3-methylglutaryl-CoA (HMG-CoA) in a condensation reaction catalyzed by HMG-CoA synthase (HMGS). These two steps take place in the cytosol. The following reaction is carried out in two reduction steps requiring NADPH as the reducing agent and resulting in MVA. This conversion is catalyzed by the main rate-determining enzyme of the pathway, the 3-hydroxy-3-methylglutaryl-CoA reductase (HMGR), which is anchored to the endoplasmic

reticulum (ER) membrane, but exposing the catalytic domain towards the cytosol. The association of HMGR to membranes has been described to regulate its activity, thus limiting the synthesis of isoprenoid end-products such as sterols (Pulido, Perello and Rodriguez-Concepcion, 2012; Vranová, Coman and Gruissem, 2013; Tholl, 2015). Two successive ATP-dependent phosphorylation steps catalyzed by MVA kinase (MVK) and phospho-MVA kinase (PMK) lead to the generation of MVA 5-diphosphate (MVPP) from MVA. The last step of IPP biosynthesis is an ATP-driven decarboxylation by MVA diphosphate decarboxylase (MVD). The two latter reactions take place in peroxisomes.

3. BIOSYNTHESIS OF STEROLS

3.1 The sterol biosynthetic pathway in plants

Sterols share a common structure based on the cyclopentane-perhydrophenanthrene ring system with methyl substitution at C10 and C13, a hydroxyl group at position C3 and a side chain of 8-10 carbon atoms attached to C17. While animals only produce cholesterol, plants synthesize a complex mixture of sterols that mainly differ in the nature of the lateral chain and the number and position of double bonds both in the skeleton and in the side chain, being β-sitosterol, stigmasterol and campesterol the most abundant species (Hartmann, 1998; Ferrer *et al.*, 2017) (Figure 5). Although cholesterol is also found in plants, it is usually present in low amounts. However, some plant families such as *Solanaceae* contain higher amounts (Hartmann, 1998). While β-sitosterol and stigmasterol are described to have a relevant role in the maintenance of cell membrane structure and function, the importance of campesterol is based on its nature as a BRs precursor (Ferrer *et al.*, 2017).

Most of the reactions within the sterol biosynthetic pathway take place in the ER. However, sterols mainly accumulate in the plasma membrane (PM), which suggests the existence of some transport mechanism between these two membranous systems. In fact, compared with other membrane compartments, the PM shows the greatest sterol content in comparison with the corresponding levels of proteins and phospholipids (Hartmann, 1998).

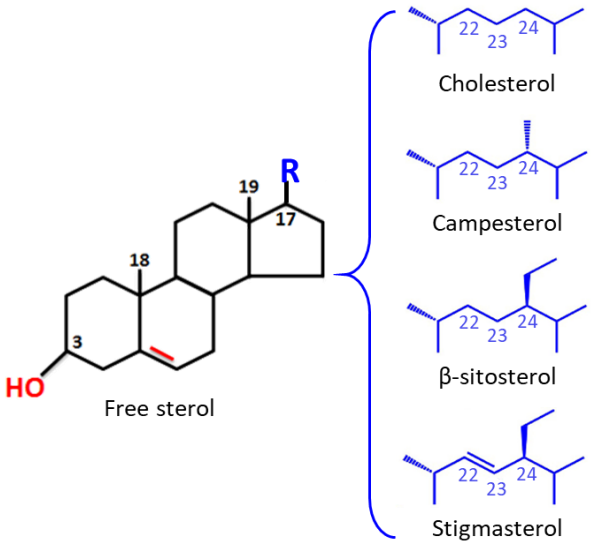

Figure 5 Chemical structure of the major free sterols present in plants. The lateral side chain at position C17 is shown in blue. Adapted from (Ferrer *et al.*, 2017)

Sterols are produced via the MVA pathway following more than 30 enzymatic reactions which are common in all eukaryotes until the generation of the sterol precursor 2,3-oxidosqualene (OS) (Hartmann, 1998; Benveniste, 2002; Aboobucker and Suza, 2019). From this point, the plant sterol biosynthetic pathway diverges from yeast or mammalian pathways, and it is characterized by specific steps that are restricted to plants. The first particularity in plants appears in the cyclization of OS into cycloartenol (instead of lanosterol, as in yeast and mammals) by cycloartenol synthase (CAS) (Hartmann, 1998; Schaller, 2003).

The flux of the different branches of the pathway leading to the main sterol end-products is regulated at specific steps (Figure 6). Cycloartenol is the first metabolite within the pathway that is susceptible to be metabolized by two different branch-point enzymes: sterol side-chain reductase 2 (SSR2) and sterol-methyltransferase 1 (SMT1). The SSR2 converts cycloartenol into cycloartanol, diverting the flux of precursors to the cholesterol branch, whose biosynthetic pathway diverges from phytosterol biosynthesis involving both unique and shared enzymes (Sonawane *et al.*, 2016). On the other hand, SMT1 catalyzes the alkylation of cycloartenol to 24-methylenecycloartanol, leading to the generation of precursors for the plant-specific sterols (β-sitosterol, stigmasterol, and campesterol) (Benveniste, 2002). Further reactions downstream of SMT1 are essentially linear until reaching 24-

methylenelophenol, where another branching point is found. While 24-methylenelophenol could be considered a specific precursor in campesterol biosynthesis, the branch-point enzymes sterol-methyltransferases 2 and 3 (SMT2/3) transforms it into 24-ethylidenlophenol, conferring to the plant kingdom the ability of producing 24-ethyl sterols as the major molecular species by directing carbon toward β-sitosterol and stigmasterol biosynthesis (Benveniste, 2002; Schaller, 2003; Carland, Fujioka and Nelson, 2010).

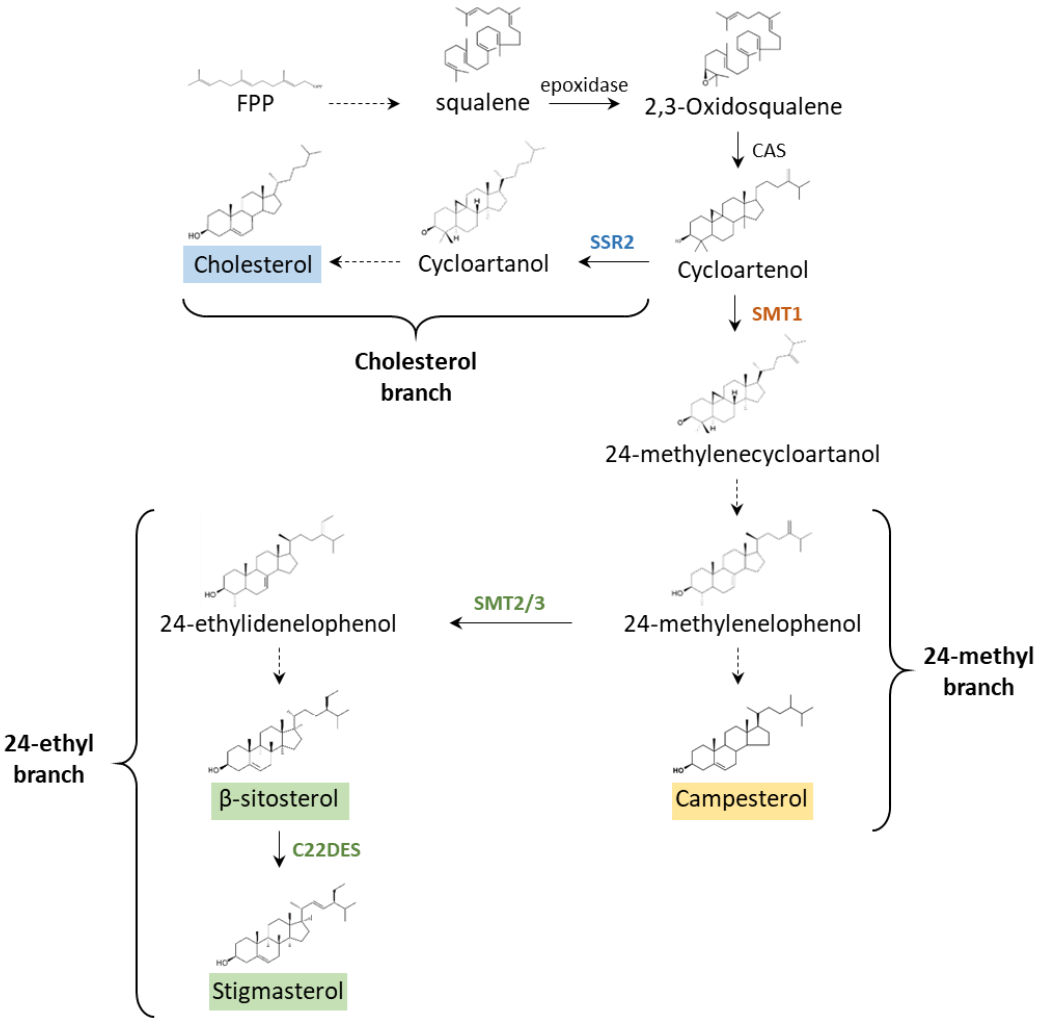

Figure 6 Schematic representation of plant sterol biosynthesis. Solid arrows represent single enzymatic step and dotted arrows indicate multiple reactions. The branching enzymes deriving the carbon flux through each sterol end-product, which are enclosed by boxes, are shown in the same color than their respective sterol species. Enzymes: C22DES, sterol C22 desaturase; SMT1, sterol methyltransferase 1; SMT2/3, sterol methyltransferases 2/3; SSR2, sterol side chain reductase 2.

Finally, sterol C22-desaturase (C22DES) is the last enzyme of the 24-ethyl branch that catalyzes the C22 desaturation reaction to yield stigmasterol from its immediate precursor, β-sitosterol. Summarizing, the key regulatory enzymes in the plant sterol biosynthetic pathway are SSR2, SMT1, SMT2/3, and C22DES.

3.2 Conjugated sterols in plants

In addition to the regulation of sterol biosynthesis, free sterol levels can be also modulated by their conversion into conjugated forms such as steryl esters (SE), steryl glycosides (SG), and acyl steryl glycosides (ASG) (Aboobucker and Suza, 2019) (Figure 7). To synthesize these conjugated forms, the free hydroxyl group in the sterol molecule at position C3 is modified by the action of several conjugating enzymes. SEs are produced by the addition of a fatty acid of different length (usually from C12 to C22) by the action of two different acyltransferases: phospholipid-sterol O-acyltransferase (PSAT) and acyl-CoA-sterol acyltransferase (ASAT) (Lara *et al.*, 2018). The sterol species present in the SE fraction are usually the same present in the FS fraction, although some sterol intermediates can also be found probably as a result of regulatory mechanisms acting on the post-squalene portion of the sterol pathway (Ferrer *et al.*, 2017; Lara *et al.*, 2018).

However, these sterol precursors cannot be found in the glycosylated fractions (SG and ASG), which have a composition similar to that of the FS fraction. They are usually the least abundant fractions in plants, with the exception of the *Solanum* genus, in which the SG+ASG fractions can reach more than 85% of the total sterol composition (Ferrer *et al.*, 2017). In SGs, the hydroxyl group of the sterol molecule is linked through a β-glycosidic bond to the C1 of a sugar molecule by the action of a sterol glycosyltransferase (SGT), increasing in this way the hydrophilicity of the sterol molecule (Hartmann, 1998; Ramírez-Estrada *et al.*, 2017). The most common monosaccharide found in SGs is glucose, but other sugars such as galactose, xylose or mannose can be also used for the sterol glycosylation (Ferrer *et al.*, 2017). Finally, ASGs are derived from SGs by the esterification of the hydroxyl group of the sugar at position C6 with palmitic or stearic acid, although some plants also use atypical fatty acid chains (Ferrer *et al.*, 2017). In the case of ASG biosynthesis, no steryl-glycoside acyltransferase (SGAT) enzyme has been identified yet.

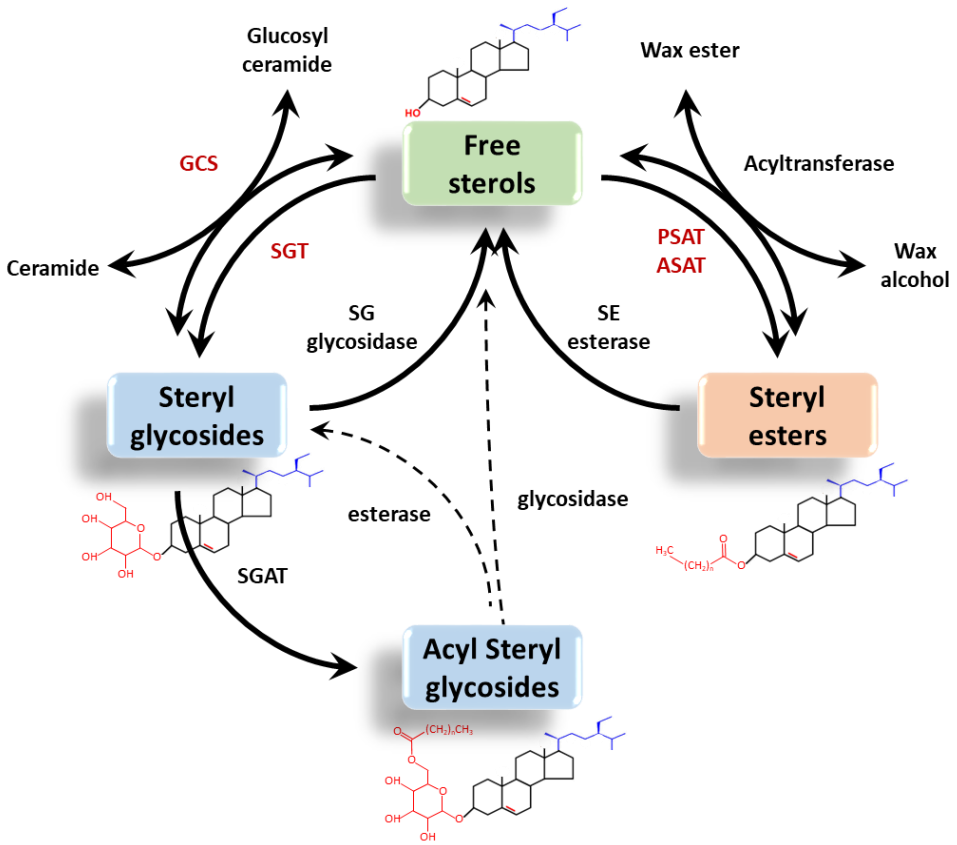

Figure 7 Schematic overview of conjugated sterol metabolism in plants. Those enzymes for which the corresponding genes have been cloned are indicated in red: ASAT, acyl-CoA:sterol acyltransferase; PSAT, phospholipid:sterol acyltransferase; SGT, UDP-glucose:sterol glycosyltransferase; SGAT, steryl glycoside acyltransferase; GCS, glucosylceramide synthase. Dashed arrows indicate enzymatic conversions not confirmed at an experimental level. The sterol molecules correspond with β-sitosterol in the free and conjugated forms. The β-sitosterol lateral side chain is shown in blue. Fatty acid and glucose moieties are shown in red. Adapted from (Ferrer *et al.*, 2017).

SE are accumulated in lipid droplets, where they are suggested to mainly serve as a reserve pool to maintain sterol homeostasis (Hartmann, 1998; Ramírez-Estrada *et al.*, 2017). In contrast, FS, SG, and ASG are commonly located in cell membranes where they are key for the maintenance of membrane fluidity and permeability (Benveniste, 2002).

Free and conjugated sterols are susceptible to a highly dynamic metabolism, in which they are potentially interconvertible by the action of different enzymes (Ferrer *et al.*, 2017) (Figure 7).

4. STEROL FUNCTIONS IN PLANTS

Sterols play essential roles in eukaryotes and, consequently, in plants. They are integral components of cell membranes that are key for regulating membrane fluidity and permeability. In the membrane environment, they can interact with other molecules such as proteins and other lipids forming specific microdomains, called lipid rafts, which serve as anchoring platforms for signaling proteins belonging to different cell signal transduction pathways (Benveniste, 2002; Valitova, Sulkarnayeva and Minibayeva, 2016). Sterols are also precursors of BRs, a kind of plant hormones related to plant growth and development. Moreover, sterols have been also described to be involved in growth and development by themselves and not only as BRs precursors (Jang *et al.*, 2000; Carland *et al.*, 2002; Schaller, 2003). Furthermore, several reports have indicated the possible role of alterations in the sterols composition of cell membranes with the response of plant cells to several biotic and abiotic stresses (Aboobucker and Suza, 2019).

The correct function of plant membranes depends on balanced levels of 24-methyl and 24-ethyl sterols, as well as the specific ratio between stigmasterol and β-sitosterol along the different developmental stages or during stress situations (Valitova, Sulkarnayeva and Minibayeva, 2016).

4.1 Sterols on cell membranes

Lipid membranes are one of the most important components of cells as they confer protection, transport, and structural functions. The PM is able to maintain intracellular ion homeostasis thanks to its selective permeability to several molecules and ions. The main lipid components of membranes are glycerolipids, sphingolipids, and sterols (Valitova, Sulkarnayeva and Minibayeva, 2016). The interaction of sphingolipids with sterols leads to the formation of lipid rafts, which are important membrane domains involved in the correct assembly and localization of membrane enzymes and signaling proteins. The composition analysis of lipid rafts from different plant species has revealed the presence of different sterol species including β-sitosterol, stigmasterol, campesterol, cholesterol and brassicasterol in their free and glycosylated forms (SGs and ASGs) (Valitova, Sulkarnayeva and Minibayeva, 2016).

Although the amount of total sterols is different in each cell membranous system, (*e.g.* their levels are lower in the ER than in the PM and are absent from thylakoid membranes) the sterol composition and proportions are similar for all of them (Hartmann, 1998).

Sterols can modulate membrane fluidity and permeability by interacting with the saturated fatty acids of phospholipids and sphingolipids and limiting their motility as cholesterol does in animal cells. The ability to organize membranes resides in the requirement of several structural characteristics such as a planar ring system, a free 3β-hydroxyl group and an aliphatic side chain of 8-10 carbons, which are all satisfied by the major plant sterols (Hartmann, 1998; Grosjean *et al.*, 2015) . Each sterol species has different ordering abilities on membrane structures depending on their structure and physicochemical properties, which have been widely studied by biophysical methods. Campesterol has been described to provide a strong ordering effect, similar to that of cholesterol. It is followed by β-sitosterol and being stigmasterol the less efficient one (Hartmann, 1998; Grosjean *et al.,* 2015; Valitova, Sulkarnayeva and Minibayeva, 2016).

The presence of saponins in membranes can also influence their permeability. It has been described that sterols can interact with saponins generating pores in the membrane with the subsequent increase in membrane permeability (Valitova, Sulkarnayeva and Minibayeva, 2016).

4.2 Role of sterols in plant growth and development

Several plant mutants affected in the early steps of the sterol biosynthetic pathway have phenotypic abnormalities related to plant growth, and most of them show reduced size (Schrick *et al.*, 2000; Benveniste, 2002; Carland *et al.*, 2002; Schaller, 2003). Relative to the dwarf phenotype of these mutants, two hypothesis have been proposed: i) The change in the sterol content may affect the physical properties of the PM and, consequently, cell growth could be constrained; ii) alterations in the sterol composition may alter BR synthesis, necessary for the correct development of the plant (Valitova, Sulkarnayeva and Minibayeva, 2016). Although the size of most of these dwarf mutants was recovered after exogenous addition of BRs, some of them (such as those affected in *FACKEL* or *SMT2* genes) were insensitive to BRs

treatment, suggesting that the growth abnormalities were caused directly by alterations in the sterol composition (Benveniste, 2002; Carland *et al.*, 2002).

Another reported phenotype for sterol mutants is embryo lethality, involving abnormal embryogenic cell divisions and aberrant differentiation of primary structures such as cotyledons. Such a severe phenotype suggests the essential role of sterols as cellular components and even as signaling molecules for correct development (Schaller, 2003; Valitova, Sulkarnayeva and Minibayeva, 2016). Sterol metabolism is very active during the early stages of seed development and germination, in which cell divisions and membrane synthesis are essential processes (Carland, Fujioka and Nelson, 2010; Valitova, Sulkarnayeva and Minibayeva, 2016). The observation of elongated nuclei and cell expansion defects in several sterol mutants support the hypothesis that sterols are involved in cell division and expansion (Carland, Fujioka and Nelson, 2010). Moreover, these mutants have also been reported to show defects on cell wall during divisions of embryo and root cells due to a reduction in cellulose formation. Cellulose is synthesized by a hexameric protein complex consisting of multiple cellulose synthase catalytic subunits which are associated with the PM. Therefore variations in sterol composition may influence the stability and function of these cellulose biosynthetic enzyme complexes (Schrick *et al.*, 2004).

Mutants affected in the *SMT2* gene show a discontinuous cotyledon venation pattern due to defects in vascular cell polarization and axialization (Benveniste, 2002; Carland *et al.*, 2002). The integrity of the PM is compromised due to alterations in sterol levels and thus may affect the localization of proteins involved in cell polarization that reside in lipid rafts (*e.g.* PIN proteins) (Carland *et al.*, 2002; Valitova, Sulkarnayeva and Minibayeva, 2016). It has been shown that PIN proteins, which belong to a protein family implicated in auxin transport, and therefore in cell polarity, require SMT1 function for correct positioning in *A. thaliana* (Willemsen *et al.*, 2003).

4.3 Sterols in stress responses

The PM is considered a physical barrier that protects the cell and, as such, it is assumed to play an essential role during stress responses. The lipids integrating the

PM, and specifically sterols, have dynamic responses to every external perturbation on the cells (Valitova, Sulkarnayeva and Minibayeva, 2016). Alterations in the sterol composition of the PM have been observed during different stress responses in plants. The response mechanism of roots to wounding includes, among others, an overall increase in total sterol levels which may be necessary for increasing membrane rigidity (Valitova, Sulkarnayeva and Minibayeva, 2016).

Big variations in temperature also influence the physicochemical properties of cell membranes. After cold exposure, the expression of several enzymes within the sterol biosynthetic pathway is increased as well as the synthesis of membrane sterols (Senthil-Kumar, Wang and Mysore, 2013). The extra ethyl group in 24-ethyl sterols may be key to improve the resistance to cold temperature by reinforcing the Van der Waals interactions and therefore increasing the strength of membrane coupling (Valitova, Sulkarnayeva and Minibayeva, 2016). The higher diversity of sterol species in plants coincides with the necessity of these sessile organisms to adapt to varying stress conditions to survive (Valitova, Sulkarnayeva and Minibayeva, 2016).

A number of studies have also highlighted the role of sterols in improving the biotic stress resistance in plants (Aboobucker and Suza, 2019). Pathogens colonize a host and take up nutrients from the apoplast, where they grow. The apoplast usually contains minimal nutrients that come from the exchange with the cytosol via PM permeability (Sattelmacher, 2001). Some enzymes such as squalene synthase (involved in the synthesis of sterol precursor) and C22DES are overexpressed after pathogen infections and regulate nutrient efflux into the apoplast by modifying membrane permeability (Wang *et al.*, 2012). Moreover, the antifungal properties of some phytosterols including β-sitosterol, campesterol, and stigmasterol have been proven (Choi *et al.*, 2017).

5. STIGMASTEROL: THE LAST PRODUCT OF THE 24-ETHYL STEROL BRANCH

As mentioned above, 24-ethyl sterols are derived from 24-ethylidenelophenol as a specific characteristic of the green world. Within this group of sterols, two major end products are found: β-sitosterol and stigmasterol. These sterols only differ by the presence of a double bond at position C22 in the stigmasterol side chain (Figure 8).

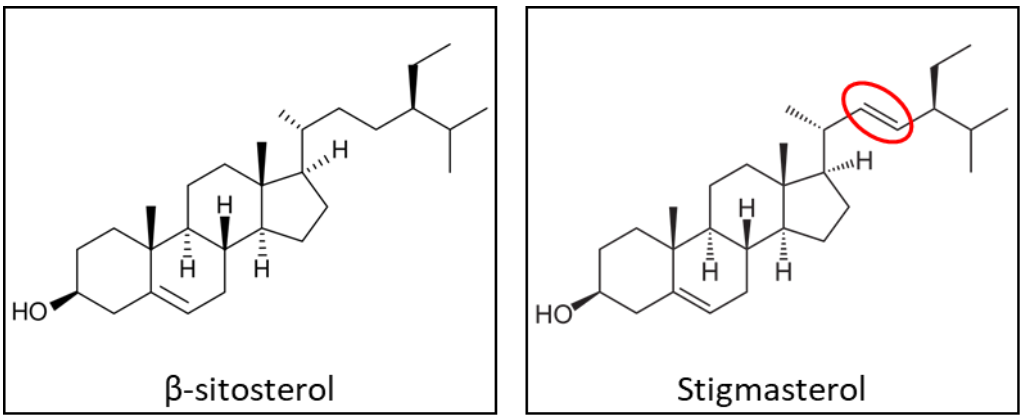

Figure 8 Molecular structure of β-sitosterol and stigmasterol. The double bond at position C22 in the lateral chain of stigmasterol is highlighted.

The existence of C22-unsaturated sterols is restricted to fungi and plants and are produced by the action of the cytochrome P450 (CYP) enzymes CYP61 and C22DES (also referred to as CYP710) in fungi and plants, respectively (Morikawa *et al.*, 2006; Ohta and Mizutani, 2013). Both enzymes have sterol C22 desaturase activity but act on different substrates and produce different products (Chen *et al.*, 2014). CYP61 and C22DES show a high level of amino acid sequence identity and consequently a very close phylogenetic relationship. CYP61 and C22DES are also phylogenetically related to CYP51, another CYP enzyme having sterol 14-demethylase activity. CYP51 is common to the plant, yeast, and animal sterol biosynthetic pathways (Morikawa *et al.*, 2006; Ohta and Mizutani, 2013).

There is evolutionary evidence suggesting that all these P450 enzymes already existed in the most ancient eukaryotes, with CYP51 appearing first and CYP61/C22DES soon after (Nelson, 2018). The orthologs of CYP61/C22DES have been lost during the evolution of the animal lineage (Chen *et al.*, 2014; Nelson, 2018) (Figure 9). Since C22DES acts downstream of CYP51 in sterol biosynthesis, an accepted hypothesis is that the C22DES evolved later from a CYP51 duplication. Thus, it has been speculated that animals descended from an ancestor originated before the occurrence of CYP51 duplication (Chen *et al.*, 2014; Nelson, 2018).

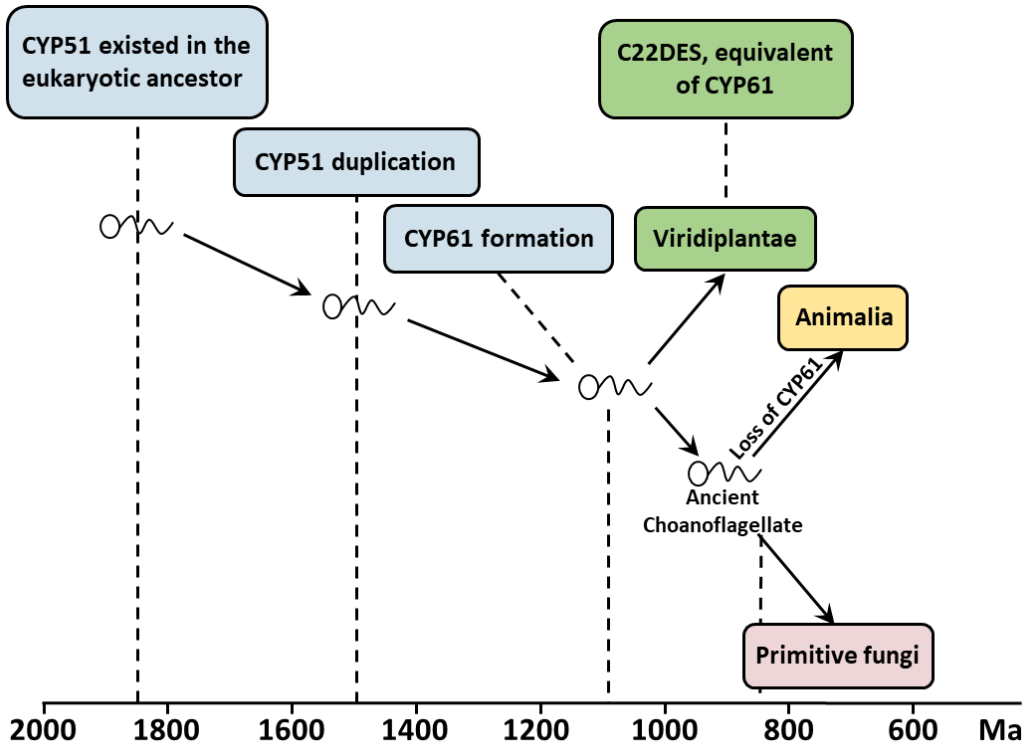

Figure 9 A possible evolutionary scenario of C22DES. The earliest eukaryotes date from 1,850 Ma in unicellular, flagellated, and aquatic forms. CYP51 is thought to be the first eukaryotic CYP. Around 1,500 Ma, CYP51 duplication occurred in the ancestral eukaryote. The CYP51 duplicate had evolved into the progenitor CYP61 before the separation of *Viridiplantae* ancestor. C22DES (CYP710), an equivalent of CYP61, is widespread in *Viridiplantae.* CYP61 existed in the choanoflagellates, ancestors of fungi, and animals, but later likely lost in the early Animalia. Adapted from Chen *et al.* (2014).

C22DES catalyzes the desaturation reaction of the C22 carbon of β-sitosterol to generate a double bond at this position in the presence of NADPH to yield stigmasterol. Like other CYPs, this enzyme needs the action of NADPH-cytochrome P450 reductase as an electron donor. Two H_2O molecules are released in the reaction (Figure 10).

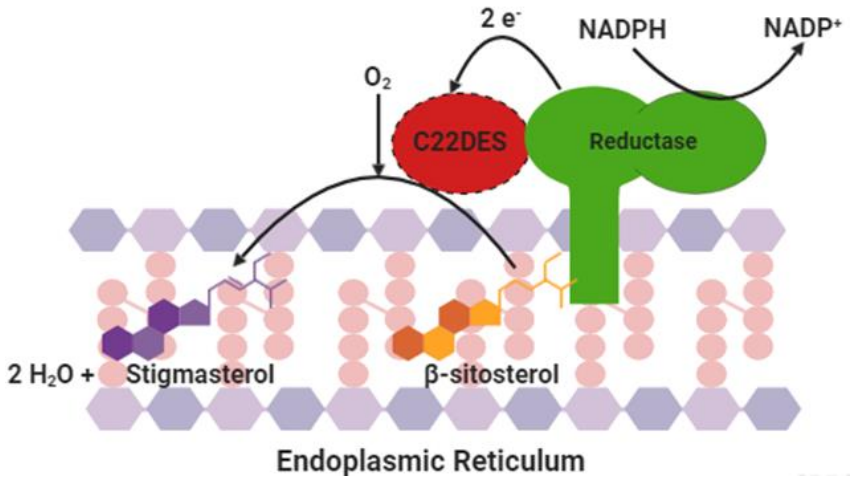

Figure 10 Schematic representation of the reaction catalyzed by C22DES. C22DES converts β-sitosterol into stigmasterol in an oxygen-dependent desaturation reaction. This enzyme requires NADPH-cytochrome P450 reductase as electron donor, which is located in the ER as an integral membrane protein. The dotted line around C22DES represents the lack of information about its subcellular localization.

C22DES is highly conserved among phylogenetically distant plant species, supporting in this way the view that stigmasterol biosynthesis is an essential process in the plant kingdom (Morikawa *et al.*, 2006; Ohta and Mizutani, 2013). In agreement with this, the presence of stigmasterol is a common feature among these organisms.

Several studies in different plant species have described the differential expression of *C22DES* genes during plant growth and development as well as in response to different biotic and abiotic stresses (e.g. cold, salinity, pathogenic bacteria, and fungal infections, etc.) with the concomitant changes in stigmasterol levels (Aboobucker and Suza, 2019).

C22 DES was cloned and characterized in various plant species more than one decade ago (Morikawa *et al.*, 2006, 2009; Arnqvist *et al.*, 2008). However, and despite the relevance of this enzyme in plant biology, no significant progress has been since then towards the characterization of this enzyme at the structural and functional levels.

OBJECTIVES

OBJECTIVES

The main objective of this thesis was to extend the current knowledge of plant sterol metabolism with a special focus on the elucidation of the role of stigmasterol during plant growth and development as well as in their response to environmental challenges. The achievement of this general objective was based on the development of the following specific objectives using tomato (*Solanum lycopersicum* cv. MicroTom*)* as a model system:

1. The functional and structural characterization of sterol C22-desaturase (C22DES), the enzyme specifically involved in the conversion of β-sitosterol into stigmasterol, using biochemical and cell biology approaches.

2. The evaluation of the role of stigmasterol on plant growth, development, and its involvement in plant and fruit responses to biotic and abiotic stresses, using transgenic and genome editing strategies.

CHAPTER I

Structural and functional analysis of tomato sterol C22 desaturase

1. ABSTRACT

Sterols are essential components of eukaryotic cells that modulate membrane fluidity and permeability. Plants produce a complex mixture of sterols, among which β-sitosterol, stigmasterol, and campesterol are the most abundant. Many reports have shown that the stigmasterol to β-sitosterol (STIG/SIT) ratio changes during plant development and in response to stresses, suggesting that it may play a role in the regulation of these processes. In tomato (*S. lycopersicum*), changes in the STIG/SIT ratio correlates with the induction of the only gene encoding sterol C22-desaturase (C22DES), the enzyme specifically involved in the conversion of β-sitosterol to stigmasterol. Despite the biological interest of this enzyme, there is still a lack of knowledge about several relevant aspects related to its structure and function. In this study, we report the endoplasmic reticulum (ER) subcellular localization of tomato C22DES based on confocal fluorescence microscopy and cell fractionation analysis. Modeling studies have also revealed that C22DES consists of two well-differentiated domains: a single N-terminal transmembrane-helix domain (TMH1), anchored into the ER-membrane, and a globular (or catalytic) domain that is oriented towards the cytosol but also in contact with the ER-membrane. Although TMH1 is involved in the targeting and retention of the enzyme in the ER, the globular domain may also interact and be retained in the ER in the absence of the N-terminal transmembrane domain. The observation that a truncated version of C22DES lacking the TMH1 is enzymatically inactive revealed the unexpected requirement of the N-terminal membrane domain for enzyme activity. The *in silico* analysis of the TMH1 region revealed several features that could be involved in substrate recognition and binding. Overall, this study contributes to expand the current knowledge on the structure and function of plant C22DES and to unveil novel aspects related to sterol metabolism.

Structural and functional analysis of tomato sterol C22 desaturase

LAURA GUTIÉRREZ-GARCÍA[1], MONTSERRAT ARRÓ[1,2], TERESA ALTABELLA[1,4], ALBERT FERRER[1,2] AND ALBERT BORONAT[1,3]

[1]CENTER FOR RESEARCH IN AGRICULTURAL GENOMICS (CSIC-IRTA-UAB-UB), CAMPUS UAB, BELLATERRA, BARCELONA; [2]DPTO DE BIOQUÍMICA Y FISIOLOGÍA, [3]DPTO DE BIOQUÍMICA Y BIOMEDICINA MOLECULAR, [4]DPTO DE BIOLOGÍA, SANIDAD Y MEDIO AMBIENTE, UB, BARCELONA.

2. INTRODUCTION

Sterols are isoprenoid-derived lipids that play an essential role in the regulation of membrane fluidity and permeability in eukaryotic cells (Demel and De Kruyff, 1976; Hartmann-Bouillon and Benveniste, 1978). Plants produce a complex mixture of sterols, among which β-sitosterol, stigmasterol, and campesterol are the most abundant. In most plants, sterols are mainly found in free form (FS) but also conjugated as steryl esters (SEs), steryl glycosides (SGs) and acyl steryl glycosides (ASGs). While FSs, SGs, and ASGs are mainly found in the plasma membrane (PM), SEs accumulate in lipid droplets (Ferrer *et al.*, 2017).

Modifications in the sterol composition of the plasma membrane (PM) are known to influence the function of membrane-bound proteins, channels, receptors, and components of different signal transduction pathways (Schaller, 2004). The maintenance of PM integrity and function has also been reported to play a relevant role in conferring biotic and abiotic stress tolerance (Senthil-Kumar, Wang and Mysore, 2013). Moreover, campesterol acts as a precursor for the synthesis of brassinosteroids, a group of steroid hormones having a key function in plant growth and development (Vriet *et al.*, 2015).

Structural variations in the plant sterol backbone arise from different substitutions in the side chain at position C17 and the number and position of double bonds in both the side chain and in the cyclopentanoperhydrophenanthrene ring system (Hartmann, 1998). Among these structural variations, the specific occurrence of a double bond at C22 in the side chain of ergosterol in fungi and stigmasterol in plants

represents one of the most remarkable features in the sterol composition among biological kingdoms (Morikawa, Mizutani and Ohta, 2006).

Stigmasterol is structurally similar to β-sitosterol. As shown in Figure 1 they only differ in the double bond present at position C22 of stigmasterol. Despite their high structural similarity, both sterols differentially affect the physicochemical properties of the PM. In this regard, sterols are known to be crucial for the stability of the PM as they modulate the formation of liquid-ordered (*lo*) lipid domains (also known as lipid rafts) which influence several biological processes such as signal transduction, cellular sorting or infectious diseases (Dufourc, 2008). Recent studies had reported the different capacities of the major plant sterols to modulate the order level of lipid membranes, being stigmasterol the less efficient (Grosjean *et al.*, 2015). Stigmasterol-enriched membranes are less permeable, and therefore they show a decreased leakage (Grunwald, 1971).

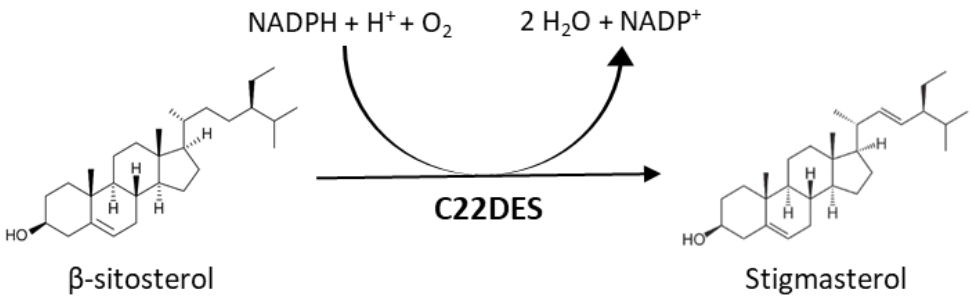

Figure 1 Enzymatic reaction of C22DES leading to stigmasterol. Stigmasterol is synthesized from β-sitosterol by the action of sterol C22DES, that catalyzes the desaturation of carbon 22 using $NADPH+H^+$ and O_2 as co-factors. This enzyme acts at the final steps of the sterol biosynthetic pathway. C22DES belongs to the cytochrome P450 enzyme family that are heme-b containing monooxygenases.

Stigmasterol is synthesized from β-sitosterol by the action of the enzyme sterol C22-desaturase (C22DES), also known as CYP710. C22DES belongs to the cytochrome P450 (CYP) protein family, which includes enzymes involved in numerous biosynthetic and xenobiotic pathways in all living organisms, from bacteria to human. CYP proteins share a common catalytic center including the heme-iron-binding domain. Although these proteins show a low primary amino acid sequence identity, all CYPs display a common overall topology and tridimensional fold (Bak *et al.*, 2011).

Many reports have shown that changes in stigmasterol levels usually correlate with increases that take place during plant development and in response to stresses (Douglas, 1985; Whitaker, 1988, 1991; Griebel and Zeier, 2010). This suggests that the conversion of β-sitosterol to stigmasterol may modulate plant development and responses to environmental stimuli (Aboobucker and Suza, 2019). Therefore, the level of these major sterols in the PM is expected to be tightly regulated and highlights the requirement of an equilibrated sterol composition for plant growth, development, and interactions with the environment. In this respect, the stigmasterol to β-sitosterol (STIG/SIT) ratio has been considered a relevant biochemical marker that has extensively been analyzed in regard to different plant developmental processes and environmental responses (Whitaker, 1991; Griebel and Zeier, 2010). Changes in the STIG/SIT ratio may be explained either by the conversion of β-sitosterol to stigmasterol, catalyzed by the action of C22DES, or by sterol homeostasis among the different conjugated fractions, especially the esterification of β-sitosterol.

All plant CYPs described so far are membrane-bound and they are mainly found in the ER membrane. However, some CYPs have also been reported in other subcellular localizations such as mitochondria, plastids and the PM (Schuler *et al.*, 2006; Šrejber *et al.*, 2018). According to current knowledge, C22DES may likely use as a substrate β-sitosterol present in two different subcellular pools: i) β-sitosterol synthesized *de novo* in the endoplasmic reticulum (ER), and ii) β-sitosterol already present in the PM (either in free form and/or conjugated as SG and ASG). Although it is widely accepted that free sterol biosynthesis occurs in the ER (Fujioka and Yokota, 2003; Schaller, 2003; Benveniste, 2004), the participation of the PM in the final steps of the sterol pathway (*e.g.* stigmasterol biosynthesis) has not been excluded (Hartmann, 1998). Therefore, C22DES could be active in the ER and/or in the PM. Based on this, the study of the precise subcellular location(s) of plant C22DES and its membrane topology is a very relevant issue to understand the mechanism of action of this enzyme and its functional role during plant growth and development and in response to stress (Aboobucker and Suza, 2019). The aim of the present work has been the study of novel structural and functional aspects of C22DES. Tomato (*Solanum lycopersicum*) was chosen for these studies as is one of the few species in which C22DES is encoded by a single-copy gene.

3. RESULTS

3.1 C22DES-GPF localizes in the ER

As indicated above, C22DES is likely to be located in the ER and/or in the PM. To study the subcellular location of this enzyme, a chimeric protein containing the entire C22DES sequence fused to the green fluorescent protein (GFP) (C22DES-GFP) was transiently expressed in *Nicotiana benthamiana* leaves.

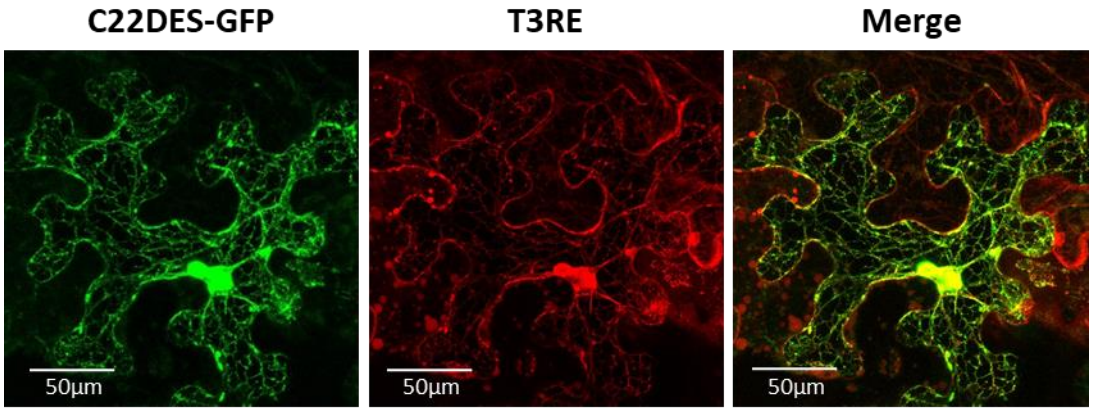

Figure 2 Subcellular localization of C22DES fused to GFP. Confocal optical sections showing the GFP and RFP fluorescence pattern of *N. benthamiana* cells expressing the C22DES-GFP fusion protein (left) and the ER marker T3R3 (middle). The merge of both images is shown in the image on the right. Bars = 50 µm.

As revealed by confocal fluorescence microscopy, C22DES-GFP exhibited a typical ER-like pattern (Figure 2). This localization pattern was equivalent to that observed in cells expressing T3RE fused to the red fluorescent protein (RFP), which was used as a specific marker for ER-localization (Forés *et al.*, 2006) (Figure 2). Merging of the fluorescence of both channels revealed a clear overlapping of the two images, despite T3RE-RFP was an ER-luminal protein and C22DES-GFP was supposed to be anchored in the membrane and facing towards the cytosol.

To make sure that the C-terminal GFP tag was not affecting either the correct targeting of C22DES nor its catalytic activity, the stigmasterol level of the agroinfiltrated *N. benthamiana* leaves expressing the native C22DES and the chimeric C22DES-GFP variant was determined. As shown in Figure 3, the total stigmasterol level increased in a similar way in the samples expressing either C22DES or C22DES-GFP. These results are relevant as reveal that the chimeric enzyme is

correctly targeted to the right subcellular compartment(s) were its substrate (β-sitosterol) is found. Moreover, this observation is also of interest as it opens the feasibility of a rapid and easy *in vivo* assay to evaluate enzyme activity of C22DES-GFP. Furthermore, the expression level of the recombinant proteins could easily be determined by immunoblot analysis using anti-GFP antibodies

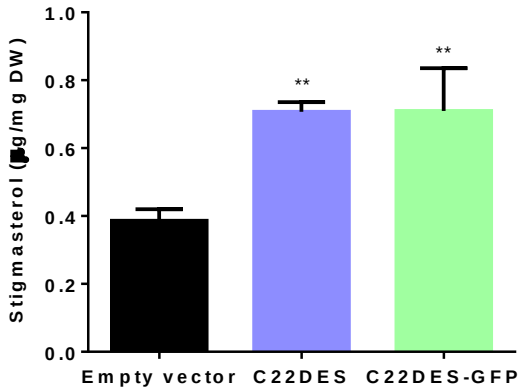

Figure 3 C22DES in vivo enzymatic activity. Stigmasterol levels in the total sterol fraction of *N. benthamiana* leaves expressing C22DES and C22DES-GFP. Values are mean values ± SD of three technical replicates (*n*=3). Asterisks indicate significant differences among means relative to those in leaf samples expressing the empty vector (one-way ANOVA with Dunnett's multiple comparisons test, *p<0.05, **p<0.01). DW: Dry weight

3.2 3D modeling of tomato C22DES predicts the presence of an N-terminal α-helix involved in ER-anchoring

The tertiary structure of tomato C22DES (481 residues out of 501) was modeled with 100 % confidence by the single highest scoring template of the Cytochrome P450 (CYP) *Saccharomyces cerevisiae* lanosterol 14α-Demethylase (CYP51) crystal structure (Monk *et al.*, 2014). Yeast CYP51 was previously reported to be an ER-membrane-associated enzyme (Ott *et al.*, 2005). As shown in (Figure 4) the tertiary structure of both proteins is very similar. The most striking difference concerns the N-terminal transmembrane domain which is much shorter in C22DES. Yeast CYP51 is attached to the ER-membrane through an amphipathic α-helix followed by a transmembrane α-helix. The amphipathic α-helix is lacking in C22DES. The rest of the protein (the globular domain and the predicted membrane interacting regions) is

very similar, with only slight differences in the region preceding the heme-iron binding domain. This region corresponds to residues 438-447 and 463-472 in C22DES and yeast CYP51, respectively. In the case of C22DES, the coiled sequence upstream the heme-iron binding domain is shorter than in CYP51, which may be due to a structural requirement related to their different enzymatic activity. The length of the C-terminal region of these proteins also differs, being shorter in the case of C22DES. Nevertheless, the multiple alignment of plant C22DES proteins indicates that there is no clear consensus for the C-terminal region among species (Figure S.3), which suggests that this region is not important for enzyme function.

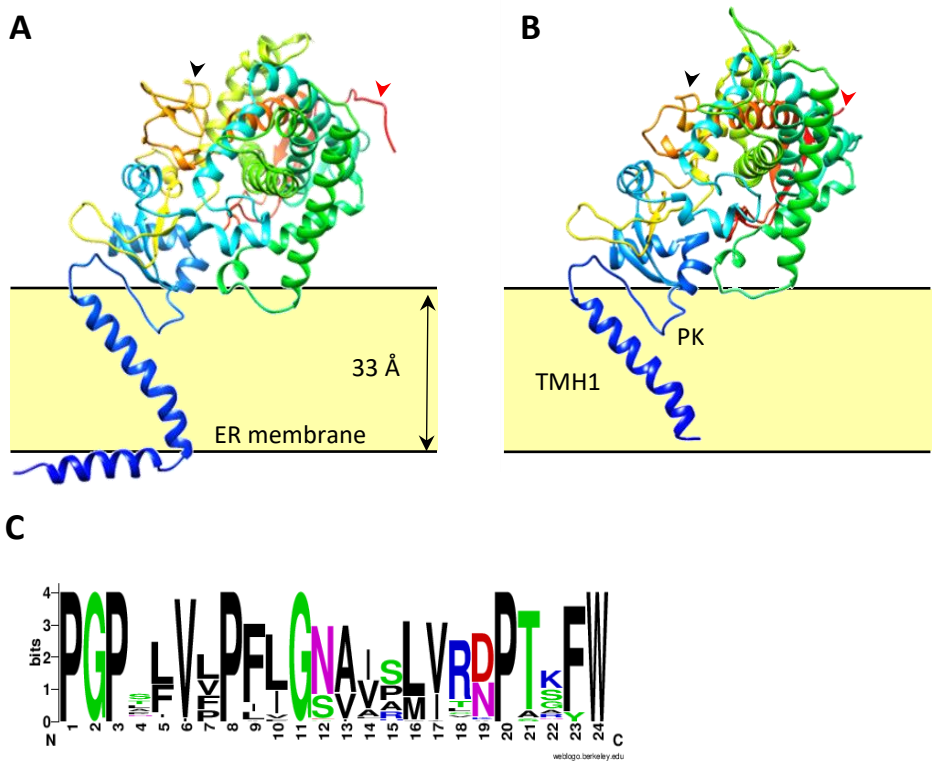

Figure 4 Prediction of tomato C22DES protein tertiary structure. (A) The tertiary structure of yeast CYP51 obtained by X-ray crystallography (adapted from Monk et al., 2014) **(B)** Overall predicted fold of tomato C22DES. The predicted N-terminal transmembrane helix (TMH1) and the proline kink (PK) motif are shown. Black arrows point the region preceding the heme-iron binding domain, and red arrows point the C-terminal region. **(C)** Sequence logo analysis of the PK motif identified in the C22DES of different plant species, in which the conservation of the proline residues can be observed. Sequences from 56 different species were used for this study (Table S.1).

An interaction model of C22DES with cell membranes was generated using the PPM web server of the OPM database (Lomize *et al.*, 2012). The obtained membrane interacting model of C22DES was very similar to that of yeast CYP51 (Monk *et al.*, 2014) (Figure 4A), a type III bitopic membrane protein, and predicts the presence of an N-terminal transmembrane helix (TMH1) (residues 1-28) followed by a proline-kink (PK) motif (residues 38-58) that could partially submerge into the lipid bilayer (Figure 4B). The primary sequence of the PK motif of C22DES is highly conserved among plant species (Figure 4C) as well as among other CYP proteins (Szczesna-Skorupa, Straub and Kemper, 1993). Other regions of C22DES were also predicted to be in contact with the lipid membrane (Figure 4B). In particular, the sequence ProGlyPheAlaPheArgAsn (residues 227-233) located at the N-terminal position of a long amphipathic α-helix. This amphipathic α-helix is predicted in all plant C22DES (data not shown), although its primary sequence is not conserved. Since this amphipathic α-helix is very close to a membrane-interacting region, it is likely that it could contribute to conformational changes of the enzyme that may result in the submersion of the globular domain into the membrane to facilitate the capture of the substrate and its channeling to the active site.

3.3 The N-terminal TMH1 sequence is involved in the targeting and retention of C22DES in the ER membrane

To study the role of the predicted membrane interacting sequences present in the N-terminal region of C22DES (TMH1 and PK), the sequences containing residues 1 to 75 (including THM1 and PK), residues 1 to 37 (including only TMH1) and residues 28 to 66 (including only PK) were fused at the N-terminal end of GFP (Figure 5A) and the subcellular localization of the corresponding chimeric proteins (TMH+PK-GFP and TMH1-GFP, and PK-GFP, respectively) was analyzed by confocal microscopy. The fluorescence distribution of TMH+PK-GFP and TMH1-GFP in agroinfiltrated *N. benthamiana* leaves resulted in a typical ER reticular pattern (Figure 5B). Co-localization studies showed an overlapping of TMH1-GFP and T3RE-RFP distribution (Figure 5C). However, PK-GFP showed a typical cytosolic pattern, with fluorescence also present inside the nucleus (Figures 5B, 5C).

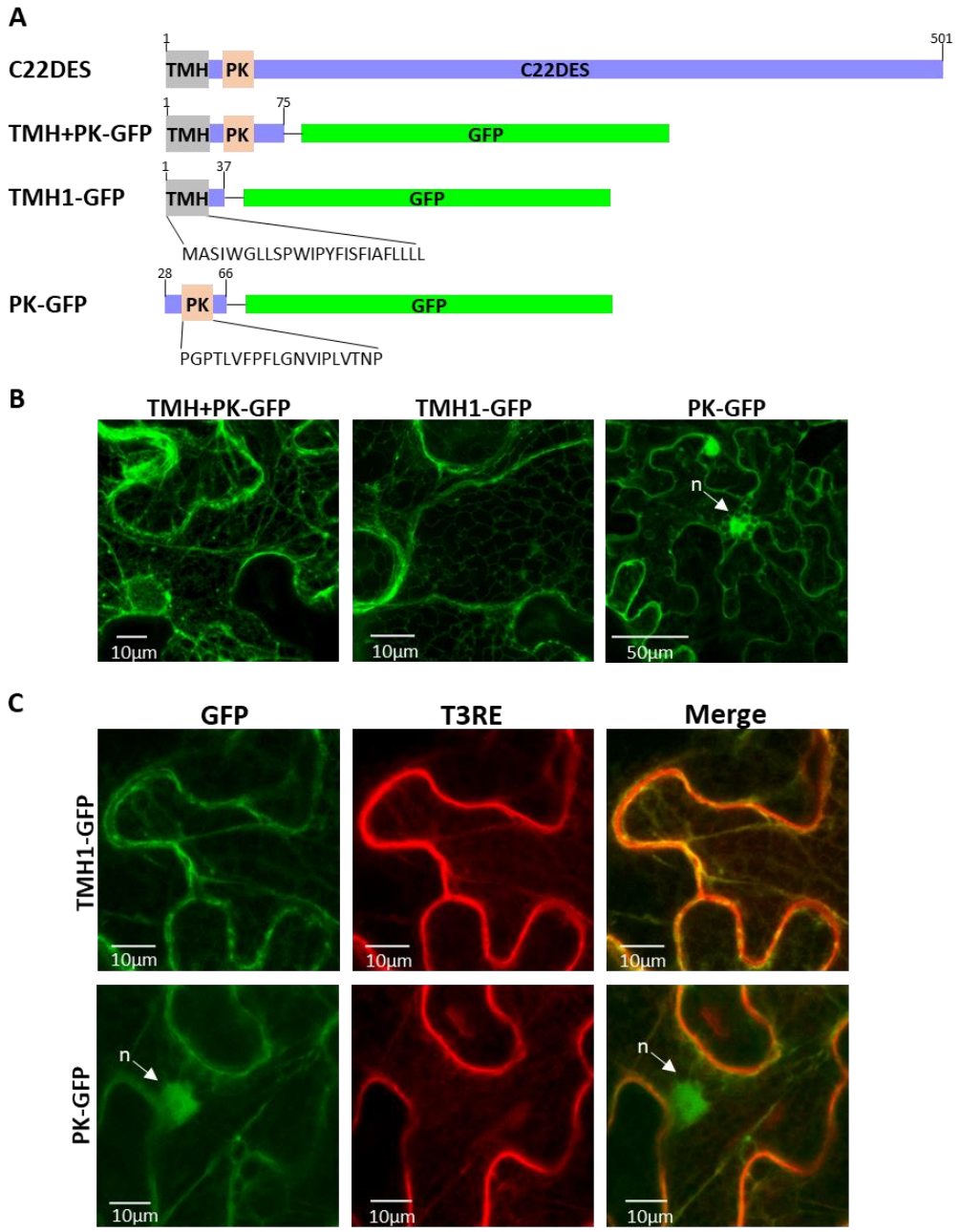

Figure 5 ER-targeting and anchoring structures analysis. (A) Schematic representation of GFP fusion constructs generated to study the role of TMH1 and PK in the ER-targeting and -anchoring of the protein. The blue boxes indicate C22DES sequences, grey boxes the transmembrane helix motif (TMH1), light-red boxes the proline kink motif (PK), and green boxes the GFP protein. The amino acid sequence of TMH1 and PK is shown. Aminoacidic coordinates are shown above the constructions. **(B)** Confocal optical sections showing the GFP fluorescence pattern of *N. benthamiana* cells expressing TMH+PK-GFP, TMH1-GFP, and PK-GFP fusion proteins. The arrow indicates the cell nucleus (n). Bars=

10 and 50µm respectively. **(C)** Close-up view of selected regions of the TMH1-GFP and PK-GFP fusion proteins showing fluorescence of GFP (left), T3RE (middle), and the corresponding merged images (right). Bars = 10 µm.

Altogether these results are in agreement with TMH1 being sufficient for the targeting and retention of C22DES in the ER-membrane. The proximity of the conserved PK motif to the TMH1 sequence suggests its structural role to promote the right orientation of the globular domain towards the ER-membrane.

3.4 The globular domain of tomato C22DES is targeted and retained in the ER-membrane in the absence of TMH1

The globular domain of several CYPs have been reported to interact with the ER-membrane in the absence of the transmembrane domain (Gnanasekaran *et al.* 2015; Mustafa *et al.* 2019; Sagara *et al.* 1993; Yabusaki *et al.* 1988). However, the enzymatic activity of these truncated forms of the enzyme remains controversial. In some cases, the globular domain by itself was reported to be catalytically competent (Clark and Waterman, 1991), while in other cases the activity was demonstrated *in vitro* but not *in vivo* (Sagara, Barnes and Waterman, 1993).

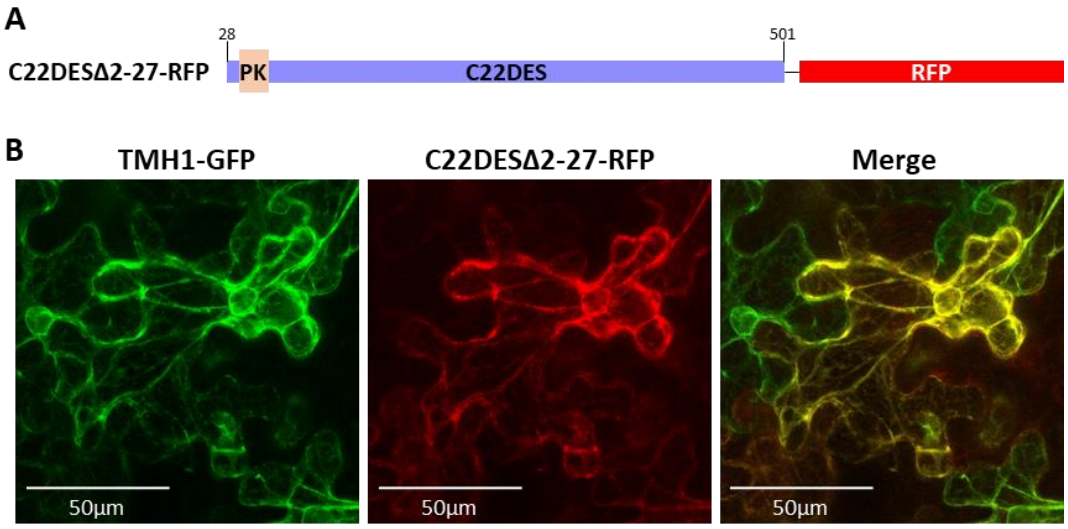

Figure 6 TMH1 is not necessary for targeting and retention of C22dES in the ER. (A) Schematic representation of the C22DESΔ2-27-RFP fusion protein. The blue box corresponds to C22DES, the light-red box the proline-rich motif (PK), and the red box the RFP protein. Amino acidic coordinates

are shown above the construct. **(B)** Confocal optical sections showing fluorescence of TMH1-GFP (left) and C22DESΔ2-27-RFP (middle), and the corresponding merged images (right) Bars = 50 µm.

To study this particular issue in C22DES, a truncated form of the enzyme lacking the TMH1 sequence (residues 2 to 27) was fused to RFP (construct C22DESΔ2-27-RFP) (Figure 6A) and transiently expressed in *N. benthamiana* leaves. As shown in Figure 6B, the fluorescence of C22DESΔ2-27-RFP and TMH1-GFP perfectly overlapped, thus indicating that the globular domain of tomato C22DES can also be targeted and retained in the ER-membrane in the absence of TMH1.

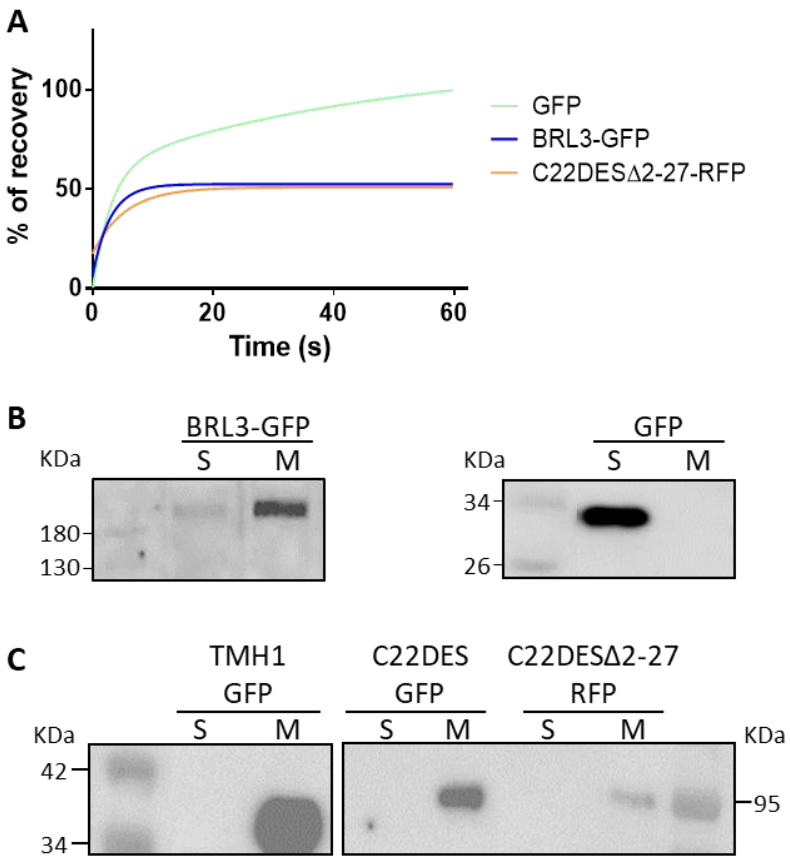

Figure 7 Subcellular localization of C22DESΔ2-27 fused to RFP using FRAP and cell fractionation analysis. (A) FRAP curves representing the fluorescence recovery rates of C22DESΔ2-27-RFP, BRL3-GFP, and GFP. BRL3-GFP and GFP were used as membrane-associated and cytosolic control proteins, respectively. The regions of interest (ROI) in cells expressing the fusion proteins were photobleached with a pulse (4s) of high-intensity laser light and the fluorescence recovery (expressed as a percentage of fluorescence at time point 0s) was measured during 60s. Fluorescence recovery curves represent the best fits from normalized datasets of at least 6 independently bleached ROIs points spots (Figure

S1). **(B)** Immunoblot analysis of soluble (S) and microsomal (M) cell fractions from *N. benthamiana* leaves expressing BRL3-GFP (≈153 KDa) and GFP (≈26.85 KDa) as microsomal and soluble control proteins, respectively. **(C)** Immunoblot analysis of soluble (S) and microsomal (M) cell fractions from *N. benthamiana* leaves expressing C22DESΔ2-27-RFP (≈84.22 kDa), TMH1-GFP (≈34.06 kDa), and C22DES-GFP (≈87.24 kDa).

Fluorescence Recovery after Photobleaching (FRAP) analysis was performed to reinforce these results. FRAP analysis is based on the photo-destruction of a fluorescent molecule in a localized area of a living cell by the action of a short and intense laser pulse. Then, fluorescence intensity is analyzed and the recovery rate will depend on the mobility of molecules from adjacent non-bleached areas (Bunt and Wouters, 2004; Goehring *et al.*, 2010). Thereby, soluble (cytosolic) proteins that can easily move within the cell have a faster fluorescent recovery than integral membrane proteins. Brassinosteroid receptor BRL3 fused to GFP (BRL3-GFP) (Caño-Delgado *et al.*, 2004) and GFP were used as membrane-bound and cytosolic control proteins, respectively. C22DESΔ2-27-RFP showed a recovery rate similar to that of BRL3-GFP (Figure 7A), confirming its behavior as a membrane-associated protein. This result was further confirmed by immunoblot analysis of the cytosolic and microsomal fractions obtained from of *N. benthamiana* leaves expressing TMH1-GFP, C22DES-GFP, and C22DESΔ2-27-RFP. The results that are shown in Figure 7C, clearly indicate that C22DESΔ2-27-RFP is found in the microsomal membrane fraction, as well as C22DES-GFP, TMH1-GFP, and BRL3-GFP (Figure 7B).

3.5 TMH1 is required for C22DES activity

The results reported above suggest that TMH1 could have an alternative functional role in addition to the targeting and retention of the enzyme in the ER. As a first approach to study the functional role of TMH1, C22DESΔ2-27-RFP and C22DES-GFP were expressed in *N. benthamiana* leaves to evaluate their enzymatic activity. An immunoblot assay was performed to estimate the expression levels of the recombinant proteins (Figure 8A).

As expected, sterol analysis of *N. benthamiana* leaves expressing C22DES-GFP showed an increase in the stigmasterol content of the total sterol fraction (Figure 8B) which resulted in an increase in the overall STIG/SIT ratio (Figure S2, Table S2).

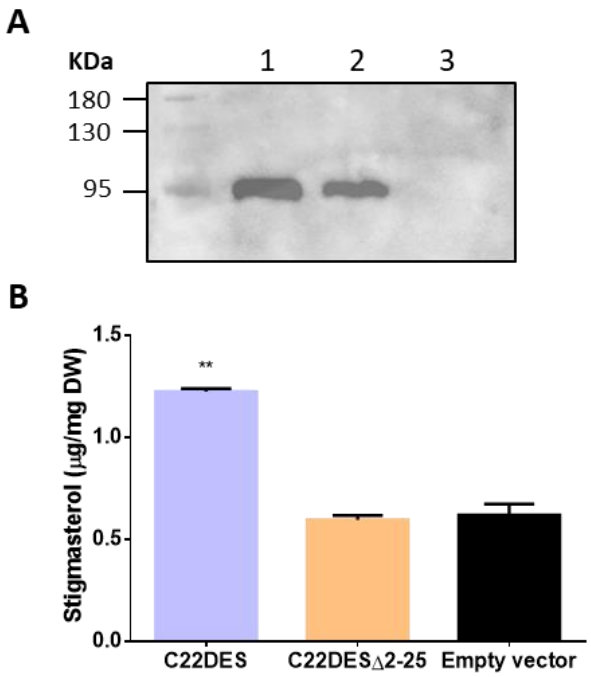

Figure 8 C22DESΔ2-27 in vivo enzymatic activity. (A) Immunoblot analysis of C22DES-GFP and C22DESΔ2-27-RFP levels of agroinfiltrated *N. benthamiana* leaves. Lane 1, C22DES-GFP (≈87.24 KDa); lane 2, C22DESΔ2-27-RFP (≈84.22 KDa); lane 3, empty vector. **(B)** Stigmasterol levels (µg/mg of dry weight) in total steryl lipids from *N. benthamiana* leaves expressing C22DES-GFP and C22DESΔ2-27-RFP. Values are mean values ± SD of three technical replicates (*n*=3). Asterisks indicate significant differences among means relative to those in leaf samples expressing the empty vector (one-way ANOVA with Dunnett's multiple comparisons test, *p<0.05, **p<0.01).

However, in the case of C22DESΔ2-27-RFP, the stigmasterol levels were similar to those present in the leaves agroinfiltrated with the empty vector, thus indicating that TMH1 is necessary for the activity of C22DES. Similar results were obtained in two independent biological replicates, but the results were treated independently due to high variations in the expression levels of the recombinant proteins and, consequently, in the final sterol composition.

3.6 The TMH1 region of plant C22DES share some common features that may be relevant for enzyme function

The sequence alignment of C22DES from different plant species showed that both the length and the primary sequence of the TMH1 region was highly divergent

(Figure 9A). However, a careful inspection of this sequence revealed the presence of several common features shared by all plant C22DES. On the one hand the high number of threonine and serine residues in the N-terminal half of THM1. This may be relevant since some studies have described the role of hydroxylated residues in protein transmembrane domains in providing substrate specificity or correct associations with other membrane components through interactions with the hydroxyl group of their polar side chains (Danek Burgess and Justice, 1999; Martínez-Garay *et al.*, 2014). Another interesting feature was the existence of at least one proline residue in the middle of the N-terminal half of most TMH1 sequences. It is well known that proline residues induce a turn of about 30 degrees in the α-helix. Consequently, the TMH1 sequence of most plant C22DES may have one or more turns in their N-terminal half.

The sequence alignment also revealed a glutamine and a tyrosine residues conserved in all plant C22DES proteins (corresponding to residues Q27 and Y30 in the tomato sequence). Interestingly, these conserved residues are included in the cholesterol recognition/interaction amino acid consensus (CRAC) motif, which is defined with the consensus –L/V-X_{1-5}-Y-X_{1-5}-R/K (Epand *et al.*, 2010) (Figure 9A). This motif has also been reported to interact with β-sitosterol in the same manner as with cholesterol in some proteins (Desai, Dong and Miller, 2016).

Additional conserved CRAC and CARC (the CRAC specular sequence which is defined with the consensus K/R-X_{1-5}-Y/F-X_{1-5}-L/V) motifs were identified when the full-protein alignment was analyzed. However, only those CRAC and CARC motifs present in an α-helix were considered for further examination (Figure 9B). There is no general rule regarding the precise prediction of a protein domain with the ability to recruit sterols in a membrane, but the presence of a CRAC/CARC motifs adjacent to a transmembrane helix is suggestive of this kind of interaction (Epand, 2006).

With these considerations, two CRAC (CRAC1 and CRAC2) and two CARC (CARC1 and CARC3) motifs, and an additional one in which the two motifs were included surrounding tyrosine residue Y358 (CRAC3/CARC2) were identified (Figure 9B and positioned in the tertiary structure of C22DES (Figure 10).

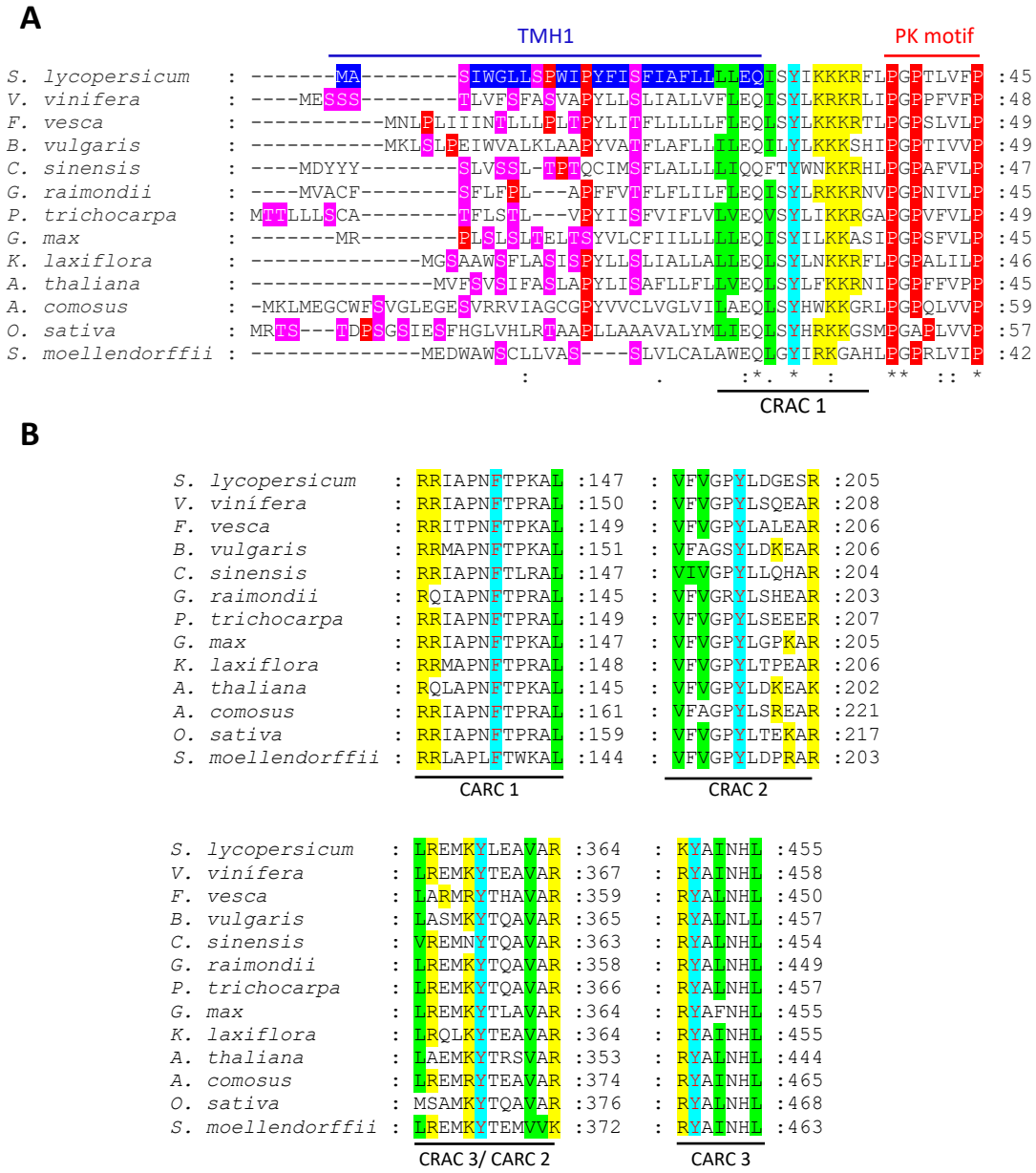

Figure 9 C22DES sequence analysis. (A) Sequence alignment of the N-terminal sequence of C22DES from 13 non-phylogenetically related plant species. Tomato C22DES TMH1 domain is highlighted in blue; prolines (P) are shown in red, and serine (S) and threonine (T) residues are shown in magenta. The CRAC1 motif including the conserved Q27 and Y30 residues is also shown **(B)** Sequence alignments of additional CRAC and CARC motifs found in C22DES protein sequence. Branched-chain amino-acids [leucine (L), valine (V) and isoleucine (I)] from the CRAC motif are shown in green; the tyrosine (Y) in the CRAC motif is shown in cyan; and dibasic residues [arginine (R) and lysine (K)] in the

CRAC motif are shown in yellow. The position of the last amino acid residue of the motif from each plant species is shown on the right.

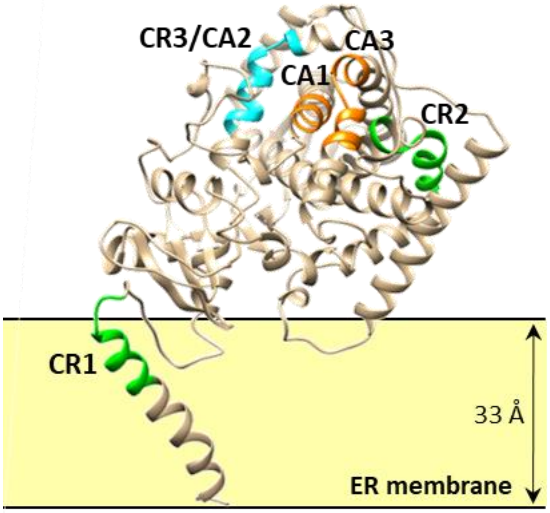

Figure 10 Identification of CRAC and CARC motifs in the tertiary structure of C22DES. CRAC motifs are represented in green, CARC motifs in orange, and the CRAC/CARC motif in cyan. CA, CARC; CR, CRAC

Two of these motifs, CARC1, and the CRAC3/CARC2 are of special interest as they are present in an α-helix with a high level of amphipathicity. It may be speculated that their location in a hydrophobic region within the helix could provide the right environment for the recognition and/or binding of a sterol molecule. In this regard, Stolowich *et al.* (2002) postulated that amphipathic α-helixes may serve not only as membrane interaction domains but also as binding sites of lipids.

3.7 TMH1 could be required for the right positioning of the globular domain in the ER-membrane during catalysis

As indicated above, the TMH1 domain is required for the catalytic activity of C22DES. According to the topological model shown in Figure 4B, it may be speculated that the primary role of TMH1 could be the positioning of the globular domain in the right orientation with respect to the ER-membrane. To get some insight into this issue, a structural model of C22DESΔ2-27 and C22DES interacting with a 1,2-dioleoyl-sn-glycero-3-phosphocholine (DOPC) bilayer was generated using the PPM web server software. The results shown in Figure 11 indicate that the positioning of the globular domain with respect to the membrane is very similar in both cases.

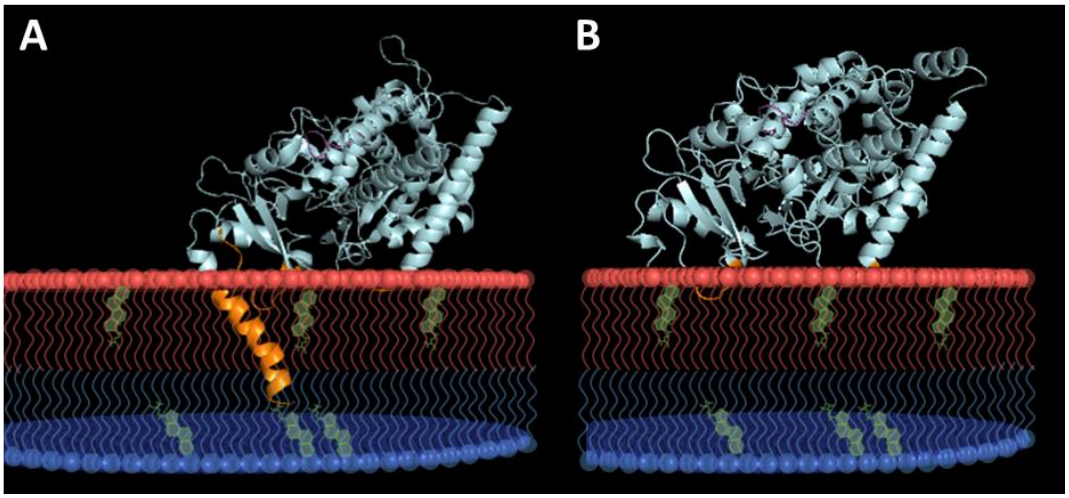

Figure 11 Prediction of the interaction of C22DES with a membrane lipid bilayer. Overall predicted fold of **(A)** C22DES and **(B)** C22DESΔ2-27 interacting with a 1,2-dioleoyl-sn-glycero-3-phosphocholine (DOPC) bilayer. The heme domain is shown in pink and predicted residues contacting the lipid membrane are shown in orange. Phospholipids of the bilayer are shown in red and blue, and β-sitosterol is represented in green.

However, several studies have reported that the globular domain of some CYP proteins shifts to become partially immersed into the lipid membrane during catalysis to facilitate the uptake/release of substrates or products from/to the ER-membrane (Berka *et al.*, 2013; Yu *et al.*, 2015). Therefore, the possibility that TMH1 could be involved in this process cannot be ruled out.

4. DISCUSSION

The subcellular localization studies of tomato C22DES presented in this work strongly support that this enzyme is an ER-resident protein (ERRP). This result was somehow expected considering that stigmasterol is a non-polar molecule synthesized in the ER (Vriet, Russinova and Reuzeau, 2013; Quon *et al.*, 2018) and that other enzymes involved in the sterol biosynthetic pathway, such as SMT1, CPI1, HYD1, and DWF/DIM, are known to localize in the ER (Klahre *et al.*, 1998; Souter *et al.*, 2002; Boutté and Grebe, 2009; Carland, Fujioka and Nelson, 2010). Furthermore, NADPH-cytochrome P450 oxidoreductase, the P450s physiological redox partner, also localizes in the ER (Jensen and Møller, 2010). However, the localization of C22DES in the ER raises the question about how this enzyme could act on the major cellular

pool of β-sitosterol present in the PM. As discussed below, this represents a major issue that remains not fully understood in the frame of the other results described in the present work.

The high score of the predicted structural model of C22DES using the functionally related yeast CYP51 protein as a template and the fact that C22DES was localized in the ER are in agreement with the observation that this enzyme is an integral ER-membrane protein. Our modeling studies predicted the presence of an N-terminal hydrophobic transmembrane domain (TMH1) (residues 1-28) involved in the anchoring of C22DES to the ER-membrane as well as a conserved proline-kink motif (PK) (residues 38 to 57) (Figure 4C) also inserted into the lipid membrane (Figure 11). These ER-membrane-anchor motifs present in C22DES have previously been described as being responsible for the anchoring of other CYP proteins into the ER-membrane. The N-terminal hydrophobic domain of the rabbit P450 LM6, a methylcholanthrene-inducible form, (Kagawa, Mihara and Sato, 1987) as well as that of the rat P450 (M-1), a constitutively expressing male-specific form (Matsumoto *et al.*, 1986), were confirmed as important structural elements for the correct insertion of P450 in the membrane (Sato *et al.*, 1990). Concerning the PK motif, the role of hydrophobic proline-rich sequences in the intracellular targeting of proteins has also been described in other plant proteins (Abell *et al.*, 1997; Lin *et al.*, 2002; Hernández-Gras and Boronat, 2015). However, our results do not support the participation of the PK motif in the targeting of the enzyme to the ER, but rather its possible participation in the right anchoring of the globular domain to promote its correct positioning in the membrane.

Our results have shown that the TMH1 sequence has a primary role in the targeting and retention of this enzyme in the ER-membrane (Figures 5, 7). Unexpectedly, we also found that the C22DES globular domain can be targeted and retained in the ER in the absence of TMH1 (Figures 6, 7). The retention of ER-membrane-bound proteins is a process that remains poorly understood. Eukaryotic proteins within the secretory pathway are primarily transported from the ER to the Golgi apparatus, where they reach the trans-Golgi network (TGN) for their following transfer to the PM, the extracellular space or the endo-lysosomal system (Gao *et al.*, 2014). Nevertheless, ER keeps some resident membrane proteins that are retained through the “export and retrieval” mechanism, in which Coat protein complex I (COPI)

vesicles recognize some canonical motifs either in the C-terminal (KDEL, KKXX, or hydrophobic residues) or in the N-terminal region (Arg-based motifs) (Murakami, Mihara and Omura, 1994; Gao *et al.*, 2014). Conversely, we noticed that C22DES does not contain any of these well-characterized signals. A similar situation occurs in other CYP members, such as the rabbit P4502C2 or the rat P450 (M-1), in which their N-terminal transmembrane region was also reported to act as ER-retention signal without having consensus ER-retention motifs (Murakami, Mihara and Omura, 1994; Szczesna-Skorupa *et al.*, 1998). Similar results were obtained with the bovine 17α-hydroxylase CYP. In this case, a truncated form of the protein lacking its N-terminal transmembrane region expressed in *E. coli* was predominantly found as an integral membrane protein despite lacking its N-terminal signal anchor sequence (Sagara, Barnes and Waterman, 1993). The rat P450c was also found in microsomal membranes after deletion of its N-terminal transmembrane domain (Yabusaki *et al.*, 1988). Altogether, these results suggest the existence of mechanisms for the retention of ER-membrane proteins which remain to be characterized. In the case of C22DES, as well as other CYP proteins, it can be hypothesized that such novel ER-targeting mechanism may not involve alternative signal retention motifs, as these enzymes could be retained in the ER via the interaction with other ERRPs. For instance, through the interaction with NADPH-Cytochrome P450 oxidoreductase, which is required for CYPs function (Scott *et al.*, 2016; Šrejber *et al.*, 2018). The interaction between CYP proteins to form heterodimers of as wells as between CYPs and other proteins such as cytochrome b5 and UDP-glucuronosyltransferase (UGT)1A is well documented (Locuson *et al.*, 2007; Subramanian *et al.*, 2009, 2010; Im and Waskell, 2011; Nelson *et al.*, 2016).

Being in the right place at the right time is very important for the correct activity of an enzyme. However, there are many other aspects that may affect enzyme activity. For example, the correct folding of the enzyme, its accessibility to the substrate or the existence of post-translational control mechanisms. By comparing the stigmasterol content of *N. benthamiana* leaves expressing either the full-length C22DES or the C22DESΔ2-27 variant lacking the N-terminal TMH1 sequence, it was concluded that the N-terminal transmembrane α-helix is required for enzyme activity *in vivo* (Figures 8, S.2, Table S.2). These results are in contrast with the observation that the globular domain of C22DES can be targeted and retained in the ER, where it was predicted to be positioned in the same orientation than the full

enzyme containing the TMH1 sequence (Figure 10). In this respect, there is a lot of controversial data in the literature involving different CYPs. On the one hand, as previously reported, some CYPs lacking the N-terminal signal anchor were shown to be active *in vitro* (Sagara, Barnes and Waterman, 1993; Scheller *et al.*, 1994). In the case of the bovine amino-terminal truncated 17α-hydroxylase, the enzyme was not active when expressed in mammalian cells, in contrast to the results obtained *in vitro* (Clark and Waterman, 1991; Sagara, Barnes and Waterman, 1993). However, Gnanasekaran *et al.* (2015) demonstrated that CYP720B4 remained active even after complete removal of its transmembrane domain. The different behavior of different CYPs of this respect may be related to the nature and subcellular availability of the substrate. This would explain why some CYPs show activity under *in vitro* assay condition, in which the substrate may be freely available, but not under *in vivo* conditions, where substrate availability may be limited. In some CYP proteins, the N-terminal transmembrane domain has been reported to contribute to small precise movements of the globular domain to modify its angle with respect to the membrane during catalysis. This tilting of the globular domain has shown to be essential for catalytic activity as it may be required for the interaction with substrates located inside the hydrophobic core of the membrane (Berka *et al.*, 2013; Yu *et al.*, 2015).

The identification of a conserved CRAC motif in the TMH1 region as well as the high amount of serine and threonine residues present in the N-terminal half of TMH1 of plant C22DES (Figure 9A) prompted us to propose novel roles associated to the N-terminal part of the protein. Cholesterol-binding domains have been the focus of many studies involving computational methods to explore the transmembrane regions of proteins for which there is good evidence of their interaction with cholesterol (Epand *et al.*, 2010; Di Scala *et al.*, 2017). The first motif to be identified was termed cholesterol recognition/interaction amino-acid consensus (CRAC) motif which fulfills the consensus (L/V)-X_{1-5}-(Y)-X_{1-5}-(R/K), (where X is any amino-acid) (Epand *et al.*, 2010; Fantini *et al.*, 2016; Di Scala *et al.*, 2017). Another cholesterol-binding motif, named CARC, corresponds to the mirror version of the CRAC motif with the consensus sequence (K/R)-X_{1-5}-(Y/F)-X_{1-5}-(L/V), (where X is any amino acid) (Fantini *et al.*, 2016; Di Scala *et al.*, 2017). The simplicity of these consensus sequences, in which there are only three specific amino-acids and two variable segments that highly increase its variability, has raised some doubts about its

predictive value (Epand *et al.*, 2010; Fantini *et al.*, 2016). However, the fact that these motifs are adjacent to a transmembrane segment, increases the reliability of the correlation between the presence of the motif and its interaction with cholesterol (Epand *et al.*, 2010; Fantini *et al.*, 2016). Moreover, the cholesterol-binding activity of CRAC motifs has been confirmed by mutational and physicochemical approaches (Fantini and Barrantes, 2013; Fantini *et al.*, 2016).

Interestingly, a CRAC motif reported to interact with β-sitosterol has recently been described in the type 1 cholecystokinin receptor (Desai, Dong and Miller, 2016). Moreover, serine and threonine residues have also been reported to be found in cholesterol-binding regions, where their side-chains have been proposed to interact with the hydroxyl group of the cholesterol molecules based on the complex structures of several described cholesterol-binding proteins (Rosenhouse-Dantsker, 2017). Thus, it is likely that the high amount of hydroxylated amino acid residues in the N-terminal half of TMH1 could have a role in enhancing the interaction of C22DES with β-sitosterol.

The presence of other conserved CRAC/CARC motifs in plant C22DES may suggest interactions involving the globular domain to retrieve sterols from other cell membrane compartments, as it could be the case of the β-sitosterol present in the PM. In this respect, the high amphipathicity of CARC1 (residues 136-147) and CRAC3/CARC2 (residues 353-364) could facilitate the interaction of C22DES with the PM to allow the interaction with the β-sitosterol present in this cell compartment. In this way, stigmasterol formation could be understood as a dynamic process, allowing the C22DES to act not only on the β-sitosterol synthesized *de novo* in the ER but also on the β-sitosterol pool present in the PM.

In mature plant cells, the central vacuole fills most of the volume, so that the cytoplasm is restricted to a thin layer at the cell cortex, and the rest of organelles reside therefore very close to the PM (Wang, Hawes and Hussey, 2017). The ER connects the different membrane compartments of the cell including the PM. The ER-PM interactions have been extensively described as conserved structures where both membranes are closely attached (less than 10 nm apart) (Manford *et al.*, 2012; Wang, Hawes and Hussey, 2017). They are usually known as ER-PM contact sites (EPCSs). In this kind of structures, there are tethering proteins that are responsible

for the attachment of the ER to other cell membranes, forming platforms involved in the regulation of lipid-homeostasis and facilitating non-vesicular lipid exchange (Quon *et al.*, 2018). This kind of association could explain the action of C22DES on the β-sitosterol present in the PM.

5. MATERIALS AND METHODS

5.1 Biological materials

Top10 *E. coli* cells were used for all sub-cloning steps. Plasmids were transformed into chemically competent Top10 *E. coli* cells and transformants were selected on appropriate antibiotics LB plates at the following concentrations: kanamycin 100µg/mL, streptomycin 100µg/mL (Table S.4). The positive transformants were checked by colony PCR and grown overnight in liquid LB medium supplemented with the corresponding antibiotics. Plasmid DNA was isolated using the Wizard® Plus SV Miniprep DNA Purification System (Promega) according to the instructions provided by the supplier.

Agrobacterium tumefaciens GV3101 cells were transformed by thermal shock as described by (Höfgen and Willmitzer, 1988). Positive transformants were selected on YEB plates containing rifampicin 50µg/ml and gentamycin 25µg/ml and the plasmid selective antibiotic. Colony PCRs were performed for plasmid confirmation.

N. benthamiana plants were grown under standard greenhouse conditions (14 h light at 26 ± 1°C and 10 h dark at 21 ± 1°C) in individual pots of 12cm diameter.

5.2 Cloning and plasmid constructions

All the protein-coding sequences lacking the stop codon used for in-frame fusions with the GFP and RFP were amplified by PCR using 35S:C22DES plasmid as a template, which was previously obtained in the laboratory starting from leaf tomato cDNA as template (C22DES GenBank: NM_001247585). All the PCR reactions were performed using AccuPrime™ Taq DNA polymerase, high fidelity (Invitrogen) and specific primer pairs (Tables S.3, S.4). The PCR products were cloned into pDONR207 donor vector using Gateway® (GW) technology (Invitrogen). The cDNAs in the

resulting pENTRY plasmids were sequenced to confirm the absence of mutations derived from the amplification process. The verified sequences were sub-cloned into the binary vectors pEarleyGate103 (Earley *et al.*, 2006) and pGWB454 (Nakagawa *et al.*, 2007) using GW technology to generate GFP and RFP fusions at the C-terminus respectively. In all cases, the coding sequences were under the control of the *CaMV 35S* promoter. The obtained constructs were confirmed by restriction mapping and DNA sequence analysis.

5.3 Agroinfiltration of *N. benthamiana* leaves

Subcellular localization assays were performed by heterologous expression of GFP fusion proteins in *N. benthamiana* leaves, which were infiltrated with the *A. tumefaciens* strains described above (Sparkes *et al.*, 2006; Wydro, Kozubek and Lehmann, 2006). A single positive colony per construct was inoculated into 3 mL YEB supplemented with the right antibiotics and incubated overnight at 28ºC at 250 rpm continuous rotary shaking. A 1:100 dilution of the overnight culture was inoculated into 25 mL of YEB medium (containing the same antibiotics) and incubated under the same conditions. The culture was centrifuged at 5000 rpm for 15 min at 4ºC and the bacterial pellets resuspended in infiltration buffer (10mM MES pH 5.6, 10mM $MgSO_4$, and 150µM acetosyringone) to reach a final OD_{600} of 1. The transformed strains were separately mixed in a 1:1 ratio with a culture of *A. tumefaciens* strain expressing the HC-Pro silencing suppressor (HCPRO) (Goytia *et al.*, 2006) and infiltrated with a syringe in the abaxial part of leaves of 3-5 week old *N. benthamiana* plants. For co-expression analysis, the different strains were also mixed in equal proportions and also with HC-Pro (the mix never reaching an OD_{600} higher than 1). Then, plants were grown under the greenhouse conditions indicated above for 3-4 days.

5.4 Confocal microscopy

Pieces of the agroinfiltrated leaves were collected to determine the subcellular localization of fluorescent fusion proteins by analyzing their abaxial epidermis with an Olympus FV 1000 confocal laser-scanning microscope using the 60x water

immersion NA: 1.20 objective. An argon laser (at 488 nm) was used to excite the GFP and a diode laser for RFP excitation (559 nm). The emission windows for fluorescence visualization were set at 500-510 nm and 570-581 nm, respectively. All images were acquired using the same confocal parameters. FV10-ASW software (Olympus) was used for image capture. ImageJ-32 was used for different channel images merging of co-transformed cells.

5.5 Sterol analysis

For sterol composition determinations, *N. benthamiana* leaves from more than three independent agroinfiltrated plants were harvested, frozen in liquid nitrogen and ground to a fine powder and lyophilized. Around thirty milligrams of the lyophilized tissue were placed in a glass tube together with a mix of internal standards [2.5 µg of cholestanol (FS), 5 µg of palmitoyl-cholestanol (SE), 5 µg of cholestanyl-β-D-glucoside (SG) and 5 µg of palmitoyl-β-D-glucosyl-cholestanol (ASG) in chloroform-methanol 2:1]. The organic fraction was then extracted with 3 mL of a chloroform-methanol solution (2:1) by vigorous homogenization in a vortex and sonication for 10 min at room temperature. Then, 1.5 mL of 0.9% (w/v) NaCl were added to facilitate phase separations. The organic phase was recovered after centrifugation at 5.000rpm for 5 min in a JA-20 rotor (Beckman Coulter) and transferred to a new tube. The remaining aqueous phase was re-extracted with 3 mL of chloroform-methanol solution (2:1) and the two organic extracts were mixed together for subsequent evaporation to dryness using a SpeedVac® Concentrator (Savant). The dried residue was dissolved in 150 µl of chloroform and the four sterol fractions (FS, SE, SG, and ASG) were separated by thin-layer chromatography (TLC) using precoated silica gel PLC 60 F254 plates (20 cm x 20 cm) (Merck) and dichloromethane-methanol-acetic acid (92:8:2) as a mobile phase. The mix of four sterol standards was also applied onto the TLC plates as markers. For the visualization of the sterols, plates were sprayed with a 0.01% primuline (Sigma-Aldrich) solution and detected with a UV lamp. All fractions were separately scraped from the silica plates and placed in a glass tube. For the acidic hydrolysis of SG and ASG, 1.5 mL of a 0.5 N HCl methanolic solution was added to the silica powder, and for the basic hydrolysis of SE, 1.5 mL of 7.5% (w/v) KOH methanolic solution was used. After incubation at 85ºC for 2 h, the reaction was stopped with 1.5 mL of 0.9%

(w/v) NaCl, and the FS moieties were extracted twice with 3 mL of *n*-hexane and centrifuged at 5.000 rpm for 5 min in a JA-20 rotor (Beckman Coulter). The hexanic phases were collected in a new tube, mixed and evaporated to dryness. Samples were resuspended in 50µl of tetrahydrofuran (THF) and derivatized by adding 50 µl of BSTFA (Regis technologies). The mix was incubated for 30 min at 60ºC, evaporated to dryness and dissolved in 50 µl of isooctane. Samples were analyzed by gas chromatography-mass spectrometry (GC-MS) using an Agilent 7890A gas chromatograph equipped with a Sapiens-X5ms capillary column (30 m x 0.25 mm x 0.25µm) (Teknokroma) coupled with a 5975C mass spectrometer (Agilent). Peaks were integrated using MSD offline Data Analysis software (Agilent).

5.6 Photobleaching Recovery Assay

For fluorescence recovery after photobleaching (FRAP) analysis, the abaxial side of the agroinfiltrated leaf fragments was analyzed using the confocal laser microscope settings described above. A 7–10 µm region of interest (ROI) was defined and photobleached using full laser power (100%) for 4 s. To assess the recovery of fluorescence the entire focused cell area was monitored with a low laser power (15%) during 60 s. The image previous to the bleaching was acquired with the same laser power. The obtained data were normalized as previously described (Luu *et al.*, 2012), and a two-phase exponential equation was used to model the normalized data. GraphPad software (GraphPad Software Inc.) was used for FRAP curves fitting.

5.7 Subcellular fractionation

Approximately 10 g of *N. benthamiana* agroinfiltrated leaves from four independent plants were harvested, cut into small pieces and rapidly mixed with 15 mL of ice-cold homogenization buffer (HB) (0.3 M sucrose, 50 mM MOPS-KOH, 5 mM Na-EDTA, pH 7,5) (Larsson and Widell, 2003) supplemented immediately prior to its use with 0.5% (w/v) PVPP, 5 mM DTT, 5 mM ascorbic acid and a protease inhibitor cocktail (AEBSF, Bestatin, E-64, Leupeptin, Pepstatin A1,10-Phenanthroline; Sigma-Aldrich) prepared following the indications of the manufacturers. Leaf tissue was homogenized with an Ultra Turrax homogenizer (3x 30s pulse at medium speed and 30s on an ice bath).

The resulting homogenate was filtered through a nylon cloth and PMSF was added to a final concentration of 1mM. Then, the mixture was centrifuged twice at 10.000x*g* in a JA-20 rotor (Beckman Coulter) for 10 min at 4ºC to remove cell debris. The supernatant was recovered (total fraction, TF) and centrifuged at 100.000*g* in an SW40Ti rotor (Beckman Coulter) for 60 min at 4ºC to obtain a pellet (microsomal fraction, MF) and a supernatant (soluble fraction, SF). The MF was resuspended in 12 mL of resuspension buffer (0.3 sucrose, 5 mM potassium phosphate pH 7.8, 0.1 mM EDTA) supplemented immediately before use with 1 mM DTT and the protease inhibitor cocktail. Both the obtained MF and SF were centrifuged again twice at 100.000*g* for 60 min at 4ºC following the same process described above to obtain final the MF and SF fractions, keeping the pellet of the MF and the supernatant of the SF, and discarding the rest. The final MF was resuspended in 2 mL of resuspension buffer for further immunoblot analysis.

5.8 Immunoblot analysis

Protein concentrations were determined as previously described in *Bradford et al., 1976* (Bradford, 1976). Equivalent amounts of TF (around 20 ug of total protein), MF (around 5 ug of total protein) and SF (around 20 ug of total protein) from each *N. benthamiana* leaf sample were used for polyacrylamide gel electrophoresis on 10% SDS TGX™ FastCast™ Gel (Bio-Rad). After SDS-PAGE, the proteins were transferred to a 0.45 µm nitrocellulose membrane (Amersham, GE Healthcare) using the Trans-Blot® Turbo™ Transfer system (Bio-Rad). The primary antibody used was rabbit anti-GFP (Invitrogen) at a 1:1000 dilution in PBS-T (1% NaCl, 0.025% KCl, 0.18% Na_2HPO_4, 0.03% KH_2PO_4, 0.1% Tween 20, pH 7.4). Secondary donkey anti-rabbit IgG conjugated to horseradish peroxidase (GE Healthcare) was used at a 1:10000 dilution in PBS-T. Detection of protein bands was performed using the Amersham ECL Select Western Blotting Detection Reagent (GE Healthcare) according to the instructions of the supplier. Gels and membranes were visualized in the ChemiDoc™ Touch (Bio-Rad).

5.9 *In silico* analysis of protein structure

The 3D structure of the C22DES (NP_001234514.1) and C22DESΔ2-27 were modeled using Phyre2 fold recognition server (Kelley *et al.*, 2015) (http://www.sbg.bio.ic.ac.uk/phyre2). The tertiary structure was predicted using the Lanosterol 14α-Demethylase (Erg11p) of *Saccharomyces* cerevisiae [Protein Data Bank (PDB) ID: c4lxjA] as a template with 100% confidence. For membrane-protein interactions, the predicted 3D models were orientated using PPM web server from the Orientations of Proteins in Membranes (OPM) database (Lomize *et al.*, 2012) (https://opm.phar.umich.edu/ppm_server).

5.10 Protein sequence analysis

Solanum lycopersicum C22DES protein sequence was retrieved from the *SolGenomics Network* website (http://solgenomics.net/) and used as query to search for other plant species homologs using the BLAST tool on the *Phytozome* (https://phytozome.jgi.doe.gov) and the *EnsemblPlants* (http://plants.ensembl.org) websites. The accession numbers of the used homologs are listed in Table S1. Protein alignments were performed using *ClustalX v 2.0* (Larkin *et al.*, 2007) with default settings and the *GeneDoc* software was used for alignments visualization and manual edition.

For sequence logo generation, WebLogo web server was used (Crooks *et al.*, 2004) (https://weblogo.berkeley.edu/).

6. REFERENCES

Abell, B. M. *et al.* (1997) 'Role of the Proline Knot Motif in Oleosin Endoplasmic Reticulum Topology and Oil Body Targeting', *The Plant Cell*, 9(August), pp. 1481–1493.

Aboobucker, S. I. and Suza, W. P. (2019) 'Why Do Plants Convert Sitosterol to Stigmasterol?', *Frontiers in Plant Science*, 10(March), pp. 1–8. doi: 10.3389/fpls.2019.00354.

Bak, S. *et al.* (2011) *Cytochromes P450*, *The Arabidopsis Book*. doi: 10.1199/tab.0144.

Benveniste, P. (2004) 'Biosynthesis and Accumulation of Sterols', *Annual Review of Plant Biology*, 55(1), pp. 429–457. doi: 10.1146/annurev.arplant.55.031903.141616.

Berka, K. *et al.* (2013) 'Behavior of human cytochromes P450 on lipid membranes', *The Journal of Physical Chemistry B*, 117(39), pp. 11556–11564. doi: 10.1021/jp4059559.

Boutté, Y. and Grebe, M. (2009) 'Cellular processes relying on sterol function in plants', *Current Opinion in Plant Biology*, 12(6), pp. 705–713. doi: 10.1016/j.pbi.2009.09.013.

Bradford, M. M. (1976) 'A Rapid and Sensitive Method for the Quantitation of Microgram Quantities of Protein Utilizing the Principle of Protein-Dye Binding', *Analytical Biochemistry*, 72, pp. 248–254. doi: 10.1016/0003-2697(76)90527-3.

Bunt, G. and Wouters, F. S. (2004) 'Visualization of molecular activities inside living cells with fluorescent labels', *International Review of Cytology*, 237, pp. 205–277. doi: 10.1016/S0074-7696(04)37005-1.

Caño-Delgado, A. *et al.* (2004) 'BRL1 and BRL3 are novel brassinosteroid receptors that function in vascular differentiation in Arabidopsis', *Development*, 131(21), pp. 5341–5351. doi: 10.1242/dev.01403.

Carland, F., Fujioka, S. and Nelson, T. (2010) 'The Sterol Methyltransferases SMT1, SMT2, and SMT3 Influence Arabidopsis Development through Nonbrassinosteroid Products', *Plant Physiology*, 153(2), pp. 741–756. doi: 10.1104/pp.109.152587.

Clark, B. J. and Waterman, M. R. (1991) 'The hydrophobic amino-terminal sequence of bovine 17α-hydroxylase is required for the expression of a functional hemoprotein in COS 1 cells', *Journal of Biological Chemistry*, 266(9), pp. 5898–5904.

Crooks, G. E. *et al.* (2004) 'WebLogo: a sequence logo generator', *Genome Research*, 14, pp. 1188–1190. doi: 10.1101/gr.849004.1.

Danek Burgess, K. S. and Justice, J. B. (1999) 'Effects of Serine Mutations in Transmembrane Domain 7 of the Human Norepinephrine Transporter on Substrate Binding and Transport', *Journal of Neurochemistry*, 73(2), pp. 656–664.

Demel, R. A. and De Kruyff, B. (1976) 'The Function of Sterols in Membranes', *Biochemica et Biophysica Acta*, 457, pp. 109–132.

Desai, A. J., Dong, M. and Miller, L. J. (2016) 'Beneficial effects of β-sitosterol on type 1 cholecystokinin receptor dysfunction induced by elevated membrane cholesterol', *Clinical Nutrition*, 35(6), pp. 1374–1379. doi: 10.1016/j.clnu.2016.03.003.Beneficial.

Douglas, T. J. (1985) 'NaCl effects on 4-desmethylsterol composition of plasma-membrane-enriched preparations from citrus roots', *Plant, Cell and Environment*, 8, pp. 687–692.

Dufourc, E. J. (2008) 'The role of phytosterols in plant adaptation to temperature', *Plant Signaling and Behavior*, 3(2), pp. 133–134.

Earley, K. W. *et al.* (2006) 'Gateway-compatible vectors for plant functional genomics and proteomics', *The Plant Journal*, 45(4), pp. 616–629. doi: 10.1111/j.1365-313X.2005.02617.x.

Epand, R. M. (2006) 'Cholesterol and the interaction of proteins with membrane domains', *Progress in Lipid Research*, 45, pp. 279–294. doi: 10.1016/j.plipres.2006.02.001.

Epand, R. M. *et al.* (2010) *Cholesterol Interaction with Proteins That Partition into Membrane Domains : An Overview*, *Cholesteron Binding and Cholesterol Transport Proteins*. doi: 10.1007/978-90-481-8622-8.

Fantini, J. *et al.* (2016) 'Molecular mechanisms of protein-cholesterol interactions in plasma membranes : Functional distinction between topological (tilted) and consensus (CARC / CRAC) domains', *Chemistry and Physics of Lipids*. Elsevier Ireland Ltd, 199, pp. 52–60. doi: 10.1016/j.chemphyslip.2016.02.009.

Fantini, J. and Barrantes, F. J. (2013) 'How cholesterol interacts with membrane proteins : an exploration of cholesterol-binding sites including CRAC , CARC , and tilted domains', *Frontiers in Physiology*, 4(31), pp. 1–9. doi: 10.3389/fphys.2013.00031.

Ferrer, A. *et al.* (2017) 'Emerging roles for conjugated sterols in plants', *Progress in*

Lipid Research. Elsevier, 67, pp. 27–37. doi: 10.1016/j.plipres.2017.06.002.

Forés, O. *et al.* (2006) 'Arabidopsis thaliana expresses two functional isoforms of Arvp, a protein involved in the regulation of cellular lipid homeostasis', *Biochimica et Biophysica Acta*, 1761(7), pp. 725–735. doi: 10.1016/j.bbalip.2006.03.025.

Fujioka, S. and Yokota, T. (2003) 'Biosynthesis and Metabolism of Brassinosteroids', *Annual Review of Plant Biology*, 54, pp. 137–164. doi: 10.1146/annurev.arplant.54.031902.134921.

Gao, C. *et al.* (2014) 'Retention mechanisms for ER and Golgi membrane proteins', *Trends in Plant Science*. Elsevier Ltd, 19(8), pp. 508–515. doi: 10.1016/j.tplants.2014.04.004.

Gnanasekaran, T. *et al.* (2015) 'Heterologous expression of the isopimaric acid pathway in Nicotiana benthamiana and the effect of N-terminal modifications of the involved cytochrome P450 enzyme', *Journal of Biological Engineering*. Journal of Biological Engineering, 9(1), pp. 1–10. doi: 10.1186/s13036-015-0022-z.

Goehring, N. W. *et al.* (2010) 'FRAP analysis of membrane-associated proteins: Lateral diffusion and membrane-cytoplasmic exchange', *Biophysical Journal*. Biophysical Society, 99(8), pp. 2443–2452. doi: 10.1016/j.bpj.2010.08.033.

Goytia, E. *et al.* (2006) 'Production of Plum pox virus HC-Pro functionally active for aphid transmission in a transient-expression system', *Journal of General Virology*, 87(11), pp. 3413–3423. doi: 10.1099/vir.0.82301-0.

Griebel, T. and Zeier, J. (2010) 'A role for β-sitosterol to stigmasterol conversion in plant-pathogen interactions', *Plant Journal*, 63(2), pp. 254–268. doi: 10.1111/j.1365-313X.2010.04235.x.

Grosjean, K. *et al.* (2015) 'Differential Effect of Plant Lipids on Membrane Organization: hot features and specificities of phytosphingolipids and phytosterols', *Journal of Biological Chemistry*, 290, pp. 5810–5825. doi: 10.1074/jbc.m114.598805.

Grunwald, C. (1971) 'Effects of Free Sterols, Steryl Ester, and Steryl Glycoside on Membrane Permeability', *Plant Physiology*, 48(5), pp. 653–655. doi: 10.1104/pp.48.5.653.

Hartmann-Bouillon, M.-A. and Benveniste, P. (1978) 'Sterol biosynthetic capability of purified membrane fractions from maize coleoptiles', *Phytochemistry*, 17, pp. 1037–1042.

Hartmann, M.-A. (1998) 'Plant sterols and the membrane environment', *Trends in*

Plant Science, 3(5), pp. 170–175. Available at: http://www.cell.com/trends/plant-science/pdf/S1360-1385(98)01233-3.pdf.

Hernández-Gras, F. and Boronat, A. (2015) 'A hydrophobic proline-rich motif is involved in the intracellular targeting of temperature-induced lipocalin', *Plant Molecular Biology*. Springer Netherlands, 88(3), pp. 301–311. doi: 10.1007/s11103-015-0326-x.

Höfgen, R. and Willmitzer, L. (1988) 'Storage of competent cells for Agrobacterium transformation', *Nucleic Acids Research*, 16(20), p. 9877. Available at: https://www.ncbi.nlm.nih.gov/pmc/articles/PMC338805/pdf/nar00162-0496.pdf.

Im, S.-C. and Waskell, L. (2011) 'The interaction of microsomal cytochrome P450 reductase and cytochrome b5', *Archives of Biochemistry and Biophysics*, 507(1), pp. 144–153. doi: 10.1038/cdd.2010.172.MicroRNAs.

Jensen, K. and Møller, B. L. (2010) 'Plant NADPH-cytochrome P450 oxidoreductases', *Phytochemistry*. Elsevier Ltd, 71(2–3), pp. 132–141. doi: 10.1016/j.phytochem.2009.10.017.

Kagawa, N., Mihara, K. and Sato, R. (1987) 'Structural analysis of cloned cDNAs for polycyclic hydrocarbon-inducible forms of rabbit liver microsomal cytochrome P-450', *Journal of Biochemistry*, 101(6), pp. 1471–1479. doi: 10.1093/oxfordjournals.jbchem.a122017.

Kelley, L. A. *et al.* (2015) 'The Phyre2 web portal for protein modelling, prediction, and analysis', *Nature Protocols*. Nature Publishing Group, 10(6), pp. 845–858. doi: 10.1038/nprot.2015-053.

Klahre, U. *et al.* (1998) 'The Arabidopsis DIMINUTO/DWARF1 Gene Encodes a Protein Involved in Steroid Synthesis', *The Plant Cell*, 10(10), pp. 1677–1690. doi: 10.2307/3870765.

Larkin, M. A. *et al.* (2007) 'Clustal W and Clustal X version 2 . 0', *Bioinformatics*, 23(21), pp. 2947–2948. doi: 10.1093/bioinformatics/btm404.

Larsson, C. and Widell, S. (2003) 'Isolation of Plant Plasma Membranes and Production of Inside-Out Vesicles', *Methods in Biotechnology*, 11, pp. 159–166. doi: 10.1385/1-59259-028-4:159.

Lin, L.-J. *et al.* (2002) 'Steroleosin , a Sterol-Binding Dehydrogenase in Seed Oil Bodies 1', *Plant Physiology*, 128, pp. 1200–1211. doi: 10.1104/pp.010928.main.

Locuson, C. W. *et al.* (2007) 'CYP2C9 protein interactions with cytochrome b5: Effects

on the coupling of catalysis', *Drug Metabolism and Disposition*, 35(7), pp. 1174–1181.

Lomize, M. A. *et al.* (2012) 'OPM database and PPM web server: Resources for positioning of proteins in membranes', *Nucleic Acids Research*, 40, pp. 370–376. doi: 10.1093/nar/gkr703.

Luu, D.-T. *et al.* (2012) 'Fluorescence recovery after photobleaching reveals high cycling dynamics of plasma membrane aquaporins in Arabidopsis roots under salt stress', *The Plant Journal*, 69(5), pp. 894–905. doi: 10.1111/j.1365-313X.2011.04841.x.

Manford, A. G. *et al.* (2012) 'ER-to-Plasma Membrane Tethering Proteins Regulate Cell Signaling and ER Morphology', *Developmental Cell*. Elsevier Inc., 23(6), pp. 1129–1140. doi: 10.1016/j.devcel.2012.11.004.

Martínez-Garay, C. A. *et al.* (2014) 'A transmembrane serine residue in the Rot1 protein is essential for yeast cell viability', *Biochemical Journal*, 458, pp. 239–249.

Matsumoto, T. *et al.* (1986) 'Purification and characterization of three male-specific and one female-specific forms of cytochrome p-450 from rat liver microsomes', *Journal of Biochemistry*, 100(5), pp. 1359–1371. doi: 10.1093/oxfordjournals.jbchem.a121842.

Monk, B. C. *et al.* (2014) 'Architecture of a single membrane spanning cytochrome P450 suggests constraints that orient the catalytic domain relative to a bilayer', *Proceedings of the National Academy of Sciences*, 111(10), pp. 3865–3870. doi: 10.1073/pnas.1324245111.

Morikawa, T., Mizutani, M. and Ohta, D. (2006) 'Cytochrome P450 subfamily CYP710A genes encode sterol C-22 desaturase in plants', *Biochemical Society Transactions*, 34(6), pp. 1202–1205. doi: 10.1042/bst0341202.

Murakami, K., Mihara, K. and Omura, T. (1994) 'The Transmembrane Region of Microsomal Cytochrome P450 Identified as the Endoplasmic Reticulum Retention Signal', *Journal of Biochemistry*, 116, pp. 164–175.

Mustafa, G. *et al.* (2019) 'Influence of Transmembrane Helix Mutations on Cytochrome P450-Membrane Interactions and Function', *Biophysical Journal*. Biophysical Society, 116(3), pp. 419–432. doi: 10.1016/j.bpj.2018.12.014.

Nakagawa, T. *et al.* (2007) 'Improved Gateway Binary Vectors: High-Performance Vectors for Creation of Fusion Constructs in Transgenic Analysis of Plants', *Bioscience, Biotechnology, and Biochemistry*, 71(8), pp. 2095–2100. doi:

10.1271/bbb.70216.

Nelson, C. H. *et al.* (2016) 'Direct protein-protein interactions and substrate channelling between cellular retinoic acid binding proteins and CYP26B1', *FEBS letters*, 590(16), pp. 2527–2535. doi: 10.1097/CCM.0b013e31823da96d.Hydrogen.

Ott, R. G. *et al.* (2005) 'Flux of sterol intermediates in a yeast strain deleted of the lanosterol C-14 demethylase Erg11p', *Biochimica et Biophysica Acta*, 1735(2), pp. 111–118. doi: 10.1016/j.bbalip.2005.05.003.

Quon, E. *et al.* (2018) *Endoplasmic reticulum-plasma membrane contact sites integrate sterol and phospholipid regulation*, *PLoS Biology*. doi: 10.1371/journal.pbio.2003864.

Rosenhouse-Dantsker, A. (2017) *Insights Into the Molecular Requirements for Cholesterol Binding to Ion Channels*. 1st edn, *Sterol Regulation of Ion Channels*. 1st edn. Elsevier Inc. doi: 10.1016/bs.ctm.2017.05.003.

Sagara, Y., Barnes, H. J. and Waterman, M. R. (1993) 'Expression in Escherichia coli of Functional Cytochrome P450c17 Lacking Its Hydrophobic Amino-Terminal Signal Anchor', *Archives of Biochemistry and Biophysics*, pp. 272–278. doi: 10.1006/abbi.1993.1349.

Sato, T. *et al.* (1990) 'The amino-terminal structures that determine topological orientation of cytochrome P-450 in microsomal membrane', *The EMBO Journal*, 9(8), pp. 2391–2397. doi: 10.1002/j.1460-2075.1990.tb07414.x.

Di Scala, C. *et al.* (2017) *Relevance of CARC and CRAC Cholesterol-Recognition Motifs in the Nicotinic Acetylcholine Receptor and Other Membrane-Bound Receptors*. 1st edn, *Sterol Regulation of Ion Channels*. 1st edn. Elsevier Inc. doi: 10.1016/bs.ctm.2017.05.001.

Schaller, H. (2003) 'The role of sterols in plant growth and development', *Progress in Lipid Research*, 42, pp. 163–175. Available at: http://www.sciencedirect.com/science/article/pii/S0163782702000474%5Cnpapers2://publication/uuid/E01C48C7-E57A-4FAD-9057-1279540D4315.

Schaller, H. (2004) 'New aspects of sterol biosynthesis in growth and development of higher plants', *Plant Physiology and Biochemistry*, 42, pp. 465–476. doi: 10.1016/j.plaphy.2004.05.012.

Scheller, U. *et al.* (1994) 'Generation of the Soluble and Functional Cytosolic Domain of Microsomal Cytochrome P450 52A3', *The Journal of Biological Chemistry*, 269(17), pp. 12779–12783.

Schuler, M. A. *et al.* (2006) 'Arabidopsis cytochrome P450s through the looking glass: a window on plant biochemistry', *Phytochemistry Reviews*, 5, pp. 205–237. doi: 10.1007/s11101-006-9035-z.

Scott, E. E. *et al.* (2016) 'The Role of Protein-Protein and Protein-Membrane Interactions on P450 Function', *Drug Metabolism and Disposition*, 44(4), pp. 576–590.

Senthil-Kumar, M., Wang, K. and Mysore, K. S. (2013) 'AtCYP710A1 gene-mediated stigmasterol production plays a role in imparting temperature stress tolerance in Arabidopsis thaliana', *Plant Signaling and Behavior*, 8(2), pp. 1–5. doi: 10.4161/psb.23142.

Souter, M. *et al.* (2002) 'hydra mutants of Arabidopsis are defective in sterol profiles and auxin and ethylene signaling', *The Plant Cell*, 14(5), pp. 1017–1031. doi: 10.1105/tpc.001248.

Sparkes, I. A. *et al.* (2006) 'Rapid, transient expression of fluorescent fusion proteins in tobacco plants and generation of stably transformed plants', *Nature Protocols*, 1(4), pp. 2019–2025. doi: 10.1038/nprot.2006.286.

Šrejber, M. *et al.* (2018) 'Membrane-attached mammalian cytochromes P450 : An overview of the membrane's effects on structure, drug binding, and interactions with redox partners', *Journal of Inorganic Biochemistry*, 183, pp. 117–136. doi: 10.1016/j.jinorgbio.2018.03.002.

Stolowich, N. J. *et al.* (2002) 'Sterol carrier protein-2 : structure reveals function', *Cellular and Molecular Life Sciences*, 59, pp. 193–212.

Subramanian, M. *et al.* (2009) 'CYP2D6-CYP2C9 protein-protein interactions and isoform-selective effects on substrate binding and catalysis', *Drug Metabolism and Disposition*, 37(8), pp. 1682–1689. doi: 10.1124/dmd.109.026500.

Subramanian, M. *et al.* (2010) 'CYP2C9-CYP3A4 protein-protein interactions: Role of the hydrophobic N terminus', *Drug Metabolism and Disposition*, 38(6), pp. 1003–1009. doi: 10.1124/dmd.109.030155.

Szcesna-Skorupa, E., Straub, P. and Kemper, B. (1993) 'Deletion of a conserved tetrapeptide, PPGP, in P450 2C2 results in loss of enzymatic activity without a change in its cellular location', *Archives of Biochemistry and Biophysics*, 304(1), pp. 170–175.

Szczesna-Skorupa, E. *et al.* (1998) 'Mobility of cytochrome P450 in the endoplasmic reticulum membrane', *Proceedings of the National Academy of Sciences*, 95(25), pp. 14793–14798. doi: 10.1073/pnas.95.25.14793.

Vriet, C. *et al.* (2015) 'Evolutionary trails of plant steroid genes', *Trends in Plant Science*, 20(5), pp. 301–308. doi: 10.1016/j.tplants.2015.03.006.

Vriet, C., Russinova, E. and Reuzeau, C. (2013) 'From squalene to brassinolide: The steroid metabolic and signaling pathways across the plant kingdom', *Molecular Plant*, 6(6), pp. 1738–1757. doi: 10.1093/mp/sst096.

Wang, P., Hawes, C. and Hussey, P. J. (2017) 'Plant Endoplasmic Reticulum – Plasma Membrane Contact Sites', *Trends in Plant Science*. Elsevier Ltd, 22(4), pp. 289–297. doi: 10.1016/j.tplants.2016.11.008.

Whitaker, B. D. (1988) 'Changes in the steryl lipid content and composition of tomato fruit during ripening', *Phytochemistry*, 27(11), pp. 3411–3416.

Whitaker, B. D. (1991) 'Changes in lipids of tomato fruit stored at chilling and non-chilling temperatures', *Phytochemistry*, 30(3), pp. 757–761.

Wydro, M., Kozubek, E. and Lehmann, P. (2006) 'Optimization of transient Agrobacterium-mediated gene expression system in leaves of Nicotiana benthamiana', *Acta Biochimica Polonica*, 53(2), pp. 289–298.

Yabusaki, Y. *et al.* (1988) 'Genetically Engineered Modification of P450 Monooxygenases: Functional Analysis of the Amino-Terminal Hydrophobic Region and Hinge Region of the P450/Reductase Fused Enzyme', *DNA*, 7(10), pp. 701–711. doi: 10.1089/dna.1988.7.701.

Yu, X. *et al.* (2015) 'Dynamics of CYP51: Implications for function and inhibitor design', *Journal of Molecular Recognition*, 28(2), pp. 59–73. doi: 10.1002/jmr.2412.

7. SUPPLEMENTAL INFORMATION

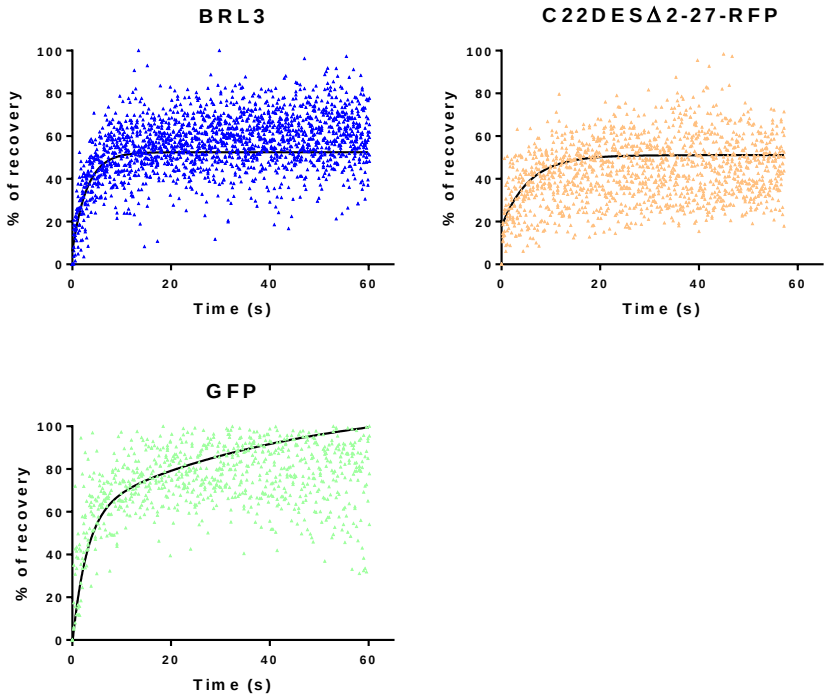

Figure S. 1 Complete data set of FRAP experiments. Plot showing each replicate (triangles in color) used to create the best fit curve, black lines represent the best fit for each the dataset calculated using the two-phase exponential association equation.

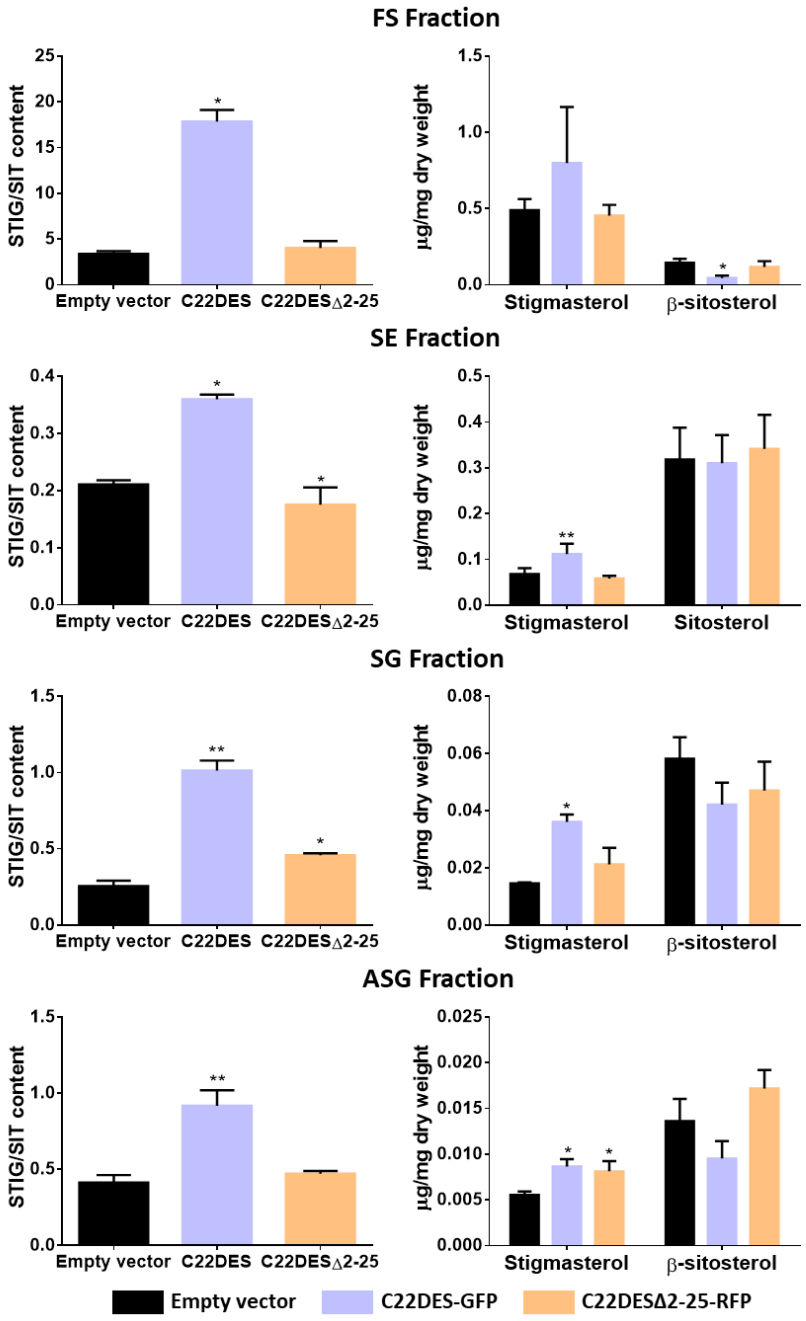

Figure S. 2 Intensive analysis of sterol composition. The left column shows the ratio of stigmasterol to β-sitosterol in each sterol fraction from *N. benthamiana* leaves expressing C22DES-GFP and C22DESΔ2-27-GFP. The right column shows the stigmasterol and β-sitosterol specific composition in each sterol fraction. Values are mean values ± SD of three technical replicates (*n*=3). Asterisks indicate significant differences among means relative to those in leaf samples expressing the empty vector (one-way ANOVA with Dunnett's multiple comparisons test, *p<0.05, **p<0.01).

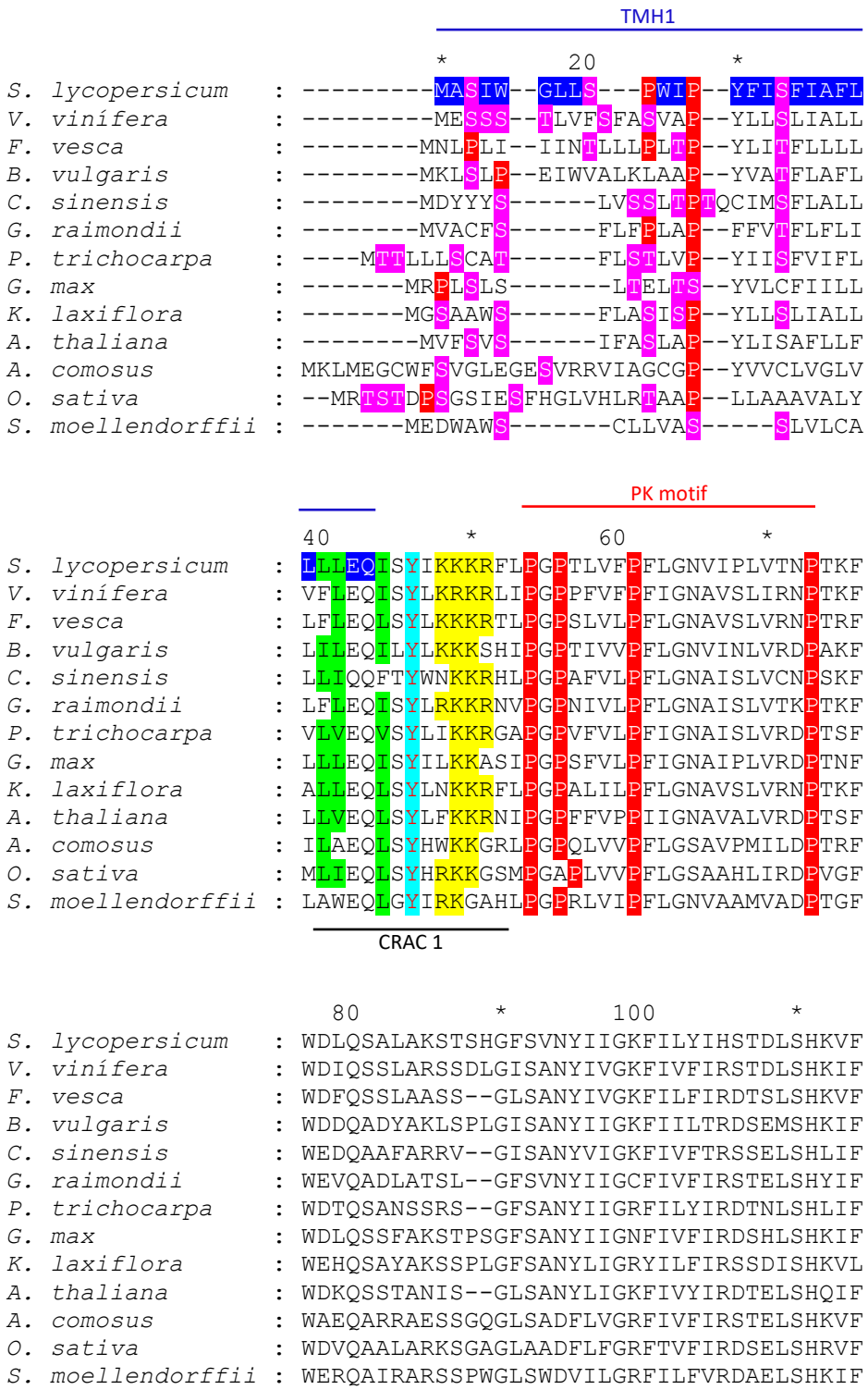
TMH1
PK motif
CRAC 1
S. lycopersicum
V. vinifera
F. vesca
B. vulgaris
C. sinensis
G. raimondii
P. trichocarpa
G. max
K. laxiflora
A. thaliana
A. comosus
O. sativa
S. moellendorffii

```
                          120         *       140         *
S. lycopersicum    : ANVRPDAFHLIGHPFGKKLFGEHNLIYMFGQEHKDLRR
V. vinífera        : ANVRPDAFHLVGHPFGKKLFGEHNLIYTMGQQHKDIRR
F. vesca           : ANVHPDAFTLVGHPFGKKLFGEHNLIYMTGQEHKDLRR
B. vulgaris        : ANVRPDAFQLIGHPFGKKLFGEHNMIYLYGQEHKDLRR
C. sinensis        : SNVRPDAFLLVGHPFGKKLFGEHNLIYMFGQDHKDLRR
G. raimondii       : ANVRPDAFLLVGHPFGKKLFGEHNMIYMFGQDHKDLRR
P. trichocarpa     : SNIRPDAFLLVGHPFGKKLFGEHNLIYKFGQEHKDLRR
G. max             : SNVRPDAFHLVGHPFGKKLFGQHNLIYMTGQVHKDLRR
K. laxiflora       : SNVSPDAFHLIGHPFGKKLFGDQNLIYMFGQDHKDLRR
A. thaliana        : SNVRPDAFHLIGHPFGKKLFGDHNLIYMFGEDHKSVRR
A. comosus         : ANVRPDAFHLIGHPFGKKLFGDHNLIYMFDQAHKDLRR
O. sativa          : ANVRADAFHVVSHPFGKKLFGEHNLVYLVGEEHKDLRR
S. moellendorffii  : ANVRPEAFHLVGHPFGKKLFGEENLIFMFGEEHKDLRR

                              160         *       180         *
S. lycopersicum    : RIAPNFTPKALGTYTDIQQRIIIKHFKSWLDEASK--S
V. vinífera        : RIAPNFTPRALAAYTSLQQVIILKHLMAWEALASK--A
F. vesca           : RITPNFTPKALATYTALQQTIILQHMKNWVSLASR--T
B. vulgaris        : RMAPNFTPKALATYTDIQQLVILKHLIRWTETGS----
C. sinensis        : RIAPNFTLRALSTYLSLQQIIILEHLKRWEKMCA---S
G. raimondii       : QIAPNFTPRALSTYTALQQIIILQHLKSWERLSSE--S
P. trichocarpa     : RIAPNFTPRALSTYTSLQQIIILKHLKKWESLSSN--S
G. max             : RIAPNFTPKALSTYTALQQIIILNHLKSWLNQSQA--P
K. laxiflora       : RMAPNFTPRALSSYISTQQRIIHRHLLSWVELCDK--S
A. thaliana        : QLAPNFTPKALSTYSALQQLVILRHLRQWEGSTS---G
A. comosus         : RIAPNFTPRALATYAALQQRVILAHLRKWLALSSASAS
O. sativa          : RIAPNFTPRALSTYAVIQQRVIISHLRRWLDRSASNGG
S. moellendorffii  : RLAPLFTWKALGVYVAIQERTIRKHIHRWLANSSSS-I
                     ---------
                     CARC 1

                                200         *       220
S. lycopersicum    : PNTPIPLRLLCRDMNLDTSQTVFVGPYLDGESRKRFNV
V. vinífera        : SPTPISLRLLCREMNLDTSQTVFVGPYLSQEARERFNR
F. vesca           : -NNGIALRFLIRDMNLDTSQTVFVGPYLALEARERFKS
B. vulgaris        : -NIPVKLRLLVREMNLETSQNVFAGSYLDKEARQRFKV
C. sinensis        : DKTPISLRLLVRDMNLETSQTVIVGPYLLQHARDKFKS
G. raimondii       : PGKPISLRLLARDMNLETSQTVFVGRYLSHEARDKFRD
P. trichocarpa     : PNKSISLRLLVRDMNLETSQTVFVGPYLSEEERERFKL
G. max             : DSHSIPLRILARDMNLQTSQTVFVGPYLGPKARERFER
K. laxiflora       : RPDPIKLRFLVRDMNLETSQTVFVGPYLTPEARHKFKQ
A. thaliana        : GSRPVSLRQLVRELNLETSQTVFVGPYLDKEAKNRFRT
A. comosus         : ASEPISLRLLCRDMNLETSQTVFAGPYLSREARERFNR
O. sativa          : KAEPI--RVPCRDMNLETSQTVFVGPYLTEKARERFDR
S. moellendorffii  : HQRPVAMRSLCRDMNLETSQEVFVGPYLDPRAREHFTR
                                          ---------
                                          CRAC 2
```

```
                        *       240         *       260
S. lycopersicum    : DYNYFNVGLMKLPVDLPGFAFRNARLAVGRLVDTLSVC
V. vinífera        : DYNLFNVGLMKLPFDLPGFAFREARLAVDRLIKTLAGC
F. vesca           : DYNFFNVGLMKLPVDLPGTAFRNARLAVGRLVETLAGC
B. vulgaris        : DYNYFNLGVIALPIDLPGFAFRRARLAVDRLVGALTNC
C. sinensis        : DYTLFNVGLMKLPIDLPGFAFRNARLAVERLVQTLAVC
G. raimondii       : DYNLFNTGLMKLPFDLPGFAFRNARLAVEQLVETLGDC
P. trichocarpa     : DYNMFNVGLMKLPIDLPGFAFRNARLAVDRLAETLSEC
G. max             : DYFLFNVGLMKLPFDFPGTAFRNARLAVDRLIAALGTC
K. laxiflora       : DYNLFNLGLLSLPFDLPGSSFRKARHAATRLVKTLADC
A. thaliana        : DYNLFNLGSMALPIDLPGFAFGEARRAVKRLGETLGIC
A. comosus         : DYNLFNVGLMALPFDLPGSAFRRARLAVSRLT--LAGA
O. sativa          : DYNLFNVGFITLPVDLPGFAFRRARLAGARLMHTLGDC
S. moellendorffii  : DYNLFNLGLLALPIDLPGFAFRRAKQAVERLVATLGEC


                           *       280         *       300
S. lycopersicum    : VEQSLNKMKNE-EEPTCLIDFWMQENLREINEAKINGL
V. vinífera        : TDDSKATMEAG-EEPRCLIDFWMQETLREIAAATDSGE
F. vesca           : AKQSRAKMEEEKQEPTCLIDFWMQEMVKELNAGGG---
B. vulgaris        : VEQSKKKMLAD-EEPKCLVDYWMQDMVREERESDTPLE
C. sinensis        : TRESKIRMAEGGE-PSCLIDFWMQEQAKEVAAARAAGR
G. raimondii       : ATQSKKRMSEGDE-PSCLIDFWMQETVREIAESKTA--
P. trichocarpa     : VMKSKKKMDNNHE-PSCLIDFWMQEMLKEISAAKSAGE
G. max             : TEMSKARMKAGGE-PSCLVDYWMQDTLREIEEAKLAGE
K. laxiflora       : ASQSRSNMLTGAE-PTCLVDFWMQDLLRETAEDPNHQ-
A. thaliana        : AGKSKARMAAGEE-PACLIDFWMQAIVAENPQ------
A. comosus         : AAASKARMRAGAE-PTCLVDFWMQNSLREIAEAEAEAE
O. sativa          : ARQSRQRMLGGGE-PECLLDYLMQETVREIDEATAAGL
S. moellendorffii  : AARSKRRMSTPGEQPACLMDFWMAETLAEIRAARESGS


                                *       320         *       340
S. lycopersicum    : QKPFQYSNKELGGYLFDFLFAAQDASTSALLWAIVLLD
V. vinífera        : PLPPHSGNAEIGGHLFDFLFAAQDASTSSLLWAVTLLD
F. vesca           : ----DISDVELGAHLFDFLFAAQDASTSSLLWAVALLD
B. vulgaris        : FQPPNCSNREIGAHVFDFLFAAQDASTSSLLWAVTLLD
C. sinensis        : PPPLHSEDHEIAGHLFDFLFAAQDASTSSLLWSVTLLD
G. raimondii       : --PPRSSDVEIGSYLFDFLFAAQDASTSSLLWAVTLLD
P. trichocarpa     : PVPPHTSEAEIGGHLFDFLFAAQDASTSSLLWAVALLD
G. max             : MPPPFSTDVEIGGYLFDFLFAAQDASTSSLLWAVALLD
K. laxiflora       : -PPPHSSDLELGGHLFDFLFAAQDASTSSLLWAVTLLS
A. thaliana        : --PPHSGDEEIGGLLFDFLFAAQDASTSSLLWAVTLLD
A. comosus         : A----ADAEEVGGHLFDFLFAAQDASTSSLCWAVALLD
O. sativa          : PPPPHTSDVEVGALLFGFLFAAQDASTSSLCWAVSALD
S. moellendorffii  : PPPPHSSDRQVGQHIFDFLFAAQDASTSSLVWVCALLE
```

```
                              *       360         *       380
S. lycopersicum    : SHPQVLEKVRSDVARFWSPES---------EEPLTAEM
V. vinífera        : SHPEVLAKVREEVAGIWSPES---------DTLITAEQ
F. vesca           : SHPEVLAKVREEVAGVWDPES---------NELITAEQ
B. vulgaris        : SHPDVLMKVRKEVETIWKVDS---------NTLITQDQ
C. sinensis        : SHPHVLSKVREEVSRIWSPES---------DKLITADQ
G. raimondii       : SHPDVLRRVREEVSRIWSPES---------DTLISAEQ
P. trichocarpa     : SNPEVLLKVRKEVSSFWSPES---------DGLINTEQ
G. max             : SHPEVLAKVRTEVAGIWSPES---------DELITADM
K. laxiflora       : SHPDILSRVRAEVSNVYTPLSS--------DTLLTYDD
A. thaliana        : SEPEVLNRVREEVAKIWSPES---------NALITVDQ
A. comosus         : AHPEVLARVRDEVAARWSPES---------GEPIPAEA
O. sativa          : SHPNVLARVRAEVAALWSPES---------GEPITAEM
S. moellendorffii  : SNPQVLGKILDEQRSLRRGGEGEFGSNFDPATPVGSEL


                                   *       400         *
S. lycopersicum    : LREMKYLEAVAREIIRIRAPATMVPHIAGEEFRLTEDY
V. vinífera        : LREMKYTEAVAREVVRIRAPATMVPHIAGEDFQLTESY
F. vesca           : LARMRYTHAVAREVVRYRAPATMVPHIAAVDFPLTETY
B. vulgaris        : LASMKYTQAVAREVVRYRAPATLVPHLAREDFQLTEKY
C. sinensis        : VREMNYTQAVAREVLRYRAPATLVPHIAVQDFPLTESY
G. raimondii       : LREMKYTQAVAREVIRYRPPATLVPHIAMKDFPLTESY
P. trichocarpa     : LREMKYTQAVAREVLRYRAPATLVPHVAMKEFALTESY
G. max             : LREMKYTLAVAREVLRFRPPATLVPHIAAESFPLTESY
K. laxiflora       : LRQLKYTEAVAREVVRYRAPATLAPHVAAQPFQLTETY
A. thaliana        : LAEMKYTRSVAREVIRYRPPATMVPHVAAIDFPLTETY
A. comosus         : LREMRYTEAVAREVVRLRPPATMVPHIAGEPFPLTEWY
O. sativa          : MSAMKYTQAVAREVVRYHPPATLVPHIAVEAFQLTAQY
S. moellendorffii  : LREMKYTEMVVKEVLRYRPPATMVPHIASVDFPITDSY
                     CRAC 3/ CARC 2


                   420         *       440         *
S. lycopersicum    : VIPKGTIVFPSVFDSSFQGFPEPEKFEPDRFMEE-RQE
V. vinífera        : TIPKGTIVFPSVFESSFQGFPDPERFEPERFMEH-RQE
F. vesca           : TVPKGTIVFPSAYESCFQGFTEPERFDPDRFSVE-RQE
B. vulgaris        : IVPKGTIVFPSPYESSFQGFTNPENFDPDRFFLEERRE
C. sinensis        : TIPKGTIVFPSVYESSFQGFSEPDRFDPERFSEE-RQE
G. raimondii       : TIPKGTIVFPSVYESSFQGFTEADRFEPERFSED-RQE
P. trichocarpa     : TIPKGTIVFPSVLDSSFQGFTKPDRFDPDRFSED-RQE
G. max             : TIPKGAIVFPSVFESSFQGFTEPDRFDPNRFSEE-RQE
K. laxiflora       : TVPKGTIVFPSLFESSFQGFTDPTQFDPDRFLDG-RQE
A. thaliana        : TIPKGTIVFPSVFDSSFQGFTEPDRFDPDRFSET-RQE
A. comosus         : TVPKGAIVFPSVYESSFQGFPDPARFDPDR-FSDERQE
O. sativa          : TIPKGTMVFPSVYESSFQGFQDADAFDPDRFFSEARRE
S. moellendorffii  : TVPKGAIVFPSLLESSFQGFREPYAFDPDRFSAA-RLE
```

```
                          460         *       480         *
S. lycopersicum    : ERVYKKNFLAFGAGPHACVGQKYAINHLMLFIAMFTAL
V. vinífera        : DRLYKKNFLAFGAGAHQCVGQRYAINHLVLFIAMFTSL
F. vesca           : DRVYRKNYLAFGAGAHQCVGQRYALNHLVLFMAMFATL
B. vulgaris        : DQLYRRNYLVFGAGGHQCVGQRYALNLLVLFIAMFSTL
C. sinensis        : GQVYKRNFLVFGAGAHQCVGQRYALNHLVLFIALFATL
G. raimondii       : EVIFKRNYLAFGAGPHQCVGQRYALNHLVLFIAMFVTV
P. trichocarpa     : DQLFKKNFLTFGAGAHQCVGQRYALNHLVLFIAMFCAL
G. max             : DQIFKRNFLAFGAGPHQCVGQRYAFNHLVLFIALFTTL
K. laxiflora       : DRLYKKNYLAFGAGPHQCVGQRYAINHLVLFIAMFTFV
A. thaliana        : DQVFKRNFLAFGWGPHQCVGQRYALNHLVLFIAMFSSL
A. comosus         : DRVYKRNFLAFGAGPHQCVGQRYAINHLVLFIALFASL
O. sativa          : DVVYKRNFLAFGAGPHQCVGQRYALNHLVIFMALFVSL
S. moellendorffii  : DVAFKRNWLLFGAGSHQCLGQRYAINHLVLFTALFSSM
                                            CARC 3

                             500         *       520         *
S. lycopersicum    : IDFKRHKTDGCDDISYIPTIAPKDDCKVFLAHRCTR--
V. vinífera        : VDFKRHRTDGCDDIAYVPTICPKDDCKVYLSRRCARYP
F. vesca           : LDFKRHRTDGCDDITFVPTICPKDDCKVFLSMR--RFP
B. vulgaris        : IEFKRHRTDGCDDLAFCPTICPKDDCLVSLSRRCAKFP
C. sinensis        : LDFKRDRTDGCDDITYSPTITPKDGCKVFLSKQ-----
G. raimondii       : LDFKRHRTEGCDEIMYCPTISPKDGCRVSLSRRCPRYP
P. trichocarpa     : LDFKRYRADGCDDIVYNPTICPKDGCIVSLKRRGTRYP
G. max             : IDFKRDESDGCDDIVYVPTICPKDDCRVFLSKRCARYP
K. laxiflora       : VDFERPISDGCDDIEYVPTICPKDDCRVFLKLRQGW--
A. thaliana        : LDFKRLRSDGCDEIVYCPTISPKDGCTVFLSRRVAKYP
A. comosus         : LDFKRNRTDGCDDIAYVPTIVPKDDCQVYLSQRCARFP
O. sativa          : VDFRRERTEGCDVPVYMPTMVPRDGCVVYLKQR-----
S. moellendorffii  : VEWERVRTPGCDEILYVPTIVPRDGCLVTLKPRRGDDD


                               540
S. lycopersicum    : ----------------
V. vinífera        : SFS-------------
F. vesca           : ALTLQ-----------
B. vulgaris        : SLSLD-----------
C. sinensis        : ----------------
G. raimondii       : NLTLN-----------
P. trichocarpa     : NLSLE-----------
G. max             : SFPSVEDFVK------
K. laxiflora       : ----------------
A. thaliana        : NFS-------------
A. comosus         : SF--------------
O. sativa          : ----------------
S. moellendorffii  : RRGREEREIEETSTES
```

Figure S. 3 Multiple protein sequence alignment of C22DES from different plant species. TMH1 domain is shown in blue; prolines (P) are shown in red; serine (S) and threonine (T) residues are shown in magenta; branched-chain amino-acids [leucine (L), valine (V) and isoleucine (I)] from the CRAC

motif are shown in green; tyrosines (Y) from CRAC motif are shown in cyan; and dibasic residues [arginine (R) and lysine (K)] from CRAC motif are shown in yellow

Specie	Family	Gene code	UniProt code
Amaranthus hypochondriacus	Amaranthaceae	AHYPO_007104-RA	-
Beta vulgaris	Amaranthaceae	BVRB_001630	A0A0J8B8L5_BETVU
Amborella trichopoda	Amborellaceae	AMTR_s00141p00052250	W1PIR2_AMBTC
Daucus carota	Apiaceae	DCAR_027922	A0A175YLR6_DAUCA
Helianthus annuus	Asteraceae	OTG29107	A0A251V0G5_HELAN
Arabidopsis thaliana	Brassicaceae	AT2G34500	C7101_ARATH
Arabidopsis lyrata	Brassicaceae	AL4G30470	D7LH13_ARALL
Boechera stricta	Brassicaceae	Bostr.23794s0661	-
Brassica oleracea	Brassicaceae	Bol027351	-
Brassica rapa	Brassicaceae	BRARA_E00976	A0A397Z8B6_BRACM
Capsella grandiflora	Brassicaceae	Cagra.7352s0002	-
Capsella rubella	Brassicaceae	CARUB_v10024737mg	R0FZJ8_9BRAS
Eutrema salsugineum	Brassicaceae	EUTSA_v10016547mg	V4M706_EUTSA
Brassica napus	Brassicaceae	BnaC04g10740D	-
Ananas comosus	Bromeliaceae	ACMD2_08728	A0A199UT02_ANACO
Carica papaya	Caricaceae	evm.model.supercontig_166.19	-
Kalanchoe fedtschenkoi	Crassulaceae	Kaladp0840s0006	-
Kalanchoe laxiflora	Crassulaceae	Kalax.0554s0026	-
Cucumis sativus	Cucurbitaceae	Csa_6G522820	A0A0A0KKM3_CUCSA
Manihot esculenta	Euphorbiaceae	Manes.01G172800	A0A2C9WLR2_MANES
Glycine max	Fabaceae	Glyma.13G217400	I1M1E5_SOYBN
Medicago truncatula	Fabaceae	Medtr2g019640	Q2MIZ9_MEDTR
Phaseolus vulgaris	Fabaceae	Phvul.006G163800	V7BPJ1_PHAVU
Trifolium pratense	Fabaceae	Tp57577_TGAC_v2_mRNA36715	-
Vigna angularis	Fabaceae	LR48_Vigan09g221000	A0A0L9VES4_PHAAN
Lupinus angustifolius	Fabaceae	TanjilG_20227	A0A1J7GN88_LUPAN
Physcomitrella patens	Funariaceae	Pp3c1_11690V3	A0A2K1L7U2_PHYPA
Klebsormidium nitens	Klebsormidiaceae	KFL_006910060	A0A1Y1IJF8_KLENI
Spirodella polyrhiza	Lemnaceae	Spipo8G0071000	-
Linum usitatissimum	Linaceae	Lus10028129	-
Gossypium raimondii	Malvaceae	B456_009G155800	A0A0D2QGW2_GOSRA
Theobroma cacao	Malvaceae	TCM_029501	A0A061GD05_THECC
Marchantia polymorpha	Marchantiaceae	MARPO_0103s0038	A0A2R6WDZ6_MARPO
Eucalyptus grandis	Myrtaceae	Eucgr.D00302	A0A059CC63_EUCGR
Mimulus guttatus	Phrymaceae	Migut.H01366	A0A022RRY1_ERYGU
Brachypodium stacei	Poaceae	Brast01G342000	-
Oryza sativa	Poaceae	Os01g11270	A2WLZ4_ORYSI

Setaria italica	Poaceae	Seita.9G366300	K4A8R3_SETIT
Setaria viridis	Poaceae	Sevir.9G372000	-
Sorghum bicolor	Poaceae	Sobic.003G021900	C5XL37_SORBI
Triticum aestivum	Poaceae	IWGSC	A0A3B6IYP2_WHEAT
Aegilops tauschii	Poaceae	AET3Gv20318700	-
Hordeum vulgare	Poaceae	IBSC_v2	G5EKM8_HORVU
Fragaria vesca	Rosaceae	mrna30586.1-v1.0-hybrid	-
Malus domestica	Rosaceae	MDP0000945293	-
Citrus sinensis	Rutaceae	CISIN_1g046882mg	A0A067GRV9_CITSI
Citrus clementina	Rutaceae	CICLE_v10014973mg	V4TQW1_9ROSI
Populus trichocarpa	Salicaceae	Potri.004G131700	B9H3Z9_POPTR
Salix purpurea	Salicaceae	SapurV1A.0560s0090	-
Solanum lycopersicum	Solanaceae	NP_001234514	A9QPL5_SOLLC
Nicotiana benthamiana	Solanaceae	NbS00037674g0002	-
Solanum tuberosum	Solanaceae	PGSC0003DMT400054511	M1BWG7_SOLTU
Nicotiana attenuata	Solanaceae	NIATTr2	A0A1J6IMN0_NICAT
Sphagnum fallax	Sphagnaceae	Sphfalx0121s0046	-
Vitis vinifera	Vitaceae	VIT_10s0003g03170	F6HLR0_VITVI

Table S. 1 List of C22DES proteins used for sequence analysis.

		Sample		
Steryl lipid	**Sterol moiety**	**Empty vector**	**C22DES-GFP**	**C22DESΔ2-27-RFP**
Free sterol	Stigmasterol	0.489 ± 0.074	0.800 ± 0.366	0.454 ± 0.070
	β-sitosterol	0.145 ± 0.025	0.044 ± 0.017	0.118 ± 0.037
Steryl ester	Stigmasterol	0.067 ± 0.013	0.112 ± 0.023	0.058 ± 0.006
	β-sitosterol	0.319 ± 0.069	0.310 ± 0.061	0.342 ± 0.074
Steryl glycoside	Stigmasterol	0.0146 ± 0.0003	0.0361 ± 0.0025	0.0212 ± 0.0057
	β-sitosterol	0.0582 ± 0.0075	0.0421 ± 0.0077	0.0471 ± 0.0101
Acylated steryl glycoside	Stigmasterol	0.0055 ± 0.0003	0.0086 ± 0.0004	0.0081 ± 0.0011
	β-sitosterol	0.0136 ± 0.0024	0.0095 ± 0.0019	0.0172 ± 0.0020

Table S. 2 Stigmasterol and β-sitosterol specific composition in each sterol fraction. Values are expressed as mean µg sterol (recovered from steryl lipid) per mg of dry weight ± SD of three technical replicates (*n*=3).

Use	Nº	Name	Primer sequence
Cloning for C-terminal fusion protein generation	1	attb1 C22DES Fw	**GGGGACAAGTTTGTACAAAAAAGCAGGCT**TCATGGCATCCATTTGGGGTTTGTTATC
	2	attb2-C22DES Rv	**GGGGACCACTTTGTACAAGAAAGCTGGGT**CTCGTGTGCACCTGTGTGCAAG
	3	attb2 TMH1 Rv	**GGGGACCACTTTGTACAAGAAAGCTGGGT**CAAGAAAACGCTTCTTCTTGATGTAAGAGAT
	4	attb1 PK Fw	**GGGGACAAGTTTGTACAAAAAAGCAGGCT**TCATGATCTCTTACATCAAGAAGAAGCGT
	5	attb2 PK Rv	**GGGGACCACTTTGTACAAGAAAGCTGGGT**CTGATTGAAGGTCCCAGAATTTAGTTGG
	6	attb1 C22DES aa28 Fw	**GGGGACAAGTTTGTACAAAAAAGCAGGCT**TCATGATCTCTTACATCAAGAAGAAGCGTTTTCTTC

Table S. 3 Primers used for GFP and RFP C-terminal fusion cloning. ATTB recombination sites are shown in bold, and the ATG start codons are underlined.

Construct	Template	Primers	Vector	Cloning method	Bacterial selection
35S:C22DES	cDNA	-	pKGW	Gateway®	Sp
C22DES-GFP	35S:C22DES	1,2	pEarleyGate103	Gateway®	Kan
TMH1-GFP	35S:C22DES	1,3	pEarleyGate103	Gateway®	Kan
PK-GFP	35S:C22DES	4,5	pEarleyGate103	Gateway®	Kan
TMH+PK-GFP	35S:C22DES	1,5	pEarleyGate103	Gateway®	Kan
C22DESΔ2-27-RFP	35S:C22DES	6,2	pGWB454	Gateway®	Sp

Table S. 4 Constructions and cloning details.

CHAPTER II

Unraveling the stigmasterol role in tomato plants

1. ABSTRACT

The C22-unsaturated sterols, which contain a double bond at the C22 position in the lateral chain, are found both in fungi and plants. In plants, CYP710 family proteins [or so-called sterol C22-desaturase (C22DES)] are the responsible enzymes of the described C22-desaturation reaction, acting in the final step of the sterol pathway leading to the conversion of β-sitosterol and campesterol into stigmasterol and brassicasterol, respectively. Increased *C22DES* transcript levels and the concomitant increase in stigmasterol concentration have been recurrently found in plants under different biotic and abiotic stresses. Several studies have proposed the C22DES role in conferring tolerance to unfavorable temperatures, salt conditions, and even pathogens attack. We have generated transgenic *S. lycopersicum* cv. Micro-Tom with altered stigmasterol levels by the overexpression, amiRNA-mediated silencing, and knock-out of *C22DES* gene. The lack of stigmasterol was confirmed in the *C22des*$^{-}$ knock-out line, and therefore, we have demonstrated that stigmasterol is not essential for completing the life cycle of tomato plants. However, we found that this mutant presented some phenotypic differences with respect to the WT, among them, its reduced plant size. Furthermore, we also report a severe problem with seed germination, which was correlated with abnormal embryo development. Finally, we have also observed increased susceptibility to *Botrytis cinerea* infection of the *C22des*$^{-}$ mutant plants.

Unraveling the stigmasterol role in tomato plants

LAURA GUTIÉRREZ-GARCÍA[1], MONTSERRAT ARRÓ[1,2], TERESA ALTABELLA[1,4], ALBERT FERRER[1,2] AND ALBERT BORONAT[1,3]

[1]CENTER FOR RESEARCH IN AGRICULTURAL GENOMICS (CSIC-IRTA-UAB-UB), CAMPUS UAB, BELLATERRA, BARCELONA; [2]DPTO DE BIOQUÍMICA Y FISIOLOGÍA, [3]DPTO DE BIOQUÍMICA Y BIOMEDICINA MOLECULAR, [4]DPTO DE BIOLOGÍA, SANIDAD Y MEDIO AMBIENTE, UB, BARCELONA.

2. INTRODUCTION

Sterols are lipid molecules belonging to the vast and heterogeneous family of isoprenoids that have essential functions in all eukaryotes, whether they are *de novo* synthesized or taken up from the environment (Hartmann, 1998; Benveniste, 2004). They are crucial structural components of cell membranes that determine their physicochemical properties, as fluidity and permeability (Hartmann, 1998; Ferrer *et al.*, 2017). In addition to this structural role, sterols also play a role as regulators of plant cell growth and development (Diener *et al.*, 2000; Schaller, 2003, 2004; Carland, Fujioka and Nelson, 2010), and some specific types of sterols are also precursors in the biosynthesis of brassinosteroids, a class of plant hormones that play diverse roles in plant growth and developmental processes (Choe *et al.*, 1999; Nomura *et al.*, 1999). Cholesterol and ergosterol are by far the major sterols in animals and fungi, respectively. In contrast, plants produce a complex mixture of sterols that mainly differ in the nature of their side chain at position C17 and the number and position of double bonds in the sterol backbone or the lateral chain (Ferrer *et al.*, 2017).

The sterol biosynthetic pathway responsible for the specific plant sterols formation (campesterol, β-sitosterol, and stigmasterol) is essentially linear except for the occurrence of two critical bifurcation steps: the cycloartenol is the first metabolite which can be transformed by the action of two different enzymes leading to the cholesterol branch (SSR2) or the phytosterols branch (SMT1); and the second bifurcation step occurs when reaching the reaction leading to 24-methylene lophenol, which can be further transformed into 24-ethylidene lophenol by the action of a sterol-methyltransferase (SMT2/3) (Schaller, 2003; Benveniste, 2004).

The later reaction involves the bifurcation of the sterol pathway into the two branches leading to the formation of 24-methyl sterols (campesterol and, in *Brassicaceae* species, brassicasterol) and 24-ethyl sterols (β-sitosterol and stigmasterol). The ratio of 24-methyl sterols to 24-ethyl sterols, determined by the activity of SMTs, is important for proper plant growth and development (Schaller, Bouvier-Navé and Benveniste, 1998; Carland *et al.*, 2002; Carland, Fujioka and Nelson, 2010).

Stigmasterol and brassicasterol are both C22-unsaturated sterols derived from β-sitosterol and campesterol, respectively. The C22-unsaturated sterols, containing a double bond at the C22 position in the side chain, are found both in fungi and plants (Morikawa *et al.*, 2006). In plants, CYP710 family proteins also referred to as sterol C22-desaturases (C22DES), are the responsible enzymes of the C22-desaturation reaction, which is the final step of the 24-ethyl sterols branch pathway.

The stigmasterol to β-sitosterol (STIG/SIT) ratio was described to be altered during different stages of plant development and in response to several biotic and abiotic stresses. A dramatic increase in the STIG/SIT ratio was found during ripening of wild type tomato fruits (Chow and Jen, 1978) which was correlated with a marked rising of *C22DES* transcript levels (Whitaker and Gapper, 2008). However, these changes were much less marked in aging fruits of *nor* and *rin* ripening mutants, indicating that this enzyme may have a specific role during tomato fruit ripening (Whitaker, 1988; Whitaker and Gapper, 2008). Nevertheless, the biological relevance of specific changes in STIG/SIT ratios during plant growth and development is currently unknown.

Stigmasterol levels are altered in response to low temperatures. This might result in substantially different packing and fluidity of membrane bilayer lipids and suggests a role for stigmasterol in the tolerance to unfavorable temperatures (Whitaker, 1991; Senthil-Kumar, Wang and Mysore, 2013). Several authors have also reported the stigmasterol raising-up after salt exposure (Douglas and Walker, 1983; Mansour, Hasselt and Kuiper, 1994). Indeed, stigmasterol treatment of flax seeds improved its salt tolerance (Hashem *et al.*, 2011).

Since the identification of *C22DES* gene for the first time in *Arabidopsis thaliana* and *Solanum lycopersicum* (Morikawa *et al.*, 2006), several studies have been carried out

to further characterize the biological role of this enzyme. The involvement of C22DES and, consequently, of stigmasterol in biotic stress tolerance has been addressed in a large range of plant pathogens, such as *Pseudomonas syringae, Botrytis cinerea, Golovinomyces cichoracearum,* and even *Phytophtora infestans* by using *A. thaliana* as a plant model (Zimmermann *et al.*, 2004; Fabro *et al.*, 2008; Wang *et al.*, 2012). Despite the *C22DES* transcript levels, as well as the STIG/SIT ratio was increased in all *P. syringae* (*Pst*)-inoculated plants, the susceptibility results presented some discrepancies among the different studies. On the one hand, Griebel and Zeier (2010) postulated that the increased STIG/SIT after pathogen inoculation attenuated pathogen-induced expression of the defense regulator flavin-dependent monooxygenase 1, promoting disease susceptibility. In contrast, Wang et al. (2012) proposed that the accumulation of stigmasterol in cell membranes makes them less permeable and hence it reduces the nutrient efflux to the apoplast, thus preventing pathogen growth. The latter attributed the discrepancies of their results to the differences in the Arabidopsis mutant lines used, since the first authors used mutant lines with reduced C22DES expression, unlike the null mutant used in the later study. This research group also demonstrated the increased susceptibility to *P. syringae* of *Nicotiana benthamiana* and *S. lycopersicum* plants with reduced transcript levels of *C22DES* gene obtained by virus-induced gene silencing (VIGS) (Wang *et al.*, 2012). Related with the biotic stress responses, the antifungal properties of some sterols were also proven recently, being stigmasterol the most efficient (Choi *et al.*, 2017).

However, more studies will be needed to clarify the role of stigmasterol in plant growth, development, and responses to stress. However, the fact that *A. thaliana* contains 4 genes encoding C22DES complicates the study of the mutants because of the gene redundancy. This is in contrast to several crop model species, such as *S. lycopersicum* that is known to contain a single copy of *C22DES* (Morikawa *et al.*, 2006), which makes this plant species a suitable organism to elucidate the role of this enzyme.

All these considerations made us to undertake this study aimed at the generation of transgenic tomato (*S.lycopersicum* cv. Micro-Tom) lines with altered STIG/SIT ratios by the overexpression, silencing and knock-out of the single *C22DES* gene, as a first step toward the elucidation of the biological role of stigmasterol biosynthesis in tomato growth and development as well as in the adaptation to stress conditions.

3. RESULTS

3.1 Transcriptional profiling of C22DES gene in tomato plants

To get a better understanding of the stigmasterol role in tomato plants, we first investigated the expression profile of the *C22DES* gene. In order to determine the specific plant organs where *C22DES* was most actively expressed, we made a search on gene expression databases (Tomato eFP Browser) and found that it was mainly expressed in roots (Figure S1). Furthermore, in order to complete these publicly available expression data, we performed RT-qPCR analysis in fruits at different developmental and ripening stages. As shown in Figure 1, the maximum expression peak of *C22DES* occurs at the early stages of fruit ripening (breaker stage) and then expression progressively decreases as the fruit ripens. These results are in agreement with those obtained from Tomato eFP Browser (Figure S1), despite being obtained in a different tomato cultivar (*Solanum lycopersicum* cv. Heinz).

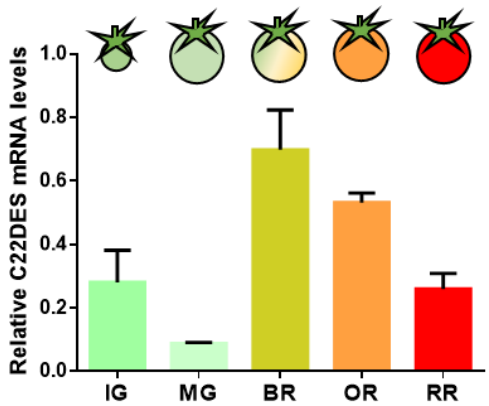

Figure 1 Expression profile of *C22DES* during fruit development and ripening. Transcript levels were measured in pericarp tissue from fruits collected at 5 different stages: Immature green (IG) [≈20 days post-anthesis (DPA)], mature green (MG) (≈30 DPA), breaker (BR) (≈35 DPA), orange (OR) (3-5 days post-breaker (DPB), and red ripe (RR) (≈15 DPB). Transcript levels were normalized using the tomato gene *CAC*. Expression values represent the mean ± SD of three independent biological replicates.

Moreover, to gain insight into the possible involvement of C22DES in the plant response to different stresses, we also analyzed the expression of *C22DES* after several treatments, including the pathogen elicitor flagellin 22 (FLA), the plant hormones ABA, MeJa and SA, and different stresses (osmotic, salt, cold and wound). The *C22DES* transcript levels were determined by RT-qPCR in RNA samples from three-week-old tomato seedlings collected before (time point 0 h) and after different

exposure times (3, 6, 12, 24 and 48 h) to the above mentioned stimuli, and from non-treated seedlings collected at the same time points (Figure 2).

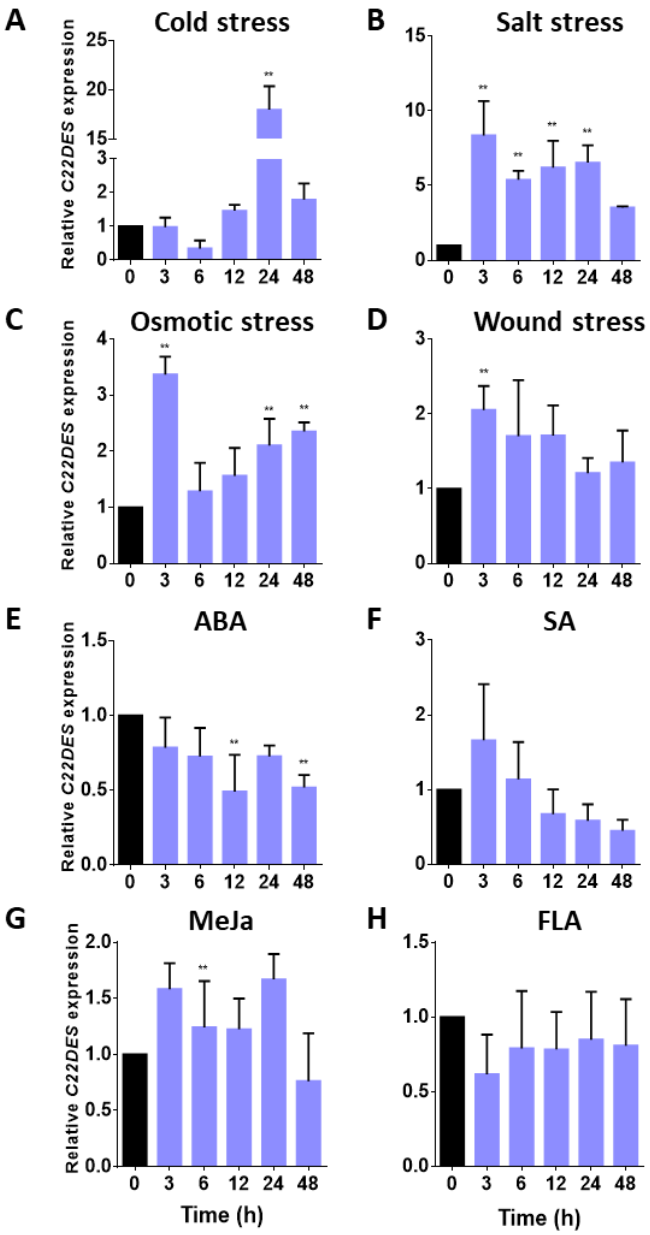

Figure 2 Expression of *C22DES* gene in tomato seedlings exposed to different stimuli. The transcript levels of *C22DES* were determined by RT-qPCR using RNA samples from 3-week-old tomato seedlings exposed to different treatments: cold (4ºC) **(A)**, NaCl (150 mM) **(B)**, mannitol (200 mM) **(C)**, wound **(D)**, ABA (0.1 mM) **(E)**, SA (0.5 mM) **(F)**, MeJa (0.5 mM) **(G)**, and flagellin 22 (1 mM) **(H)**. Samples were

collected at the indicated time points (3, 6, 12, 24, and 48 h) from the start of each treatment (0 h). Data are expressed as normalized quantity values calculated using two independent housekeeping genes (*PP2A* and *EF1a*) (Ballester, Cordón and Folch, 2013) and relative to non-treated seedlings at each time point, which is assumed to be one. Values are means ± SD (*n*= 6). Asterisks show the values that are significantly different (one-way ANOVA with Dunnett's multiple comparisons test, **p<0.01) compared to those at time 0 h.

The activation of the corresponding stress signaling pathways was confirmed by the increase in the transcript levels of different marker genes for each treatment (Ramírez-Estrada *et al.*, 2017) (Figure S2). The highest level of *C22DES* activation was reached after 24h of cold treatment (about 18-fold higher than basal levels). However, the induction by salt (about 8-fold) and wound stress (about 2-fold) was observed at earlier time points (3h) and was maintained until the end of the experiment. Osmotic stress also elicited a fast response by activating *C22DES* transcription after 3h of exposure, but transcript levels returned back to basal levels at the following time points. By contrast, the expression of *C22DES* was slightly down-regulated after 12h of ABA treatment, and the transcript levels remained below those in the non-treated plants until the end of the experiment. Finally, the transcript levels of this gene were not significantly altered in response to SA, MeJa and FLA treatments. Overall these results suggest that *C22DES* and most likely stigmasterol levels are involved in mediating the tomato response to abiotic stresses.

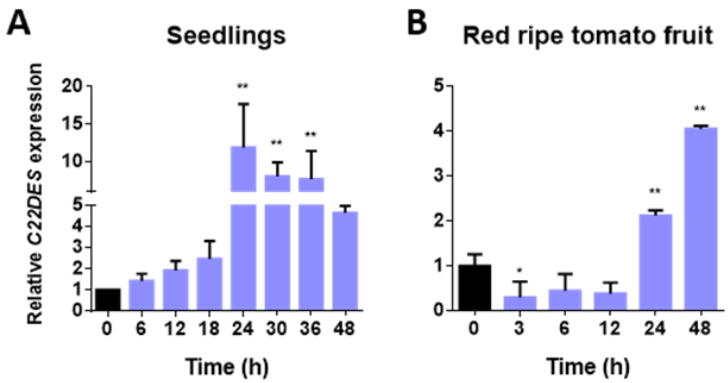

Figure 3 Expression of *C22DES* gene in tomato seedlings and red ripe fruits exposed to cold stress. The transcript levels of *C22DES* were determined by RT-qPCR using RNA samples from **(A)** tomato seedlings and **(B)** red ripe fruits (≈15 DPB) exposed to cold stress (4ºC). Samples were collected at the indicated time points from the start of each treatment (0 h). Data are expressed as normalized quantity values calculated using two independent housekeeping genes (*PP2A* and *EF1a*) (Ballester, Cordón and Folch, 2013) and relative to non-treated seedlings at each time point, which is assumed to be one. Values are means ± SD (*n*= 6). Asterisks show the values that are significantly different

(one-way ANOVA with Dunnett's multiple comparisons test, *p<0.05, **p<0.01) compared to those at time 0 h.

Considering the strong induction of *C22DES* expression after cold stress, we decided to further study this stress response by increasing the number of analyzed exposure time points (6, 12, 18, 24, 30, 36 and 48h) in seedlings and also by including tomato red ripe fruits in the analysis, which could provide interesting data related to the chilling storage temperatures at which they are exposed in post-harvest conditions, as they might help to elucidate whether the fruit chilling injury may involve stigmasterol biosynthesis to increase fruit protection or not (Figure 3). Results confirmed that the expression in seedlings peaked at 24h after cold exposure, and remained at similarly high levels until 36h after stimuli. Then expression began to decrease (Figure 3A). In the case of red ripe fruits, the induction was lower (around 4-fold higher than basal levels instead of 12-fold observed in seedlings) and clearly delayed compared to seedlings as the peak of expression was reached at 48h post-treatment (Figure 3B). These results indicate that the role of C22DES, and probably of stigmasterol, in the plant response to cold stress is not only restricted to the vegetative tissues but is also important in the fruit. The possibility that the observed differences in the induction times between seedlings and fruits could be due to faster sensing of temperature changes by the young tissues of seedlings in comparison with the fruit pericarp, which is protected by the cuticle and waxes, cannot be completely ruled out.

3.2 Stigmasterol metabolism is tightly regulated

In order to elucidate in more detail the contribution of stigmasterol to plant growth, development and stress responses, we next generated transgenic tomato lines (*S. lycopersicum* cv. Micro-Tom) with increased and decreased *C22DES* transcript levels by overexpressing a *C22DES* cDNA and artificial micro-RNA (amiRNA)-mediated *C22DES* gene silencing, respectively. Taking into account the marked up-regulation of *C22DES* expression at the early stages of fruit ripening (Figure 1), we decided to alter the *C22DES* expression levels both in the whole plant and specifically at the fruit ripening stage. For this purpose, both transgenes were expressed under the control of the constitutive CaMV35S promoter (*35S:amiC22DES, 35S:C22DES*) and the E8 fruit-ripening specific promoter (*E8:amiC22DES, E8:*C22DES) (Estornell *et al.*, 2009).

All independent T0 (hemizygous) lines were initially characterized by analyzing the *C22DES* expression levels either in leaves in the case of constitutive transgene expression lines or in orange fruits in the case of fruit-specific expression lines.

As expected, the *C22DES* transcript levels of the *E8:amiC22DES* lines were significantly lower than the WT in orange fruits, while in the *35S:amiC22DES* lines the mRNA relative levels measured in leaves remained unchanged or even increased (line #68.1) (Figure S3A). The analysis of the stigmasterol levels in the *E8:amiC22* lines was performed in red ripe fruits because of the expected gap between decreased transcript levels and its translation into reduced enzyme activity and stigmasterol levels. However, these lines did not show a concomitant reduction of stigmasterol content, but rather a slight increase (Figure S3B), suggesting no correlation between transcripts levels and C22DES activity. For this reason, we did not further work with any of the above mentioned silenced transgenic lines.

Both the constitutive and the fruit-specific *C22DES* overexpressing lines exhibited increased transcript levels albeit at different dosages (Figure 4A).

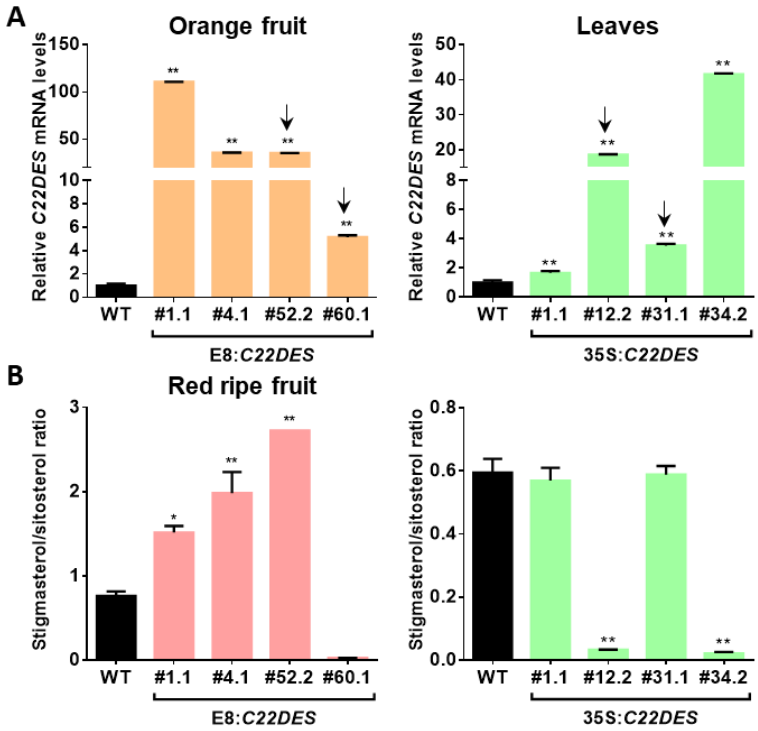

Figure 4 Analysis of *C22DES* transcript levels and sterol composition in *C22DES* overexpressing lines.
(A) *C22DES* transcript levels were measured in leaves of the constitutive *C22DES* overexpressing lines

(*35S:C22DES*) and orange fruits of the fruit-specific *C22DES* overexpressing lines (*E8:C22DES*). Values are mean values ± SD from 3 technical replicates (*n*= 3). Arrows indicate the selected lines for further segregation based on the different levels of overexpression and Stigmasterol/Sitosterol ratio changes. **(B)** Stigmasterol/Sitosterol ratio from membrane sterol fractions (FS, SG, and ASG) in red ripe fruits of the fruit specific *C22DES* overexpressing lines (*E8:C22DES*), and leaves of the constitutive overexpressing lines (*35S:C22DES*). Values are means ± SD from 3 technical replicates (*n*=3). Asterisks show the values that are significantly different (one-way ANOVA with Dunnett's multiple comparisons test, *p<0.05, **p<0.01) compared to WT

When we analyzed the sterol composition, we noticed two opposing behaviors (Figure 4B): On the one hand, the STIG/SIT ratio was increased between 2-fold and 4-fold the WT in the *E8:C22DES* lines in which the overexpression level was above 20-fold the WT (*E8:C22DES* #1.1, #4.1, #52.1) and severely decreased (38-fold lower than the WT) in the *E8:C22DES* line that showed the lowest level of overexpression (*E8:C22DES* #60.1); on the other hand, the STIG/SIT ratio did not increase in any of the *35S:C22DES* lines, but it was 95% decreased respect to the WT in the most overexpressing ones (*35S:C22DES* #12.2, #34.2). Based on the different levels of *C22DES* expression and the stigmasterol content, we selected two T0 independent lines for each construct for homozygous segregation of the transgenes, the *35S:C22DES* #12.4 and #31.1; and the *E8:C22DES* #52.2 and #60.1 (Figure 4A). Unfortunately, for the *E8:C22DES* construct we only could obtain homozygous plants from one of the two selected lines (*E8:C22DES* #60.1).

We next performed a more exhaustive characterization of the T2 transgenic homozygous lines including a detailed study of the *C22DES* gene expression and sterol profiles in different plant organs including leaves and fruits, and only sterol composition in seeds (Figure 5). In all cases, the sterol composition was analyzed in the 4 sterol fractions (FS, SE, SG, and ASG), (Tables S1, S2, S3).

As shown in Figure 5A, all the transgenic homozygous lines display different *C22DES* expression levels, which are in most cases higher than the WT, with the exception of the *35S:C22DES* #31.1 line, that showed decreased *C22DES* transcript levels in red ripe fruits.

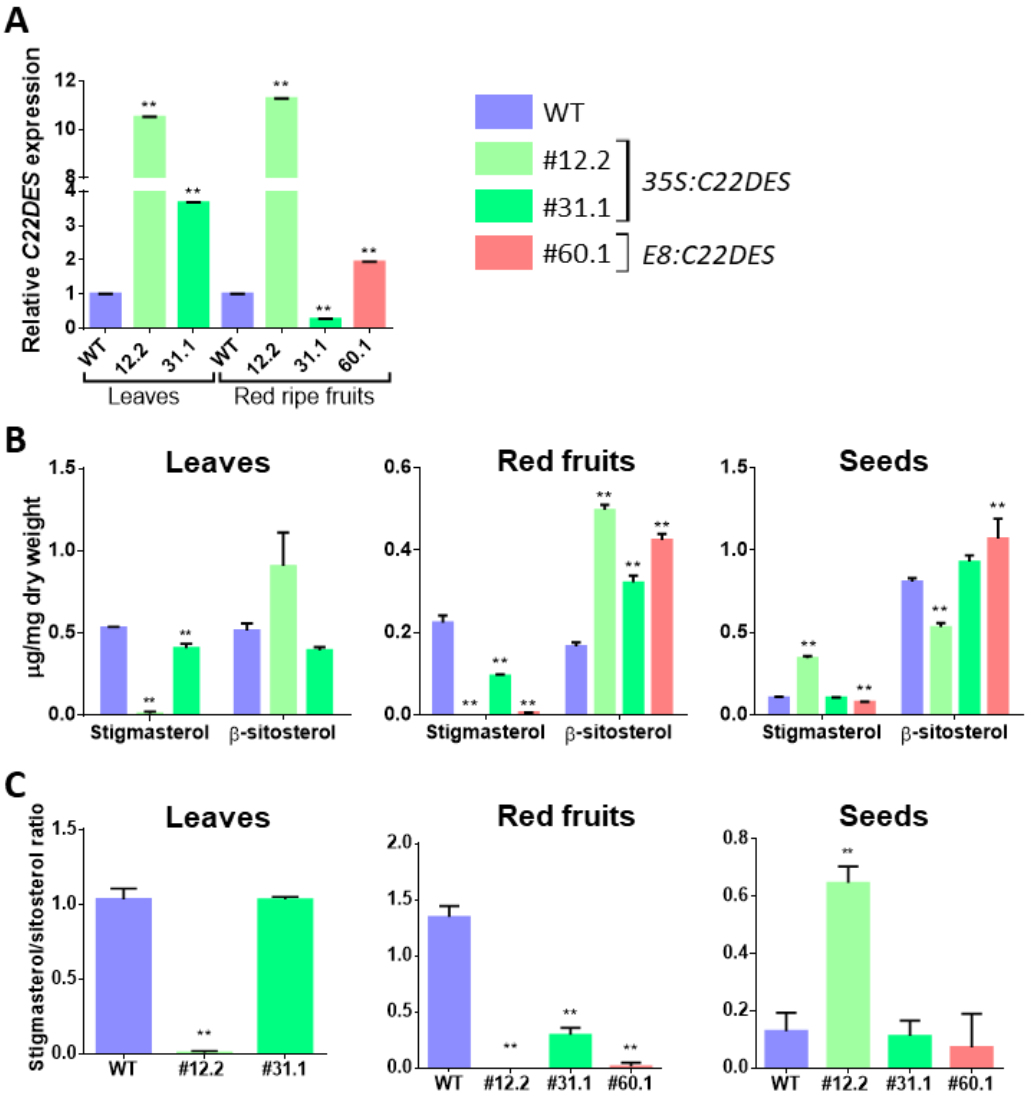

Figure 5 *C22DES* transcript levels and sterol content in transgenic homozygous lines overexpressing *C22DES*. (A) *C22DES* transcript levels were measured in leaves of the indicated constitutive *C22DES* overexpressing lines (*35S:C22DES*), and in red ripe fruits of both the constitutive and fruit-specific *C22DES* overexpressing lines (*35S:C22DES* and *E8:C22DES*, respectively). Values are means ± SD (*n*= 3) from 3 technical replicates. We determined the expression levels in three independent biological replicates, but calculations were made independently for each replicate because of the high variability of values, but the tendency of the expression for each line in comparison with the WT was identical among replicates. **(B)** Total stigmasterol and β-sitosterol levels in the four sterol fractions (FS, SE, SG, and ASG) in leaves, red fruits, and seeds, and **(C)** the resulting STIG/SIT ratios. Sterols in leaves were only analyzed in the constitutively *C22DES* overexpressing lines. Values are means ± SD from 2 biological replicates with 3 technical replicates in the case of leaves, and 3 technical replicates in the

rest of the samples. Asterisks show the values that are significantly different (one-way ANOVA with Dunnett's multiple comparisons test, **p<0.01) compared to WT.

Concerning the sterol composition, we did not detect increased levels of stigmasterol either in leaves or in red fruits in comparison with the WT (Figure 5B) despite the generalized increment of *C22DES* transcript levels. In fact, lines *35S:C22DES* #12.2 and *E8:C22DES* #60.1 practically did not exhibit stigmasterol at all, as previously reported for the T0 generation, and the remaining line, *35S:C22DES* #31.1, also had decreased levels of stigmasterol. However, in seeds, the effect of *C22DES* overexpression on the stigmasterol content was different from the other organs. In this case, two transgenic lines had similar stigmasterol content than the WT (*35S:C22DES* #31.1 and *E8:C22DES* #60.1), whereas the stigmasterol accumulation in the *35S:C22DES* #12.2 line was over 3-fold the WT. In all cases, the β-sitosterol levels were affected inversely proportional to those of the stigmasterol (Figure 5B), so that the STIG/SIT ratio was the result of a combinatory of these changes, being increased only in the seeds of *35S:C22DES* #12.2 line (Figure 5C).

Regarding the rest of the sterol species apart from stigmasterol and β-sitosterol, we can point out different observations. In leaves, the majority of sterol species showed a reduction in the membrane sterol fraction (FS, SG, ASG) of both constitutive overexpressing lines ranging from a 13% reduction of cholesterol in the ASG fraction (*35S:C22DES* #31.1) to a 79% reduction of campesterol in the SG fraction (*35S:C22DES* #12.2). However, in the case of the *35S:C22DES* #31.1 line we could observe the accumulation of some sterol species in the SE fraction such as campesterol and 24-ethylophenol, suggesting that the sterol esterification enzymes were more active. In fruits, we observed an overall increase of the major sterols except in the case of free campesterol, which was significantly reduced in the *35S:C22DES* lines. Finally, in seeds, FS, SE, and ASG fractions experimented a generalized increase of all sterol species, and only the SG fraction of the *E8:C22DES* line showed reduced levels of sterols (Tables S1, S2, S3).

To summarize, although the results were not as initially expected, we obtained several tomato lines with contrasting stigmasterol to sitosterol ratios in different organs (leaves, fruits and seeds) that are available for further use as models to investigate the effects of these altered sterol profiles on plant development and adaptation to biotic and abiotic stress. Furthermore, all these results suggest the

existence of precise regulatory mechanisms controlling stigmasterol metabolism that appear to operate differently in the distinct plant organs.

3.3 Generation and identification of homozygous *C22DES* knock-out plants

Our first attempt to generate tomato plants with reduced stigmasterol levels by amiRNA-mediated *C22DES* silencing was unsuccessful. On the other hand, despite the homozygous transgenic lines described above had an overall reduced stigmasterol content in red ripe fruits, and the *35S:C22DES* #12.2 also in leaves, this lower stigmasterol accumulation was not observed in all the plant organs, suggesting that these plants were able to increase C22DES activity when required. This fact could be a hurdle in the attempt to characterize the stigmasterol role in plant growth, development and stress responses.

For this reason, we performed CRISPR/Cas9 gene editing to generate knock-out *C22DES* mutant lines with the final aim to obtain tomato plants completely devoid of stigmasterol due to a block of its synthesis. To this end, we designed two different sgRNAs targeting a sequence located in the first third of the *C22DES* gene sequence and a second sequence that was located upstream that encoding the heme-binding motif (Figure 6A). *C22DES* gene does not contain introns, hence any mutation in the genomic sequence translates into mutations in the coding sequence. The edited proteins were expected to be inactive, the first due to the lack of more than the C-terminal half of the amino acid sequence and the second because of the lack of the heme-binding motif, which is essential for the activity of CYP family proteins (Bak *et al.*, 2011; Bansal *et al.*, 2019).

The genomic region encompassing the sgRNA target sites of the transgenic T0 plants was amplified by PCR, sequenced, and compared to the corresponding WT *C22DES* sequence. Unfortunately, transformations with the construct to express the first sgRNA did not result in any transgenic line with a mutated *C22DES* gene. Conversely, we obtained 12 independent heterozygous mutant transgenic lines with the second sgRNA, but only one of them produced seeds (*C22des*$^{-}$*)*. The mutation of this plant consisted of a deletion of 2 nucleotides (TG; positions 1055-1056 in *C22DES* ORF), with the consequent ORF change and the occurrence of a premature stop codon (Figure 6A). The resulting truncated protein lacking 150 amino acid residues of the

C-terminal end (C22des$^-$), shares with the full-length C22DES the first 351 amino acid residues followed by a short sequence of 12 residues (TQGNEVPGSGGA) resulting from the ORF shift to another reading frame caused by the 2 bp deletion.

We decided to check if the C22des$^-$ was really inactive before beginning with its segregation to homozygosis. For this purpose, we cloned the corresponding mutant cDNA (*C22des*$^-$) in frame with the GFP coding sequence, so that the resulting protein consisted of the green fluorescent protein (GFP) fused at the C-terminal end of the truncated C22DES (c22des$^-$-GFP), in a binary plasmid for *Agrobacterium*-mediated transient expression in *N. benthamiana* leaves (Figures 6B, S3) and subsequent analysis of their sterol composition. We also generated a binary expression plasmid in which the full-length C22DES protein was fused to GFP (C22DES-GFP) that was used as a positive control.

As expected, whereas the overexpression of C22DES-GFP resulted in an increment in the STIG/SIT ratio in the total steryl lipids from *N. benthamiana* agroinfiltrated leaves (Figure 6C), C22des$^-$-GFP was not able to increase the stigmasterol content in none of the analyzed sterol fractions (Figure S4, Table S4), obtaining similar results than with the overexpression of the empty vector. These results confirmed that the C22des$^-$ truncated version of the protein was catalytically inactive and reinforced the idea that the homozygous mutant plants should not be able to synthesize stigmasterol.

We next performed genotyping analysis of the T1 generation plants by PCR taking advantage of the fact that the CRISPR/Cas9 deletion of two nucleotides also removed a *Bpu*10I restriction site (RFLP, restriction fragment length polymorphism). A 558-bp fragment encompassing the sgRNA target site was amplified by PCR followed by *Bpu*10I digestion and gel electrophoresis analysis. Due to the RFLP, a single non-digested PCR fragment of 558-bp was obtained in the case of the *C22des*$^-$ homozygous plants, whereas two restriction fragments of 333 and 225 bp and a mix of the three fragments (558, 333 and 225 bp) would be obtained from WT and heterozygous plants, respectively (Figure 6D).

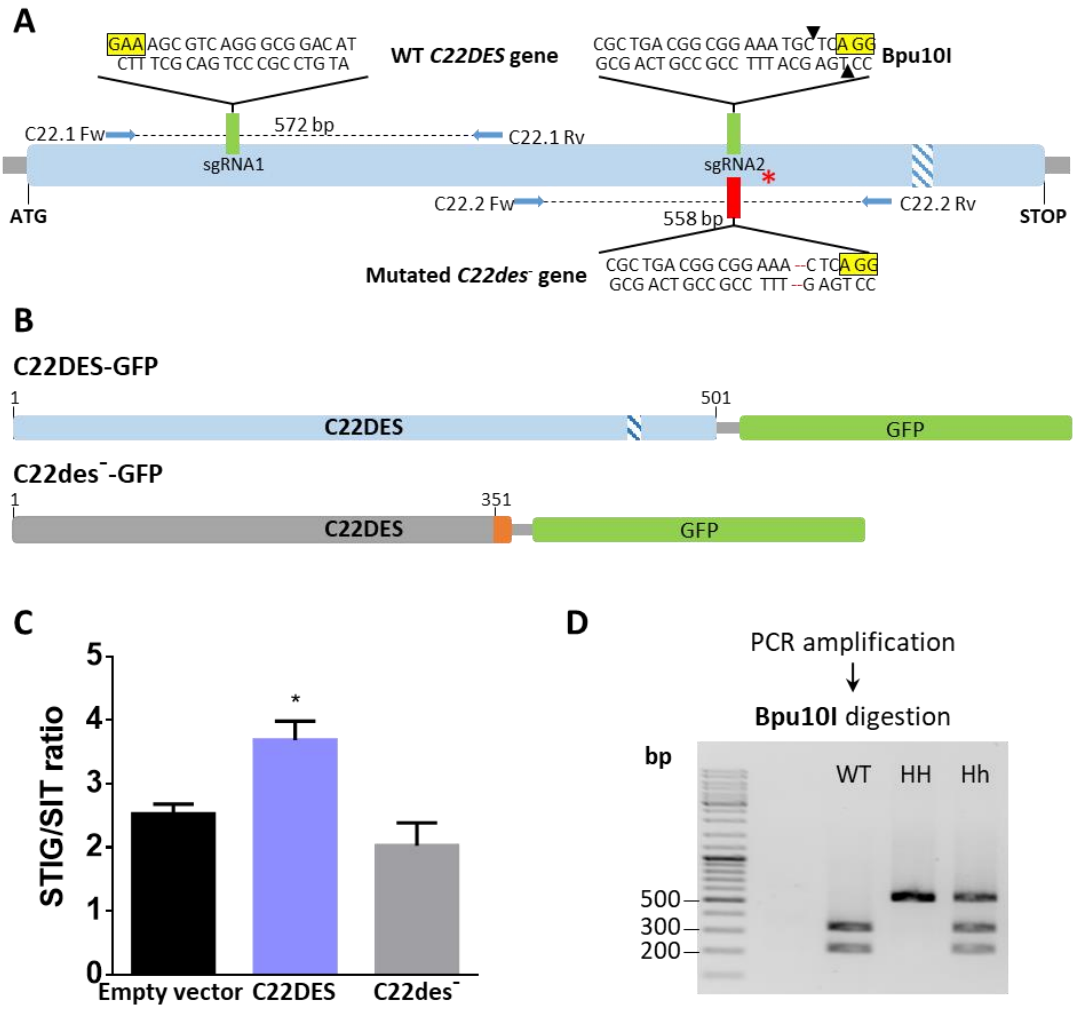

Figure 6 Strategy for the generation and identification of *C22des*⁻ homozygous mutant plants obtained by CRISPR/Cas9 genome editing technology. (A) Schematic representation of *C22DES* genomic sequence, in which the start and stop codons and the target sites of the designed sgRNAs are indicated. Green boxes indicate the sgRNA target sites; striped boxes represent the heme-iron ligand motif essential for catalysis; yellow boxes correspond with the PAM sequence recognized by the Cas9 nuclease; the red box indicates the *C22DES* mutation obtained after Cas9 action; black arrows show the *Bpu*10I restriction site in WT sequence which was removed by the mutation; blue arrows represent the pairs of primers used for the mutations screening; the red asterisk indicates the position of the premature stop codon in the mRNA derived from the edited genomic sequence. **(B)** Schematic representation of C22DES and the truncated C22des⁻ GFP fusion proteins. The blue box represents the full-length C22DES protein; green boxes, the GFP protein; grey box, the amino acid residues in the C22des⁻ protein that are identical to those in the full-length one; orange box, the resulting protein sequence from the ORF shift. Aminoacidic coordinates of C22DES protein sequence are shown above the constructions **(C)** Ratio of stigmasterol to β-sitosterol in the total steryl lipids from *N. benthamiana* leaves expressing C22DES-GFP and C22des⁻-GFP. Values are means ± SD of two

independent biological replicates (*n*=2) with their corresponding technical triplicates. Asterisks indicate significant differences among mean values relative to those in leaf samples expressing the empty vector (one-way ANOVA with Dunnett's multiple comparisons test, *p<0.05). **(D)** Homozygous line identification by RFLP analysis of the amplified region surrounding the sgRNA target site. HH: homozygous; Hh: Heterozygous.

3.4 Stigmasterol is not crucial for completing the life cycle of tomato plants

The sterol analysis of different tomato plant organs of the *C22des*$^{-}$ mutant plants revealed that neither free nor conjugated stigmasterol (SE, SG, or ASG) was accumulated in any of the samples (Table 1), thus demonstrating on the one hand the effectiveness of the CRISPR/Cas9 experimental approach and on the other hand that the lack of stigmasterol does not result lethal for the tomato plants. Moreover, *C22des*$^{-}$ plants developed normal flowers and fruits with seeds, suggesting that their reproductive capacity was also intact. As described below, the seed germination in the mutant genotype is affected but not completely abolished.

The data in Table 1 show the sterol composition of each sterol fraction (FS, SE, SG, and ASG) in three different tomato plant organs (leaves, red ripe fruits, and seeds) of WT and *C22des*$^{-}$ plants.

As shown in Table 1, the major sterols in the four steryl lipid fractions were cholesterol, campesterol, stigmasterol, and β-sitosterol, and in the case of steryl ester fraction, we also measured some desmethylsterol intermediaries such as cycloartenol and 24-ethylidenelophenol. Cycloartenol is the first tetracyclic sterol precursor in plant sterol biosynthetic pathway, whereas 24-ethylidenelophenol is the first intermediate on the C24-ethyl branch of the sterol biosynthetic pathway, which is regulated by the key regulatory enzyme SMT2/3 (Benveniste, 2004).

In the case of the *C22des*$^{-}$ leaf sterol composition, we observed an overall rise of major sterols, not only of β-sitosterol, the immediate precursor of stigmasterol, but also of cholesterol and campesterol, resulting in an overall increase of 11% of the total content of membrane sterol fractions (FS, SG, and ASG) in comparison with the WT. However, the increase in the total sterol content was not the same for each sterol fraction, being the FS the most increased (around 20% higher than FS accumulation in the WT). Despite SE levels also seem to be higher, the differences

are not statistically significant. Overall these results suggest that mutant plants upregulate the whole sterol biosynthetic pathway in leaves in an attempt to compensate for the lack of stigmasterol.

		Tomato plant organ					
		Leaves		Red ripe fruits		Seeds	
		WT	*C22des*$^-$	WT	*C22des*$^-$	WT	*C22des*$^-$
FS	Cholesterol	3.24 ± 0.22	4.62 ± 0.23	0.19 ± 0.04	0.21 ± 0.01	2.92 ± 0.20	2.62 ± 0.15
	Campesterol	0.71 ± 0.04	1.11 ± 0.16	0.84 ± 0.05	0.62 ± 0.04	2.15 ± 0.23	2.54 ± 0.03
	Stigmasterol	18.90 ± 0.51	*nd*	6.19 ± 0.27	*nd*	6.47 ± 0.49	*nd*
	β-sitosterol	8.81 ± 0.47	32.64 ± 0.64	1.35 ± 0.20	6.94 ± 0.61	43.18 ± 5.61	51.60 ± 2.81
SE	Cholesterol	3.09 ± 0.14	4.73 ± 0.70	1 ± 0.39	0.77 ± 0.18	27.20 ± 2.51	28.49 ± 1.73
	Campesterol	1.44 ± 0.04	2.33 ± 0.20	2.93 ± 0.45	0.79 ± 0.16	3.04 ± 0.36	3.26 ± 0.42
	Stigmasterol	1.12 ± 0.04	*nd*	2.90 ± 0.33	*nd*	3.74 ± 0.24	*nd*
	β-sitosterol	4.47 ± 0.58	11.15 ± 1.78	6.65 ± 0.74	7.28 ± 0.35	58.12 ± 8.28	47.07 ± 1.04
	Cycloarthenol	2.32 ± 0.52	9.78 ± 3.93	1.44 ± 0.19	0.55 ± 0.11	2.30 ± 0.34	3.68 ± 0.46
	24-Ethylidenelophenol	0.33 ± 0.05	0.97 ± 0.19	*nd*	*nd*	1.87 ± 0.34	1.76 ± 0.37
SG	Cholesterol	2.71 ± 0.11	3.40 ± 0.21	0.42 ± 0.04	0.52 ± 0.01	1.38 ± 0.34	0.96 ± 0.16
	Campesterol	0.86 ± 0.09	0.77 ± 0.06	1.62 ± 0.04	1.42 ± 0.15	2.46 ± 0.16	1.79 ± 0.36
	Stigmasterol	6.37 ± 0.51	*nd*	8.55 ± 0.56	*nd*	8.10 ± 0.74	*nd*
	β-sitosterol	12.53 ± 0.53	22.13 ± 1.3	4.58 ± 0.39	10.04 ± 0.94	47.58 ± 5.08	45.69 ± 8.58
ASG	Cholesterol	7.27 ± 0.15	8.68 ± 0.27	0.53 ± 0.02	0.82 ± 0.01	0.60 ± 0.11	0.91 ± 0.06
	Campesterol	1.83 ± 0.12	2.06 ± 0.11	1.53 ± 0.10	2.07 ± 0.06	0.59 ± 0.18	0.53 ± 0.002
	Stigmasterol	28.13 ± 1.07	*nd*	7.66 ± 1.6	*nd*	2.85 ± 0.60	*nd*
	β-sitosterol	26.45 ± 1.09	56.15 ± 0.82	4.07 ± 0.43	19.76 ± 0.10	10.33 ± 2.65	14.73 ± 1.52

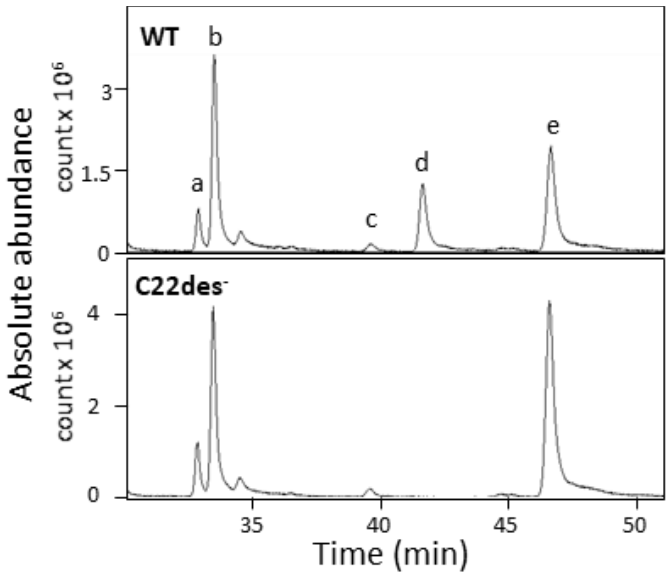

Table 1 Detailed sterol composition in different organs of WT and *C22des*$^-$ plants. Data are the mean values ± SD of three technical replicates (*n*=3). Values are given in µg/100mg dry weight. *nd.,* not detected. FS, free sterols; SE, steryl esters; SG, steryl glycosides; ASG, acyl-steryl glycosides. Below

the table: GC-MS analysis of the WT and *C22des*$^{-}$ sterol composition of the ASG fraction in leaves. The top panel represents the total ion chromatogram of the ASG fraction in WT tomato leaves and the bottom panel corresponds to the equivalent sample in the *C22des*$^{-}$ mutant. Peaks at the specific retention times correspond to (a) cholesterol, (b) cholestanol (Internal standard), (c) campesterol, (d) stigmasterol, and (e) β-sitosterol. The lower panel corresponds to the SG fraction of the *C22des*$^{-}$ leaf sample, in which the stigmasterol peak (d) is not detected.

In red ripe fruits, the sterol composition of the *C22des*$^{-}$ mutant mainly differs from the WT in stigmasterol and β-sitosterol content, that completely disappears and accumulates, respectively. In this case, the total sterol content of both genotypes is similar, but the distribution among the different steryl fractions is slightly different: on the one hand, the SE fraction experienced a 37% drop in sterol levels in comparison with the WT, mainly due to the decreased levels of campesterol and the lack of stigmasterol, which was not compensated by the slight increase of β-sitosterol; on the other hand, the *C22des*- mutant fruits showed a 64% increment in ASG levels, which balances the drop experienced in the other sterol fractions. Note that campesterol levels were also significantly different than the WT in most sterol fractions (FS, SE, and ASG). Although in the ASG fraction there is a 35% increment on campesterol levels, contrary to the reduction observed in the FS and SE fractions, it is not proportional to the 64% overall rise in the ASG fraction, so in fact, it could be considered as a decrease. This finding could be related to the regulation of the flux of intermediates to the biosynthesis of C24-ethyl sterols.

Finally, the sterol composition of *C22des*- mutant seeds was not affected except for the absence of stigmasterol, since even the β-sitosterol levels were not significantly increased.

3.5 The phenotype of *C22des*- mutant plants

We next analyzed several phenotypic traits of *C22des*$^{-}$ plants (Table 2) in order to elucidate the possible involvement of stigmasterol in different biological processes. *C22des*$^{-}$ plants, as well as their leaves, were significantly smaller than the WT and had a bushy phenotype due to their shorter internodes both between leaves and between the different leaf leaflets (Figure 7). Five-old-week mutant plants reached a height of 11.51 ± 1.29 cm, a 27% reduction in comparison with WT plant. According to these data, *35S:C22DES* #12.2 plants, in which stigmasterol content in vegetative

tissue was depleted, were also significantly smaller than the WT, reaching a final height of 12.84 ± 1.92 cm, around a 19% reduction compared to WT.

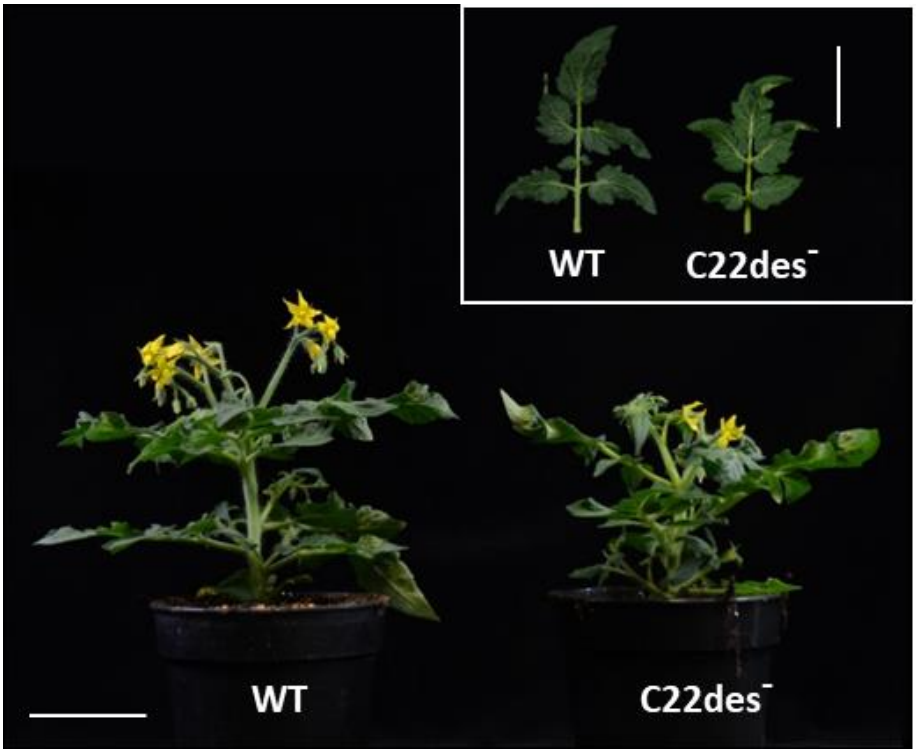

Figure 7 Morphology of mature *C22des*⁻ mutant. Main images show representative WT and *C22des*⁻ 40-days-old plants. Inset: representative 8th leaf from both genotypes. Bars = 5 cm.

The mutant's leaves were smaller not only in length (16% reduction) but also in the area (17% reduction). The reduced size of *C22des*⁻ could be a consequence of defects on cell division or cell elongation or both. To better elucidate this issue, we analyzed sections from the leaf abaxial epidermis by light microscopy to observe cell sizes. To minimize variations due to the developmental stage of the sample, we always took the fourth pair of true leaves. However, epidermal cell areas (Table 2) were similar in both genotypes, suggesting a defect in cell division rather than in cell elongation.

The onset of flowering was delayed by about 5 days in the case of *C22des*⁻ compared to WT plants, but both the mutant and the WT plants had the same number of true leaves at the onset of flowering. We also noticed a marked reduction in the weight of red ripe fruits (33%) and seeds (23%) in comparison with the WT (Table 2).

All these results suggest that stigmasterol is not only involved in plant growth processes but also in development.

	Genotype		
Measurements	WT	*C22des*$^{-}$	*n*
Height at maturity (cm) **	15.83 ± 1.79	11.51 ± 1.29	>20
Leaf length (cm) **	13.10 ± 0.45	11 ± 0.12	3
Leaf area (cm^2) *	40.86 ± 1.37	33.58 ± 3.05	3
Epidermal cell area (mm^2)	$1.99 \cdot 10^{-3} \pm 4.3 \cdot 10^{-4}$	$1.89 \cdot 10^{-3} \pm 3.97 \cdot 10^{-4}$	>20
Start of flowering (days) **	43.07 ± 2.96	48.07 ± 2.59	15
Fruit weight (g) **	4.40 ± 1.36	2.94 ± 1.04	>60
Seed weight (mg) *	3.48 ± 0,04	2,66 ± 0,29	300

Table 2 Morphometric analysis of WT and *C22des*$^{-}$ plants. Five weeks-old plants, red ripe fruits (15 DPB), and mature seeds were used for the metric analysis. Data are the mean values ± SD of *n* replicates (right column). Asterisks show the values that are significantly different (one-way ANOVA with Dunnett's multiple comparisons test, *p<0.05, **p<0.01) between the *C22des*$^{-}$ and the WT plants.

3.6 The lack of stigmasterol impairs normal seed germination

We realized that seeds of the *C22des*$^{-}$ mutant line showed severe germination problems, as only around 40% of the seeds initiated sprouting in comparison with 97% of the WT seeds (Figure 8A), which was also markedly delayed compared to WT. Furthermore, less than half of the *C22des*$^{-}$ germinating seeds resulted in seedling establishment, suggesting additional developmental abnormalities beyond germination (Figure 8B). We observed a high percentage of *C22des*$^{-}$ seeds (around 60%) that resulted in non-viable seedlings, a phenotype also observed in the WT, but much less frequently (11%), and even with a lower frequency in the case of the *35S:C22DES* #12.2 line (2%), which was reported to accumulate stigmasterol in seeds. These abnormal seedlings usually showed an apparently normal root but a callous hypocotyl that in most cases presented a constriction in the apical hook and aberrant cotyledons (Figure 8C).

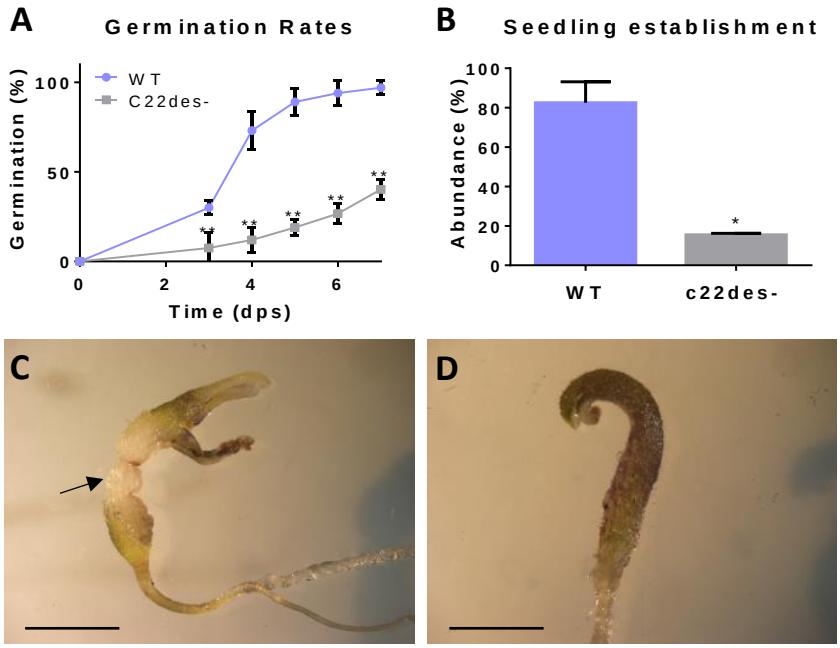

Figure 8 Germination phenotype of tomato *C22des*⁻ seeds lacking stigmasterol. (A) Germination rates showing the percentage of germinating seeds and **(B)** percentage of seedling establishment of the *C22des*⁻ mutant compared to the WT. Data are the mean values ± SD of 4 independent biological replicates (*n* = 80), except for **(B),** which was calculated from 2 independent biological replicates (*n* = 40). Asterisks show the values that are significantly different (one-way ANOVA with Dunnett's multiple comparisons test, *p<0.05, **p<0.01) compared to WT **(C and D)** Representative non-viable seedlings. Bars: 5 mm. Images are taken by a stereoscopic magnifier. Dps, days post-sowing

Taking advantage of the fact that *35S:C22DES* #12.2 accumulated stigmasterol in seeds, we wondered if it could have a positive effect on the germination rate. To check this hypothesis, we repeated the analysis by including the transgenic lines overexpressing *C22DES* under the control of the constitutive CaMV35S promoter (*35S:C22DES* #12.2 and *35S:C22DES* #31.1) and the E8 fruit-ripening specific promoter (*E8:C22DES* #60.1) (Figures 9A-B). There were no significant differences in germination between these lines and the WT, reaching almost 100% of germinated seeds (Figure 9A), but a significant increase in the abundance of viable seedlings should be noted for the *35S:C22DES* #12.2 line (Figure 9B).

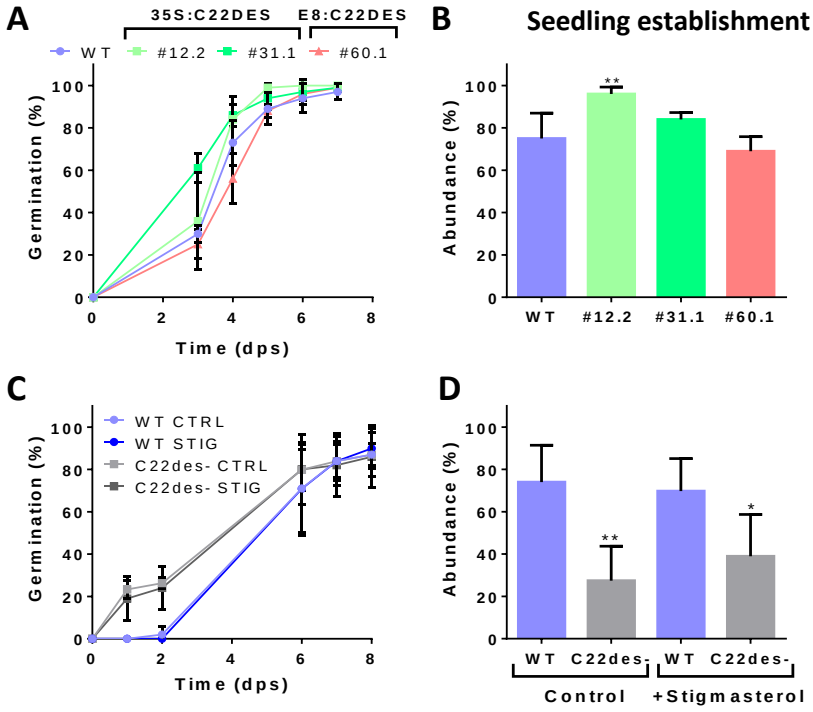

Figure 9 Germination assays of tomato *C22des*⁻ seeds lacking stigmasterol or with enhanced levels of stigmasterol (*C22DES* overexpressing lines). (A and C) Germination rates showing the percentage of germination of seeds from **(A)** the overexpressing *C22DES* lines (*35S:C22DES* #12.2, #31.1, and *E8:C22DES* #60.1) and **(C)** the *C22des*⁻ mutant soaked in a stigmasterol solution (0.02% w/v), compared to WT seeds under the same experimental conditions. **(B, D)** Percentage of viable seedlings after the above-mentioned germination assays. Control seeds in panel **C** and **D** were soaked in 4.84% ethanol (v/v), which was used to solubilize stigmasterol. Data are the mean values ± SD of 4 independent biological replicates (*n* = 80). Asterisks show the values that are significantly different (one-way ANOVA with Dunnett's multiple comparisons test, *p<0.05, **p<0.01) compared to WT. Dps, days post-sowing

Considering these results, we next wondered if the seed mutant phenotypes could be restored to WT or at least partially complemented by exogenous application of stigmasterol. To this end, we incubated *C22des*⁻ and WT seeds overnight in a stigmasterol solution (0.02% w/v), as previously described for flax seeds (Hashem *et al.*, 2011), and compared their germination rates and seedling viability. Surprisingly, the only fact of being soaked improved germination of *C22des*⁻ seeds, resulting in a similar percentage to that of WT seeds (almost 90%) (Figure 9C). In this case, the germination rate of mutant seeds was faster than the WT. Unfortunately, this improvement didn't translate into a higher seedling establishment (Figure 9D),

indicating that defective seedling establishment is not a direct consequence of germination deficiency.

Exogenously added stigmasterol did not recover normal seedling establishment in comparison with control treatments (Figure 9D) but it cannot be ruled out the possibility that the tomato seeds were not able to take up the exogenously supplied stigmasterol, or that at this developmental stage, the defects derived from the lack of stigmasterol may not be rescued.

3.7 The embryo development is affected in the *C22des*- mutant

To elucidate whether the high percentage of seedling malformations (Figure 10A) reflected embryo developmental abnormalities, we conducted tetrazolium (TZ) staining of tomato seeds and then we took the embryos out of the seed to observe their morphology. TZ is a colorless compound that is converted into a red-colored formazan by hydrogen transfer reaction catalyzed by the cellular dehydrogenases in living tissues (Verma and Majee, 2013). Moreover, this test also enables to distinguish between viable and non-viable tissues within the embryo.

A high number of *C22des*$^{-}$ mutant embryos (around 80%) showed aberrant phenotypes compared to embryos from the WT (20%) and the *C22DES* overexpressing line (*35S:C22DES* #12.2) (13%) (Figure 10B), in agreement with the percentages of non-viable seedlings observed in the same plants (Figure 10A).

Additionally, we also noticed that the structure of the non-viable seedlings (Figure 8C and D) was similar to that of the aberrant embryos: *e.g.* the embryo shown in Figure 10C had a similar constriction in the hypocotyl than the seedling shown in Figure 8C, that overlaps with a region of no TZ staining, which indicates that is a non-viable tissue. In the case of the embryo shown in Figure 10D, its cotyledons seemed to be insufficiently differentiated, and they remained unfolded similarly to the seedling shown in Figure 8D. As an additional piece of information, the tissue of mutant embryos was apparently softer than the WT.

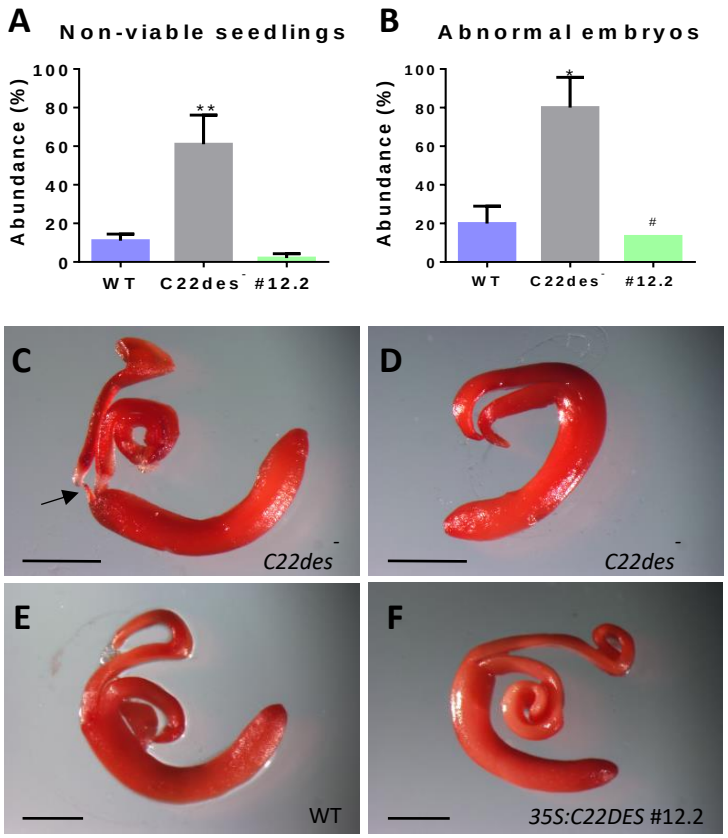

Figure 10 Embryo phenotypes of *C22des*⁻ mutant in comparison with WT plants. (A) Percentage of non-viable seedlings and **(B)** abnormal embryos from the different analyzed genotypes. Data are the means ± SD of **(A)** 4 independent biological replicates (*n* = 100) and **(B)** 2 independent biological replicates (*n* = 50). #, indicates only one replicate. Asterisks show the values that are significantly different (one-way ANOVA with Dunnett's multiple comparisons test, *p<0.05, **p<0.01) compared to WT. **(C and D)** Representative abnormal embryos from the mutant, with similar phenotypes than the abnormal seedlings showed above. Arrows indicate similar constrictions in the hypocotyl region. **(E)** Representative normal embryos from the WT and **(F)** the *35S:C22DES* #12.2 line. Images are taken by a stereoscopic magnifier. Bars: 1 mm

Taking into account the apparent coincidences not only in the phenotype but also in the occurrence frequency, we hypothesize that the problems that we found in seedling establishment were caused principally by abnormalities in the embryo development.

3.8 Stigmasterol contributes to improving *Botrytis cinerea* resistance

Botrytis cinerea is one of the most important fungal plant pathogens in terms of economic losses, as it can infect more than 200 plant species, including tomato (Dean *et al.*, 2012).

In order to investigate the role of stigmasterol in the defense response against biotic stress, we performed infection assays using *B. cinerea* and red ripe fruits from both the WT and the transgenic lines generated in this study, including *C22des*⁻ mutant and the *C22DES* overexpressing lines *35S:C22DES* #12.2, 31.1, and *E8:C22DES* #60.1, since all of them showed differentially altered stigmasterol levels in red ripe fruits in comparison with the WT. By this way, we may be able to analyze the effect of different stigmasterol levels ranging from the complete depletion of the metabolite to the WT levels.

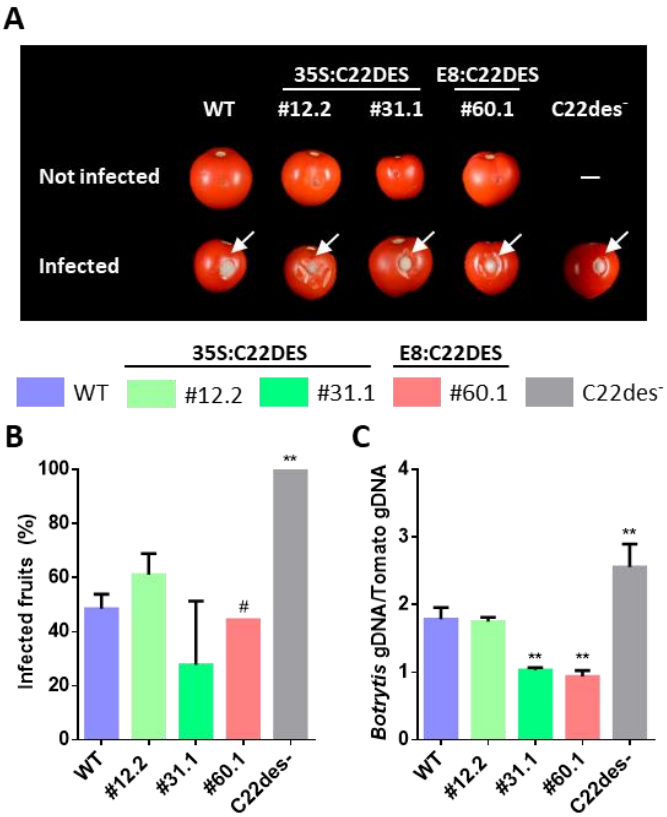

Figure 11 Infection of tomato fruits with *Botrytis cinerea*. (A) Representative images showing infected and non-infected fruits from the indicated genotypes taken at 6 days post-inoculation (DPI).

White arrows indicate lesions. **(B)** Percentage of infected fruits from the different infection assays after 6 DPI. Values are means ± SD of two independent experiments. #, corresponds with only one replicate. **(C)** Relative quantification of *B. cinerea* genomic DNA in tomato red fruits at 6 DPI. The ratio of *B. cinerea β-tubulin* gene to tomato *SlACT* gene is shown. All data represent mean ± SD of three technical replicates from a pool of fruits from only one experiment. Asterisks show the values that are significantly different (one-way ANOVA with Dunnett's multiple comparisons test, *p<0.05, **p<0.01) compared to WT.

The symptoms of infected fruits were analyzed at 6 days post-inoculation (dpi) by taking images and comparing the progression of the infection in all the genotypes (Figure 11A). *C22des*$^{-}$ fruits were more susceptible to the fungal infection than the WT infected fruits. All of the mutant fruits were successfully infected in every single experiment, whereas only half of WT fruits showed infection symptoms (Figure 11B). However, the rest of the transgenic lines had similar resistance to *B. cinerea* than the WT despite their decreased initial stigmasterol levels. These differences in fruit susceptibility against *B. cinerea* infection were confirmed by quantifying the genomic fungal DNA by qPCR, whose levels were significantly higher in the mutant fruits than in the rest of fruits (Figure 11C).

4. DISCUSSION

The results obtained in this study show that although stigmasterol seems to be involved in several biological processes (including biotic stress resistance and proper embryo development) (Figures 2, 3, 8, 10 and 11), it is not strictly necessary to sustain plant life, as the complete lack of this metabolite does not result in plant lethality. We have obtained a *C22DES* knock-out line (*C22des*$^{-}$), the gene encoding the enzyme responsible for the β-sitosterol desaturation into stigmasterol, in which the complete absence of stigmasterol in different plant tissues has been demonstrated (Table 1). These mutant plants represent an important and unique tool to further investigate the biological processes, including putative signaling pathways, in which stigmasterol is involved, since stigmasterol levels in some Arabidopsis mutants described to date are not completely depleted, most likely because of the *C22DES* gene redundancy in this plant species (Griebel and Zeier, 2010). In this respect, tomato can be considered a more suitable model to study the stigmasterol role because it has only a single gene encoding *C22DES* (Morikawa *et al.*, 2006). Furthermore, tomato is a well-described plant species and there are a

number of genetic and molecular biology tools already available to use on it (Chaudhary *et al.*, 2019).

According to our results, it can be speculated that the stigmasterol metabolism is regulated in a strong and tissue-specific manner, similar to that proposed in previous studies (Schaller, Bouvier-Navé and Benveniste, 1998). Our attempts to generate transgenic tomato plants with enhanced or decreased stigmasterol levels by overexpressing or silencing *C22DES* gene, respectively, in both cases failed to some extent (Figure S3, 4 and 5). Despite being able to modify the *C22DES* transcript levels compared to those in the WT plants, these alterations did not correlate with similar changes in the stigmasterol contents. Unexpectedly, plants with more than 10-fold down-regulation of the *C22DES* transcript levels showed no change in the stigmasterol content, which remained at the same level than the WT in ripening fruits (Figure S3). On the other hand, and contrary to what we intended, we obtained plants with decreased stigmasterol content in most of the analyzed plant organs (including leaves and red ripe fruits) by overexpressing *C22DES* cDNA under the control of a constitutive promoter (*35S:C22DES*) and a fruit-ripening specific promoter (*E8:C22DES*), with the only exception of seeds in which stigmasterol levels raised up to 3-fold (Figure 5).

The lack of success in both strategies suggests the operation of strong translational or post-translational regulatory mechanism controlling *C22DES* gene expression and/or enzyme activity. Some previous studies involving metabolic processes revealed that whilst metabolites from the same pathways changed in abundance in a coordinated manner, the transcripts abundance was less strictly synchronized, suggesting that post-translational mechanisms dominate metabolic regulation (Carrari *et al.*, 2006). Altogether these results are in agreement with the existence of very precise sensing mechanism for stigmasterol, or even for *C22DES* mRNA levels, by which each specific organ could maintain appropriate stigmasterol content by regulating the gene expression or the enzymatic activity. According to this hypothesis, stigmasterol has been previously reported as a metabolite involved in modulating other enzymatic activities, such as HMG-CoA reductase (HMGR) activity, which was reduced by 30-35% in pea seedlings treated with stigmasterol (Russell and Davidson, 1982). Further investigations including measuring C22DES protein levels

should be performed to elucidate whether translational or post-translational regulatory mechanism are involved in modulating C22DES activity.

To overcome the limitation due to the proposed tight post-transcriptional regulation of tomato C22DES, we decided to use a different approach in order to generate tomato plants with depleted stigmasterol levels. For this purpose, the *C22DES* knock-out (*C22des*$^{-}$) based on the CRISPR-Cas9 technology seemed the most appropriated strategy. The *C22des*$^{-}$ mutation generated an inactive truncated version of C22DES lacking 150 amino acids of the C-terminal region, which includes the heme-binding domain (Figure 6). The lack of activity of the truncated protein was demonstrated both by biochemical and cell biology approaches and is in agreement with the reported necessity of the heme-binding domain for the activity of CYP family proteins (Bak *et al.*, 2011; Bansal *et al.*, 2019).

The sterol profile of these mutant plants was analyzed in order to assess the impact of C22DES inactivation, and consequently of stigmasterol biosynthesis, in the overall sterol composition (Table 1). The most profound changes were observed in leaves, where the sterol content of the membrane sterol fractions (FS, SG, and ASG) increased by 11% in comparison with the WT. This result raises the possibility that stigmasterol role might be related to the vegetative stages of tomato plants, likely in growing processes as discussed below, and suggests that the whole sterol biosynthetic pathway is upregulated, in what seems to be a compensatory attempt to restore normal stigmasterol levels. In red ripe fruits, the most remarkable differences compared to the WT were the notable increment of ASG levels and the significant reduction in the total campesterol levels. Regarding the increase of ASGs, it is worth noting that they localize in the membrane fraction. Thus it is likely that the lack of stigmasterol may affect the membrane integrity and stability, being necessary for the plant to balance the sterol composition to maintain proper physicochemical membrane properties. Membranes that are enriched in ASGs and SGs are described to show a significant increment in the order level (Grosjean *et al.*, 2015). On the other hand, it can be speculated that the reduction in the total campesterol level in fruits may be related with an increased flux of the 24-ethyl sterol branch of the pathway driven by an increased SMT2/3 activity (*see* General Introduction, Figure 6).

We have reported in this study that *C22des*$^{-}$ mutant shows a moderate dwarf phenotype, including also smaller fruits. This growth reduction could be due to a reduction in cell length, in the number of cells or both (Figure 7, Table 2). Our data demonstrated that the cell length was not affected in comparison with the WT, which suggest that the reduced plant size is most likely due to a decrease in cell number.

In plants, the sterols intermediaries are essential substrates acting in two different metabolic routes: the biosynthesis of brassinosteroids (BRs), which are campesterol-derived plant hormones with a key role in controlling plant growth through acting on both cell expansion and division (Zhiponova *et al.*, 2012); and the synthesis of bulk sterols β-sitosterol, stigmasterol, campesterol and the minor sterol, cholesterol. Plant size is a common trait known to be altered in several mutants affected in genes of the early steps of the sterol biosynthetic pathway, and has been recurrently related with both alterations on BRs homeostasis (Choe *et al.*, 1999; Nomura *et al.*, 1999) and the sterol composition by itself (Diener *et al.*, 2000; Schaller, 2003, 2004; Carland, Fujioka and Nelson, 2010). C22DES has no direct relation with campesterol biosynthesis, as it acts downstream the branch point enzymes SMT1 and SMT2/3 controlling sterol precursors partitioning between the different branches of the sterol pathway (precursors-flux-deriving enzymes) (*see* General Introduction, Figure 6). Thus, it cannot be ruled out the possibility that changes in stigmasterol levels might alter the activity of these branching-point enzymes. In this manner, the deregulation of the SMT2/3 enzyme might alter the flux of precursors through the ethyl-branch of the sterol pathway and affect brassinosteroid levels. However, the sterol analysis showed decreased levels of campesterol only in red ripe fruits but not in leaves or seeds (Table 1), thus suggesting that brassinosteroid metabolism is not affected. Hence, the problems in cell division seem to be caused directly by the lack of stigmasterol and/or the consequent β-sitosterol accumulation. This hypothesis is consistent with previous results in which only stigmasterol was able to restore celery cells full-growth when treated with the growth retardant PGR tetcyclacis, which acts as an inhibitor of CYP51, an enzyme involved in the early sterol pathway, therefore blocking the sterol biosynthesis (Goad, 1990). This result sets stigmasterol as a key metabolite controlling cell proliferation. Such a function might be related to its importance as a building block for the assembly of biological membranes, in which the correct composition is key for the right positioning of signal transduction

proteins (Aboobucker and Suza, 2019), and for the growth or expansion of the membranes themselves.

The phenotypic abnormalities of the mutants within the sterol pathway have been analyzed with regard to their specific sterol profiles (Carland, Fujioka and Nelson, 2010). Severe defects including abnormal meristem and root patterning, altered pattern of embryo development, reduced size and seedling lethality are described in Arabidopsis plants with mutations in genes of the early sterol pathway as *sterol C14-reductase* or *CYP51* (Jang *et al.*, 2000; Kim *et al.*, 2005). All of these mutants have an overall reduction in the plant sterol end-products but not in cholesterol, which is synthesized by a separate branch of the pathway independently of the mentioned enzymes (Souter *et al.*, 2002; Schrick *et al.*, 2004). Particularly, the above-mentioned mutants are impaired in embryo development and most of them show abnormal cotyledon morphology. Specifically, in *fackel* mutants, the embryos at the heart stage failed to develop cotyledon primordia (Jang *et al.*, 2000). On the other hand, *smt2/3* Arabidopsis mutants represented a more accurate tool for assessing specifically the role of β-sitosterol and stigmasterol (24-ethyl sterol species) in adult plants. Reduction of these sterols from the 24-ethyl branch led to a less severe phenotype, including a loss of polarity both at the vascular cell level and the organ level, rounded cotyledons, short roots, and reduced plant stature, and most importantly, they were able to grow to maturity. Carland *et al.* (2010) proposed all of these mild phenotypes to be a consequence of the reduced β-sitosterol levels, although the stigmasterol levels were also decreased to only 1% of WT levels. We show here that the lack of stigmasterol resulted in marked defects on embryo development, including cotyledon differentiation (Figures 8, 10). In agreement with these results, the transgenic plants that accumulate stigmasterol in seeds (*35S:C22DES* #12.2) showed the opposite phenotype: a higher percentage of well-differentiated embryos were found in comparison with the WT, thus remarking the pivotal role of stigmasterol during embryogenesis.

In general, the most remarkable changes in the sterol composition of the *C22des*$^{-}$ mutant were the depletion of stigmasterol in all tomato plant organs (leaves, red ripe fruit, and seeds) and the accumulation of its immediate precursor, β-sitosterol, which only occurred in leaves and red ripe fruits (Table 1). In fact, the sterol composition in seeds, which is the analyzed plant organ most related to embryos,

only differs from the WT in the stigmasterol levels, with no concomitant accumulation of β-sitosterol. These data are in agreement with our previous hypothesis that the stigmasterol sensing and regulation mechanism is laxer or even inexistent in seeds. Therefore, we have accurately delimited this phenotype in seeds to the altered composition of only one sterol end-product, stigmasterol, which represents one of the most specific mutants so far described in the plant sterol biosynthetic pathway.

In several plant species, the observed accumulation of sterols in developing seeds correlates with an increase in the expression of different sterol biosynthetic genes and the activity of some biosynthetic enzymes (Harker, Hellyer and Clayton, 2003; Schrick *et al.*, 2011; Suza and Chappell, 2016). It has been reported that in *smt1* mutants, an aberrant sterol composition in cell membranes cause defects in cell polarity due to an incorrect localization of PIN proteins, which are active transporters involved in the efflux of auxin (Willemsen *et al.*, 2003; Möller and Weijers, 2009). This plant hormone is considered the principal component regulating the embryo patterning since the regulated auxin maxima and activity are required for the organization of both the apical and basal embryo domains (Steinmann *et al.*, 1999; Al-hammadi *et al.*, 2003; Möller and Weijers, 2009). When PIN1 is not well-positioned it is intracellularly accumulated and the auxin efflux is affected, generating problems in embryonic cell and tissue polarity (Steinmann *et al.*, 1999). In WT tomato, *C22DES* expression also increases during seed development (Figure S6), and it is possible that *C22des*$^{-}$ embryo defects and subsequent seedling establishment defects could be also a consequence of PIN mislocalization due to an altered sterol composition of the plasma membrane.

It was not possible to rescue seedling viability in the *C22des*$^{-}$ mutant by the exogenous application of stigmasterol (Figure 9D) neither before seed germination nor after germination on agar plates containing stigmasterol (data not shown). It is likely that embryonic defects cannot be rescued once the embryo is already formed with abnormal characteristics. However, seed germination highly improved in previously soaked seeds (Figure 9C) suggesting that the lower germination rate of the mutant could be due to problems in the radicle protrusion, which led us to propose that soaking would soften the testa allowing an easier seed-coat cracking. The testa rupture involves a number of biological processes including hormone

homeostasis as well as embryo cell expansion/elongation in the embryonic axis (Steinbrecher and Leubner-Metzger, 2018). We hypothesize that either some defect on the embryo growth and/or in the physical properties of the radicle tissue, which could be losing its firmness and consequently its strength to emerge from the seed, could be responsible for the reduced germination ability of *C22des*$^{-}$ mutant seeds.

Plants are typically exposed to various and complex types of environmental factors that lead to biotic and abiotic stresses. The exposure of plants to these type of stresses seriously affects plant metabolism implying severe reductions in their growth and yield (Rejeb, Pastor and Mauch-Mani, 2014; Pandey *et al.*, 2017). To deal with this kind of stressful situations, plants have evolved specific mechanisms activating defense responses in order to improve their adaptation. These responses involve signaling pathways regulated by phytohormones (ABA, JA or SA, among others). Genes encoding *C22DES* in Arabidopsis have been described to be phytohormone-responsive, suggesting the stigmasterol involvement in various stress responses (Aboobucker and Suza, 2019). Our gene expression results in tomato seedlings are in agreement with the results obtained by several studies in various species. The stigmasterol levels were described to experience some perturbations when plants were exposed to different stresses such as salinity stress (Douglas and Walker, 1983; Mansour, Hasselt and Kuiper, 1994; Hashem *et al.*, 2011), cold stress (Whitaker, 1991; Senthil-Kumar, Wang and Mysore, 2013) and pathogen infections (Griebel and Zeier, 2010; Wang *et al.*, 2012). This is in contrast to the possible involvement of C22DES in the biotic stress responses since our results showed that *C22DES* transcript levels did not show significant differences after FLA, JA, and SA treatments (Figure 2). With all these data, the involvement of C22DES and stigmasterol in abiotic stress responses seems to be clear, but a role in the biotic stress responses still remains to be unequivocally established.

However, the results obtained in the *Botrytis cinerea* infection experiments, suggest that stigmasterol is important to improve pathogen resistance in tomato fruits since the *C22des*- mutant showed higher susceptibility than the WT and the *C22DES* overexpressing lines (Figure 11). Although the red ripe fruits of these last lines showed reduced stigmasterol levels in control conditions (Figure 5), it is likely that C22DES activity may be increased under stress situations.

Previous studies concerning infections with *Botrytis cinerea* in *Arabidopsis* plants with reduced levels of stigmasterol showed increased nutrient efflux into the apoplast. The apoplastic fluid from these plants promoted pathogen multiplication compared to WT (Wang *et al.*, 2012). Membrane permeability plays an important role in nutrient efflux into the apoplast, and sterols are known to modify the physicochemical properties of the plasma membrane. Specifically, stigmasterol, due to its less planar structure than other sterols such as cholesterol or campesterol, is less efficient in stabilizing the plasma membrane and therefore is unable to influence membrane permeability (Grunwald, 1971; Grosjean *et al.*, 2015).

Moreover, Choi *et al.* (2017) reported the antifungal properties of stigmasterol when sprayed onto seedlings before inoculation. During tomato fruit ripening, multiple metabolic changes occur contributing, among other effects, to increase the pathogen susceptibility. Therefore, ripe fleshy fruits are more susceptible to disease and decomposition than unripe green fruits (Cantu *et al.*, 2009). Based on the fact that stigmasterol provides protection against pathogens, it is possible that the observed increase of *C22DES* expression during the early stages of tomato fruit ripening (Figure 1) could be part of defense mechanisms to reduce fruit susceptibility. As the fruit ripens, the *C22DES* expression progressively drops down (Figure 1), which could be somehow related to the increased susceptibility of over-ripened fruits. Considering the results obtained in the gene expression analysis in seedlings under stress conditions (Figure 2) and the results of the Botrytis infection experiments in fruits (Figure 11), it is likely that *C22DES* is not involved in biotic defense mechanisms at the seedling stage and for this reason, *C22DES* expression levels were not altered by the FLA, JA, and SA treatments. In agreement with this hypothesis, several studies have reported the differential efficiency of pathogen resistance among different plant organs, thus pointing to tissue-specific mechanisms (Strugala, Delventhal and Schaffrath, 2015).

In conclusion, we demonstrated that stigmasterol is not essential for plant life, at least in tomato, although it contributes significantly to the normal functioning of several biological processes such as embryo development and cell division. We also provide evidence that stigmasterol plays a role in tomato plant defense against biotic stress, although further studies would be necessary to conclusively demonstrate this issue. Lastly, the generation of the first to-date stigmasterol-free plant might be

considered one of the most interesting contributions of this work since it provides a valuable tool to evaluate the physiological role of stigmasterol in plants.

5. MATERIALS AND METHODS

5.1 Plant material, growth condition, and treatments

Tomato (*Solanum lycopersicum* cv. Micro-Tom) plants were used for most experiments. Seeds were surface-sterilized as described by Ramirez-Estrada *et al*., 2017. For stigmasterol-supplemented germination experiments, seeds were soaked overnight at room temperature in a stigmasterol solution [0.02% stigmasterol (w/v), 0.1 % Tween-20 (v/v), 4.84% EtOH (w/v)], or a control solution [4.84% EtOH (v/v), 0.1% Tween-20 (v/v)] prior to sowing.

Sterile seeds were sown on MS plates (0.5 x Murashige and Skoog basal salts medium supplemented with Gamborg B5 vitamins, sucrose (3% w/v) and agar (0.8% w/v). Kanamycin (100 µg/mL) was also added when required to select transgenic plants. After stratification for 2 days in darkness at 24ºC, plates were transferred to a climate-controlled growth chamber set for long-day conditions (16 h light/8 h darkness) at an irradiance of 150 $\mu mol^{-2}s^{-1}$ and 24ºC. 7 to 10-days-old seedlings were transferred to pots filled with soil (peat, vermiculite and perlite 5:1:1) and grown under standard greenhouse conditions (14 h light at 27 ± 1 °C and 10 h dark at 22 ± 1 °C).

For stress experiments, seeds were sown in glass jars instead of plates. Pools of five 12-day-old seedlings were transferred to glass jars containing 30 mL of MS liquid medium lacking sucrose and allowed to grow for an additional week under the same conditions described above. Then, growth medium was replaced by new MS liquid medium supplemented with the desired effectors: 200 mM mannitol, 150 mM NaCl, 0.1 mM abscisic acid (ABA), 0.5 mM salicylic acid (SA), 1 mM flagellin 22 (FLA) or 0.5 mM methyljasmonate (MeJa). For wounding experiments leaves of seedlings in the MS liquid medium were injured with forceps, whereas for cold treatment seedlings were transferred to a growth chamber set for long-day conditions (16 h light/8 h darkness) at an irradiance of 150 $\mu mol^{-2}s^{-1}$ and at 4ºC. Samples were collected at different exposure time points (0, 3, 6, 12, 24 and 48 h), immediately frozen in liquid

nitrogen and ground to a fine powder using a mortar. All the treatments were performed in three independent biological replicates.

For determining the expression profile of *C22DES* gene during fruit ripening and cold stress, fruits were collected at 5 different developmental (growth and ripening) stages established on the basis of the days post-anthesis (DPA) or post-breaker (DPB): small green (SG, ≈20 DPA), mature green (MG, ≈30 DPA), breaker (BR, ≈35 DPA), orange (OR, ≈3-5 DPB), and ripe red (RR, ≈15 DPB). The fruit pericarp was collected, frozen in liquid nitrogen and ground to a fine powder. Three independent biological replicates were collected for each experiment, and each biological replicate consisted of a pool of 4 tomato fruits. Both fruit and seedling samples were stored at -80ºC until further analysis.

Nicotiana benthamiana plants were grown under standard greenhouse conditions (14 h light at 26 ± 1°C and 10 h dark at 21 ± 1°C) in individual pots of 12cm diameter.

5.2 Cloning and plasmid constructions

All constructs for CRISPR/Cas9-mediated genome editing were generated as described by Schiml *et al.* (2017), with a single modification: the phosphinothricin resistance gene (*BAR*) in the pDE-Cas9 was replaced by the kanamycin resistance gene (*NPTII*) by restriction digest with *Hind*III and subsequent ligation to generate pDE-Cas9-Kan^{R} (Table S7). The sgRNAs for *C22DES* gene disruption (Figure 6A) were designed using the Breaking-Cas tool (http://bioinfogp.cnb.csic.es/tools/breakingcas/) (Oliveros *et al.*, 2016), and the corresponding primer pairs are shown in Table S5.

The binary plasmids used for overexpression (*35S:C22DES* and *E8:C22DES*) and silencing (*35S:amiC22DES* and *E8:amiC22DES*) of the *C22DES* gene were previously obtained in the laboratory (Bonilla Jaime, 2015).

The C22DES coding sequences lacking the stop codon for in-frame fusions with the GFP coding sequence were amplified by PCR using the *35S:C22DES* plasmid as a template, which was previously obtained in the laboratory (C22DES GenBank: NM_001247585). All the PCR reactions were performed using high-fidelity AccuPrime^{TM} Taq DNA polymerase (Invitrogen) and specific primer pairs (Tables S5,

S7). The PCR products were cloned into pDONR207 donor vector using Gateway® (GW) technology (Invitrogen). The cDNAs in the resulting pENTRY plasmids were sequenced to exclude the presence of amplification mutations, and subcloned into the binary vectors pEarleyGate103 (Earley *et al.*, 2006) by GW recombination to generate binary plasmids coding for C22DES-GFP fusions. In all cases, the coding sequences were under the control of the *CaMV35S* promoter. Constructs were confirmed by restriction mapping and DNA sequence analysis.

5.3 Bacterial strains and media

Chemically competent Top10 *Escherichia coli* strain was used for all subcloning steps as described previously (Pope and Kent, 1996). Transformants were selected on LB plates supplemented with the appropriate antibiotics (Table S7). *Agrobacterium tumefaciens* GV3101 was used for transient and stable transformations of *N. benthamiana* and tomato plants, respectively. Binary plasmids were introduced into this strain by thermal shock as described by Höfgen and Willmitzer (1988). Positive transformants were selected on YEB plates supplemented with rifampicin 50 µg/mL, gentamycin (25 µg/mL) and the respective plasmid selection antibiotics: kanamycin (100 µg/mL) or streptomycin (100µg/mL). In all cases, the presence of the recombinant plasmids in the antibiotic-resistant bacterial colonies was analyzed by colony PCR.

5.4 Gene expression analysis by RT-qPCR

Total RNA was isolated from around 100 mg of ground frozen tissue (tomato fruit pericarp, seedlings, or leaves) using the *Maxwell® RSC Plant RNA Kit* with the *Maxwell® RSC Instruments* (Promega) according to manufacturer's instructions. The cDNA samples for RT-qPCR were prepared from 0.5-1 µg of DNA-free RNA using the *Transcriptor First Strand cDNA Synthesis Kit* (Roche) following the provided recommendations. Prior to use, the cDNA was diluted ten-fold and its integrity was checked by PCR using specific primers for the ACTIN gene *Solyc03g078400*. Relative mRNA abundance of target genes was evaluated by Real-Time Quantitative Polymerase Chain Reaction (RT-qPCR) that was performed with a *LightCycler 480*

Real-Time PCR System (Roche) in a total volume of 10 µl containing 5 µl *LightCycler 480 SYBR Green I Master Mix* (Roche), 0.25 µM of each specific forward (Fw) and reverse (Rv) primer (Table S5), 2.5 µl water and 2 µl of ten-fold diluted cDNA. The LightCycler experimental run protocol used was: 95°C for 10 min followed by 40 cycles of 95°C for 10 s, 60°C for 30 s, and a final cooling step to 4°C. The raw PCR data from LightCycler software 1.5.0 was used in the analysis. For stress experiments and ripening expression profile, the analysis was conducted using three independent biological replicates of each condition and their respective technical triplicates. For transgenic lines characterization, three technical replicates of a single pool of samples from different individual plants were used. Normalized transcript abundances were calculated as follows:

$$\Delta Ct = Ct_{target} - Ct_{reference}$$

and the fold-change value was calculated using the $2^{-\Delta Ct}$ expression (Livak and Schmittgen, 2001), using tomato *CAC* (*Solyc08g006960*) or *PP2A* (*Solyc02g093800*) as endogenous reference genes. Primer efficiencies were calculated in triplicate using six serial dilution points (ranging from 6.25 to 200 ng) of genomic or plasmid DNA.

5.5 Generation and genotyping of tomato transgenic lines

A. tumefaciens GV3101 strain carrying the appropriate constructs (Table S7) was used to stably transform tomato cv MicroTom cotyledons as previously described by Fernandez *et al.* (2009).

The genomic DNA was obtained from leaf tissue using the cetyltrimethyl ammonium bromide (CTAB) method. A piece of tomato leaf of about 100 mg of fresh weight was immediately frozen in liquid nitrogen, ground to a fine powder using a TissueLysser II (Qiagen), and mixed with 600 µl of ice-cold extraction buffer (50 mM Tris-HCl pH 8.0 and 20 mM EDTA). After adding 80 µl of SDS 10% (w/v), samples were vortexed and incubated at room temperature for 15 min. Then, 180 µl of NaAc pH 5.2 3M was added to the mix and incubated on ice for 30 min. Samples were centrifuged at 10,000 rpm for 15 min and the supernatant was transferred to a new tube. The same volume of isopropanol was added and incubated on ice for 30 min. Samples were

centrifuged at 10,000 rpm for 10 min and the pellet was resuspended in 300 µl 10mM Tris-HCl pH 8.0. After that, the sample was mixed with 300 µl CTAB [2% CTAB (w/v), 2M NaCl, 0.2 M Tris-HCl pH 8, 0.05 M EDTA] and incubated at 65º C for 15 min. Finally, 600 µl of chloroform were added, mixed and centrifuged for 5 min at maximum speed. The aqueous phase was recovered, mixed with the same volume of isopropanol and incubated at -20ºC for at least 2 hours. Finally, samples were centrifuged at maximum speed for 10 min and the DNA pellet was resuspended with 50 µl of water.

The presence of the transgenes was checked by PCR with pairs of primers specific for *NPTII* and selected regions of the transgenes. In the case of the overexpressing and silenced *C22DES* lines, 2 different gene-specific pairs of primers were used (Table S5, Table S6) to check the integrity of the whole transgene: one corresponding to the promoter region, either E8 or CaMV35S, and the other one corresponding to the *C22DES* cDNA coding sequence or the amiRNA coding gene. The transgene copy number in the different plant generations was determined by qPCR as described in Yang *et al.* (2005) using tomato *LAT52* (*Solyc10g007270*) as the endogenous single-copy gene and *NPTII* as the target gene. At least three generations were analyzed to assure homozygosis for the transgene in segregating plants.

For the CRISPR-Cas9 lines, the genomic region encompassing the sgRNA target sites (Figure 6A) was amplified by PCR and the resulting products were cloned into *pGEM®-T Easy Vector* (Promega). Plasmid DNA from 10 positive colonies from each transgenic line was isolated using *Wizard® Plus SV Minipreps DNA Purification systems* (Promega) according to manufacturer's instructions and sequenced for genomic mutations identification. All the specific primers used in these experiments are described in Table S5.

5.6 Transient overexpression in *Nicotiana benthamiana* leaves

A. tumefaciens GV3101 cells harboring *35S:C22DES-GFP* or *35S:c22des⁻-GFP* constructs were used to transiently transform *Nicotiana benthamiana* leaves as previously described (Sparkes *et al.*, 2006; Wydro, Kozubek and Lehmann, 2006). The resulting strains were separately mixed in a 1:1 ratio with an *Agrobacterium tumefaciens* strain harboring the HC-Pro silencing suppressor (Goytia *et al.*, 2006)

and infiltrated in leaves of 3- to 5-week-old *N. benthamiana* plants employing the syringe infiltration method. Plants were kept growing under long-day conditions at 25°C for 3-4 days until further analysis.

5.7 Sterol analysis

Different plants species and tissues were used for sterol composition determinations. *N. benthamiana* leaves from more than three independent agroinfiltrated plants were harvested in pools. Two independent biological replicates were performed with their respective technical triplicates.

In tomato plants, the sterol composition from leaves, red ripe fruits, and seeds was determined. Leaf samples consisted of a pool of the third pair of leaves from 5 different plants. In the case of fruit samples, pools of the pericarp of 5 red fruits (10 DPB) from different plants were made, and finally, about 300 mg of seeds were pooled for determining seed sterol composition. Three technical replicates were analyzed for each sample.

All plant tissue samples, including leaf, fruit pericarp, and seed, were frozen in liquid nitrogen, ground to a fine powder and lyophilized prior to use. Around thirty milligrams of the lyophilized tissue was placed in a glass tube and 100 µl of a mix of internal standards containing 2.5 µg of cholestanol (FS), 5 µg of palmitoyl-cholestanol (SE), 5 µg of cholestanyl-β-D-glucoside (SG) and 5 µg of palmitoyl-β-D-glucosyl-cholestanol (ASG) dissolved in chloroform-methanol 2:1] was added. In the case of seeds, two aliquots of lyophilized tissue were used for each sample, one for FS and SE extraction and the other one for SG and ASG extraction, since the high amount of triacylglycerols in seeds may impair the visualization of sterol fractions in the TLC separation. Therefore, in the first tube a mix of FS and SE internal standards [2.5 µg of cholestanol (FS) and 5 µg of palmitoyl-cholestanol (SE) in chloroform-methanol 2:1] was added, and in the second one a mix of SG and ASG internal standards [5 µg of cholestanyl-β-D-glucoside (SG) and 5 µg of palmitoyl-β-D-glucosyl-cholestanol (ASG) in chloroform-methanol 2:1] was included.

Sterols were then extracted with 3 mL of a chloroform-methanol solution (2:1). Samples were vigorously homogenized, sonicated for 10 min at room temperature

and incubated at room temperature for 1h to complete the sterol extraction. Then, 1.5 mL of 0.9% (w/v) NaCl were added to facilitate further phase separation. The organic phase was recovered by centrifugation at 5000rpm for 5 min in a JA-20 rotor (Beckman Coulter) and filtered through a Pasteur pipette with a glass wool filter. The remaining aqueous phase was re-extracted with 3 mL of the chloroform-methanol solution (2:1) and the two organic extracts were mixed together for subsequent evaporation to dryness using a SpeedVac® Concentrator (Savant). The dried residue was dissolved in 150 µl of chloroform and the four sterol fractions were separated by thin-layer chromatography (TLC) using precoated silica gel PLC 60 F254 plates (20 cm x 20 cm) (Merck) and three different mobile phases depending on the separated fractions: For the four fractions separation dichloromethane-methanol-acetic acid (92:8:2) was used; for FS and SE fractions separation, TLC plates were placed in petroleum ether-diethyl ether-acetic acid (70:30:2) until the mobile phase reached half of the plate and then in petroleum ether-diethyl ether (98:2) until reaching 1 cm from the top of the plate; and for SG and ASG fractions separation, dichloromethane-methanol-acetic acid (90:10:2) was used. A mix of the respective standards was also applied onto the TLC plates as markers. For the fractions visualization, plates were sprayed with a 0.01% primuline (Sigma-Aldrich) solution and detected with a UV lamp. All fractions were separately scraped from the silica plates and placed in a glass tube. For the acidic hydrolysis of SG and ASG, 1.5 mL of a 0.5 N HCl methanolic solution was added to the silica powder, and for the basic hydrolysis of SE, 1.5 mL of 7.5% (w/v) KOH methanolic solution was used. After incubation at 85ºC for 2 h, the reaction was stopped with 1.5 mL of 0.9% (w/v) NaCl, and the FS moieties were extracted twice with 3 mL of *n*-hexane and centrifuged at 5000 rpm for 5 min in a JA-20 rotor (Beckman Coulter). The hexanic phases were collected in a new tube, mixed and evaporated to dryness. Sterol samples were resuspended in 50µl of tetrahydrofuran (THF) and derivatized by adding 50 µl of BSTFA (Regis technologies). The mix was incubated 30 min at 60ºC, evaporated to dryness and dissolved in 50 µl of isooctane. Samples were then analyzed by GC-MS using an Agilent 7890A gas chromatograph equipped with a Sapiens-X5ms capillary column (30 m x 0.25 mm x 0.25µm) (Teknokroma) coupled with a 5975C mass spectrometer (Agilent). Peaks were integrated using MSD offline Data Analysis software (Agilent).

5.8 Morphometric and physiological analysis

The different morphological traits listed in Table 2 were measured in plants at 5 weeks old. Epidermal cell sizes were analyzed by light microscopy and the area was calculated using ImageJ software. The average fruit weight was determined at 15 DPB.

5.9 Germination tests

Four replicates of >20 seeds each per lot were sown in solid medium as mentioned above. Radicle emergence was observed from 1 to 8 days after sowing (DPS) and results were expressed as the mean percentage of germination per seed lot. Seedling viability was calculated as the mean percentage of normal seedlings per experiment.

5.10 Embryo analysis

Seeds were preconditioned before tetrazolium salt (TZ) staining to have proper penetration of the solution and to prevent damage of the embryos while cutting seeds. The preconditioning consisted of the hydration of the seeds between moistened paper-towel sheets for 18 h at 37ºC and the subsequent puncture of the seed coat with a thin awl or a needle in the one-third section of the seed, between the micropyle and the embryo. Then, seeds were placed on a multi-well dish, covered with 5 mL of 0.1% TZ (w/v) and incubated in darkness at 37ºC overnight. The TZ solution was discarded, the seeds rinsed thoroughly with cool, running tap water and left immersed in water until embryo analysis. For embryo observations, seeds were cut longitudinally through the midsection of the embryonic axis with a scalpel, the embryos were carefully taken out from the seed with a forceps, and observed under magnification (40x). Embryos were classified in normal and abnormal based on their appearance and the presence of non-stained tissues.

5.11 Inoculation of *B. cinerea* spores onto tomato fruits

Botrytis cinerea was kindly provided by Dr. M. Coca (CRAG, Barcelona). Tomato (*Solanum lycopersicum* cv. Micro-Tom) red ripe fruits were harvested at 15 DPB and surface-cleaned with EtOH 30% (v/v). A small lesion was made on each fruit with a punch to improve the inoculum penetration. Then, spores of *B. cinerea* were suspended in glucose 0.2% (w/v) at a final concentration of $5 \cdot 10^6$ conidia/mL and a drop of 10 µl was applied onto the fruit lesions. Inoculated fruits were kept in a glass container hermetically sealed to maintain high humidity necessary for fungal infection progression. The progression of symptoms was followed visually in 9 fruits of 9 independent plants for each genotype.

5.12 Quantification of *B. cinerea* DNA in infected tomato fruits

Infected tomato fruits were incubated for 6 days post-infection (dpi) under the conditions mentioned above. Then, 3 g of a pool of the infected area of 9 fruits were collected, of, immediately frozen in liquid nitrogen and ground to a fine powder. Samples were stored at -80ºC until use. DNA from each sample was extracted using the CTAB method as described above. DNA quantifications were conducted by qPCR using about 100 ng of total gDNA as a template and specific pairs of primers for *B. cinerea* β-tubulin gene (GenBank: KC620303) and for the tomato actin gene (*SlACT,* Solyc11g005330.1), which was used as reference endogenous gene (Ueda *et al.*, 2018). Primers are listed in Table S5.

6. REFERENCES

Aboobucker, S. I. and Suza, W. P. (2019) 'Why Do Plants Convert Sitosterol to Stigmasterol?', *Frontiers in Plant Science*, 10(March), pp. 1–8. doi: 10.3389/fpls.2019.00354.

Al-hammadi, A. S. A. *et al.* (2003) 'The polycotyledon Mutant of Tomato Shows Enhanced Polar Auxin Transport', *Plant Physiology*, 133(September), pp. 113–125. doi: 10.1104/pp.103.025478.cells.

Bak, S. *et al.* (2011) *Cytochromes P450*, *The Arabidopsis Book*. doi: 10.1199/tab.0144.

Ballester, M., Cordón, R. and Folch, J. M. (2013) 'DAG Expression : High-Throughput Gene Expression Analysis of Real-Time PCR Data Using Standard Curves for Relative Quantification', *PLOS ONE*, 8(11), pp. 1–5. doi: 10.1371/journal.pone.0080385.

Bansal, R. *et al.* (2019) 'A Plant like Cytochrome P450 Subfamily CYP710C1 Gene in Leishmania donovani Encodes Sterol C-22 Desaturase and its Over- expression Leads to Resistance to Amphotericin B', *PLoS Neglected Tropical Diseases*, 13(4), pp. 1–23.

Benveniste, P. (2004) 'Biosynthesis and Accumulation of Sterols', *Annual Review of Plant Biology*, 55(1), pp. 429–457. doi: 10.1146/annurev.arplant.55.031903.141616.

Bonilla Jaime, J. (2015) *Nuevas aproximaciones al estudio del metabolismo de los esteroles en tomate*. Universitat de Barcelona.

Cantu, D. *et al.* (2009) 'Ripening-Regulated Susceptibility of Tomato Fruit to Botrytis cinerea Requires NOR But Not RIN or Ethylene', *Plant Physiology*, 150(3), pp. 1434–1449. doi: 10.1104/pp.109.138701.

Carland, F., Fujioka, S. and Nelson, T. (2010) 'The Sterol Methyltransferases SMT1, SMT2, and SMT3 Influence Arabidopsis Development through Nonbrassinosteroid Products', *Plant Physiology*, 153(2), pp. 741–756. doi: 10.1104/pp.109.152587.

Carland, F. M. *et al.* (2002) 'The Identification of CVP1 Reveals a Role for Sterols in Vascular Patterning', *The Plant Cell*, 14(9), pp. 2045–2058. doi: 10.1105/tpc.003939.

Carrari, F. *et al.* (2006) 'Integrated analysis of metabolite and transcript levels reveals the metabolic shifts that underlie tomato fruit development and highlight regulatory aspects of metabolic network behavior', *Plant physiology*, 142(4), pp. 1380–1396. doi: 10.1104/pp.106.088534.

Chaudhary, J. *et al.* (2019) 'Mutation Breeding in Tomato: Advances, Applicability and Challenges', *Plants*, 8(128), pp. 1–17.

Choe, S. *et al.* (1999) 'The Arabidopsis dwf7/ste1 Mutant Is Defective in the Δ 7 Sterol C-5 Desaturation Step Leading to Brassinosteroid Biosynthesis', *The Plant Cell*, 11(2), pp. 207–221. doi: 10.2307/3870851.

Choi, N. H. *et al.* (2017) 'Antifungal activity of sterols and dipsacus saponins isolated from Dipsacus asper roots against phytopathogenic fungi', *Pesticide Biochemistry and Physiology*. Elsevier B.V., 141, pp. 103–108. doi: 10.1016/j.pestbp.2016.12.006.

Chow, E. T. S. and Jen, J. J. (1978) 'Phytosterol biosynthesis in ripening tomatoes', *Journal of Food Science*, 43(5), pp. 1424–1426.

Dean, R. *et al.* (2012) 'The Top 10 fungal pathogens in molecular plant pathology.', *Molecular plant pathology*, 13(4), pp. 414–30. doi: 10.1111/j.1364-3703.2011.00783.x.

Diener, A. C. *et al.* (2000) 'STEROL METHYLTRANSFERASE 1 Controls the Level of Cholesterol in Plants', *The Plant Cell*, 12(6), pp. 853–870. doi: 10.2307/3871215.

Douglas, T. J. and Walker, R. R. (1983) '4-Desmethylsterol composition of citrus rootstocks of different salt exclusion capacity', *Physiologia Plantarum*, 58, pp. 69–74.

Earley, K. W. *et al.* (2006) 'Gateway-compatible vectors for plant functional genomics and proteomics', *The Plant Journal*, 45(4), pp. 616–629. doi: 10.1111/j.1365-313X.2005.02617.x.

Estornell, L. H. *et al.* (2009) 'A multisite gateway-based toolkit for targeted gene expression and hairpin RNA silencing in tomato fruits', *Plant Biotechnology Journal*, 7, pp. 298–309. doi: 10.1111/j.1467-7652.2009.00402.x.

Fabro, G. *et al.* (2008) 'Genome-Wide Expression Profiling Arabidopsis at the Stage of Golovinomyces cichoracearum Haustorium Formation', *Plant Physiology*, 146, pp. 1421–1439. doi: 10.1104/pp.107.111286.

Fernandez, A. I. *et al.* (2009) 'Flexible Tools for Gene Expression and Silencing in Tomato', *Plant Physiology*, 151(4), pp. 1729–1740. doi: 10.1104/pp.109.147546.

Ferrer, A. *et al.* (2017) 'Emerging roles for conjugated sterols in plants', *Progress in Lipid Research*. Elsevier, 67, pp. 27–37. doi: 10.1016/j.plipres.2017.06.002.

Goad, L. J. (1990) 'Application of sterol synthesis inhibitors to investigate the sterol requirements of protozoa and plants', *Biochemical Society Transactions*, 18(1), pp. 63–65. doi: 10.1042/bst0180063.

Goytia, E. *et al.* (2006) 'Production of Plum pox virus HC-Pro functionally active for

aphid transmission in a transient-expression system', *Journal of General Virology*, 87(11), pp. 3413–3423. doi: 10.1099/vir.0.82301-0.

Griebel, T. and Zeier, J. (2010) 'A role for β-sitosterol to stigmasterol conversion in plant-pathogen interactions', *Plant Journal*, 63(2), pp. 254–268. doi: 10.1111/j.1365-313X.2010.04235.x.

Grosjean, K. *et al.* (2015) 'Differential Effect of Plant Lipids on Membrane Organization: hot features and specificities of phytosphingolipids and phytosterols', *Journal of Biological Chemistry*, 290, pp. 5810–5825. doi: 10.1074/jbc.m114.598805.

Grunwald, C. (1971) 'Effects of Free Sterols, Steryl Ester, and Steryl Glycoside on Membrane Permeability', *Plant Physiology*, 48(5), pp. 653–655. doi: 10.1104/pp.48.5.653.

Harker, M., Hellyer, A. and Clayton, J. C. (2003) 'Co-ordinate regulation of sterol biosynthesis enzyme activity during accumulation of sterols in developing rape and tobacco seed', *Planta*, 216, pp. 707–715. doi: 10.1007/s00425-002-0913-3.

Hartmann, M.-A. (1998) 'Plant sterols and the membrane environment', *Trends in Plant Science*, 3(5), pp. 170–175. Available at: http://www.cell.com/trends/plant-science/pdf/S1360-1385(98)01233-3.pdf.

Hashem, H. A. *et al.* (2011) 'Stigmasterol seed treatment alleviates the drastic effect of NaCl and improves quality and yield in flax plants', *Australian Journal of Crop Science*, 5(13), pp. 1858–1867.

Höfgen, R. and Willmitzer, L. (1988) 'Storage of competent cells for Agrobacterium transformation', *Nucleic Acids Research*, 16(20), p. 9877. Available at: https://www.ncbi.nlm.nih.gov/pmc/articles/PMC338805/pdf/nar00162-0496.pdf.

Jang, J.-C. *et al.* (2000) 'A critical role of sterols in embryonic patterning and meristem programming revealed by the fackel mutants of Arabidopsis thaliana', *Genes and Development*, 14(12), pp. 1485–1497.

Kim, H. B. *et al.* (2005) 'Arabidopsis cyp51 Mutant Shows Postembryonic Seedling Lethality Associated with Lack of Membrane Integrity', *Plant Physiology*, 138, pp. 2033–2047. doi: 10.1104/pp.105.061598.as.

Livak, K. J. and Schmittgen, T. D. (2001) 'Analysis of Relative Gene Expression Data Using Real- Time Quantitative PCR and the 2 -☒☒CT Method', *METHODS*, 25, pp. 402–408. doi: 10.1006/meth.2001.1262.

Mansour, M. M. F., Hasselt, P. R. Van and Kuiper, P. J. C. (1994) 'Plasma membrane

lipid alterations induced by NaCl in winter wheat roots', *Physiologia Plantarum*, 92, pp. 473–479.

Möller, B. and Weijers, D. (2009) 'Auxin Control of Embryo Patterning', *Cold Spring Harbor Perspectives in Biology*, pp. 1–13.

Morikawa, T. *et al.* (2006) 'Cytochrome P450 CYP710A Encodes the Sterol C-22 Desaturase in Arabidopsis and Tomato', *The Plant Cell*, 18(4), pp. 1008–1022. doi: 10.1105/tpc.105.036012.

Nomura, T. *et al.* (1999) 'Brassinosteroid / Sterol Synthesis and Plant Growth as Affected by lka and lkb Mutations of Pea', *Plant Physiology*, 119, pp. 1517–1526.

Oliveros, J. C. *et al.* (2016) 'Breaking-Cas —– interactive design of guide RNAs for CRISPR-Cas experiments for ENSEMBL genomes', *Nucleic Acids Research*, 44(May), pp. 267–271. doi: 10.1093/nar/gkw407.

Pandey, P. *et al.* (2017) 'Impact of Combined Abiotic and Biotic Stresses on Plant Growth and Avenues for Crop Improvement by Exploiting Physio-morphological Traits', *Frontiers in Plant Science*, 8(537), pp. 1–15. doi: 10.3389/fpls.2017.00537.

Pope, B. and Kent, H. M. (1996) 'High efficiency 5 min transformation of Escherichia coli', *Nucleic Acids Research*, 24(3), pp. 536–537.

Ramírez-Estrada, K. *et al.* (2017) 'Tomato UDP-Glucose Sterol Glycosyltransferases : A Family of Developmental and Stress Regulated Genes that Encode Cytosolic and Membrane-Associated Forms of the Enzyme', *Frontiers in Plant Science*, 8(June), pp. 1–21. doi: 10.3389/fpls.2017.00984.

Rejeb, I. Ben, Pastor, V. and Mauch-Mani, B. (2014) 'Plant Responses to Simultaneous Biotic and Abiotic Stress: Molecular Mechanisms', *Plants*, 3(4), pp. 458–475. doi: 10.3390/plants3040458.

Russell, D. W. and Davidson, H. (1982) 'Regulation of cytosolic HMG-CoA reductase activity in pea seedlings: Contrasting responses to different hormones, and hormone-product interaction, suggest hormonal modulation of activity', *Biochemical and Biophysical Research Communications*, 104(4), pp. 1537–1543. doi: 10.1016/0006-291X(82)91426-7.

Schaller, H. (2003) 'The role of sterols in plant growth and development', *Progress in Lipid Research*, 42, pp. 163–175. Available at: http://www.sciencedirect.com/science/article/pii/S0163782702000474%5Cnpapers2://publication/uuid/E01C48C7-E57A-4FAD-9057-1279540D4315.

Schaller, H. (2004) 'New aspects of sterol biosynthesis in growth and development of higher plants', *Plant Physiology and Biochemistry*, 42, pp. 465–476. doi: 10.1016/j.plaphy.2004.05.012.

Schaller, H., Bouvier-Navé, P. and Benveniste, P. (1998) 'Overexpression of an Arabidopsis cDNA Encoding a Sterol-C24 1 -Methyltransferase in Tobacco Modifies the Ratio of 24-Methyl Cholesterol to Sitosterol and Is Associated with Growth Reduction', *Plant Physiology*, 118(2), pp. 461–469. doi: 10.1104/pp.118.2.461.

Schiml, S., Fauser, F. and Puchta, H. (2017) 'CRISPR/Cas-Mediated In Planta Gene Targeting', *Plant Genomics: Methods and Protocols*, 1610, pp. 3–11. doi: 10.1007/978-1-4939-7003-2.

Schrick, K. *et al.* (2004) 'A link between sterol biosynthesis, the cell wall, and cellulose in Arabidopsis', *Plant Journal*, 38(2), pp. 227–243. doi: 10.1111/j.1365-313X.2004.02039.x.

Schrick, K. *et al.* (2011) 'A dynamic role for sterols in embryogenesis of Pisum sativum', *Phytochemistry*. Elsevier Ltd, 72(6), pp. 465–475. doi: 10.1016/j.phytochem.2011.01.009.

Senthil-Kumar, M., Wang, K. and Mysore, K. S. (2013) 'AtCYP710A1 gene-mediated stigmasterol production plays a role in imparting temperature stress tolerance in Arabidopsis thaliana', *Plant Signaling and Behavior*, 8(2), pp. 1–5. doi: 10.4161/psb.23142.

Souter, M. *et al.* (2002) 'hydra mutants of Arabidopsis are defective in sterol profiles and auxin and ethylene signaling', *The Plant Cell*, 14(5), pp. 1017–1031. doi: 10.1105/tpc.001248.

Sparkes, I. A. *et al.* (2006) 'Rapid, transient expression of fluorescent fusion proteins in tobacco plants and generation of stably transformed plants', *Nature Protocols*, 1(4), pp. 2019–2025. doi: 10.1038/nprot.2006.286.

Steinbrecher, T. and Leubner-Metzger, G. (2018) 'Tissue and cellular mechanics of seeds', *Current Opinion in Genetics and Development*. The Authors, 51, pp. 1–10. doi: 10.1016/j.gde.2018.03.001.

Steinmann, T. *et al.* (1999) 'Coordinated polar localization of auxin efflux carrier PIN1 by GNOM ARF GEF', *Science*, 286(5438), pp. 316–318. doi: 10.1126/science.286.5438.316.

Strugala, R., Delventhal, R. and Schaffrath, U. (2015) 'An organ-specific view on non-host resistance', *Frontiers in Plant Science*, 6(526), pp. 1–5. doi:

10.3389/fpls.2015.00526.

Suza, W. P. and Chappell, J. (2016) 'Spatial and temporal regulation of sterol biosynthesis in Nicotiana benthamiana', *Physiologia Plantarum*, 157, pp. 120–134. doi: 10.1111/ppl.12413.

Ueda, H. *et al.* (2018) 'Disease severity enhancement by an esterase from non-phytopathogenic yeast Pseudozyma antarctica and its potential as adjuvant for biocontrol agents', *Scientific Reports*, 8, pp. 1–12. doi: 10.1038/s41598-018-34705-z.

Verma, P. and Majee, M. (2013) 'Seed Germination and Viability Test in Tetrazolium (TZ) Assay', *bio-protocol*, 3(17), pp. 5–8.

Wang, K. *et al.* (2012) 'Phytosterols Play a Key Role in Plant Innate Immunity against Bacterial Pathogens by Regulating Nutrient Efflux into the Apoplast', *Plant Physiology*, 158(4), pp. 1789–1802. doi: 10.1104/pp.111.189217.

Whitaker, B. D. (1988) 'Changes in the steryl lipid content and composition of tomato fruit during ripening', *Phytochemistry*, 27(11), pp. 3411–3416.

Whitaker, B. D. (1991) 'Changes in lipids of tomato fruit stored at chilling and non-chilling temperatures', *Phytochemistry*, 30(3), pp. 757–761.

Whitaker, B. D. and Gapper, N. E. (2008) 'Ripening-Specific Stigmasterol Increase in Tomato Fruit Is Associated with Increased Sterol C-22 Desaturase (CYP710A11) Gene Expression', *Journal of Agri*, 56, pp. 3828–3835.

Willemsen, V. *et al.* (2003) 'Cell Polarity and PIN Protein Positioning in Arabidopsis Require', *The Plant Cell*, 15, pp. 612–625. doi: 10.1105/tpc.008433.1999.

Wydro, M., Kozubek, E. and Lehmann, P. (2006) 'Optimization of transient Agrobacterium-mediated gene expression system in leaves of Nicotiana benthamiana', *Acta Biochimica Polonica*, 53(2), pp. 289–298.

Yang, L. *et al.* (2005) 'Validation of a Tomato-Specific Gene , LAT52 , Used as an Endogenous Reference Gene in Qualitative and Real-Time Quantitative PCR Detection of Transgenic Tomatoes', *Journal of Agricultural and Food Chemistry*, 53, pp. 183–190.

Zhiponova, M. K. *et al.* (2012) 'Brassinosteroid production and signaling differentially control cell division and expansion in the leaf', *New Phytologist*, 197, pp. 490–502. doi: 10.1111/nph.12036.

Zimmermann, P. *et al.* (2004) 'GENEVESTIGATOR . Arabidopsis Microarray Database

and Analysis Toolbox', *Plant Physiology*, 136, pp. 2621–2632. doi: 10.1104/pp.104.046367.1.

7. SUPPLEMENTAL INFORMATION

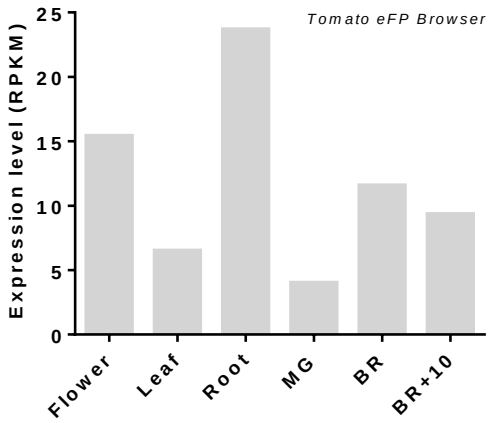

Figure S1 Transcript levels of *C22DES* in different tomato organs. Expression data were retrieved from the Tomato eFP Browser database (http://bar.utoronto.ca/efp_tomato/cgi-bin/efpWeb.cgi). Graph shows the transcript levels of *C22DES* in flowers, leaves, roots, and fruits in three different stages (MG – Mature green; BR – Breaker; BR+10 – Breaker + 10 days).

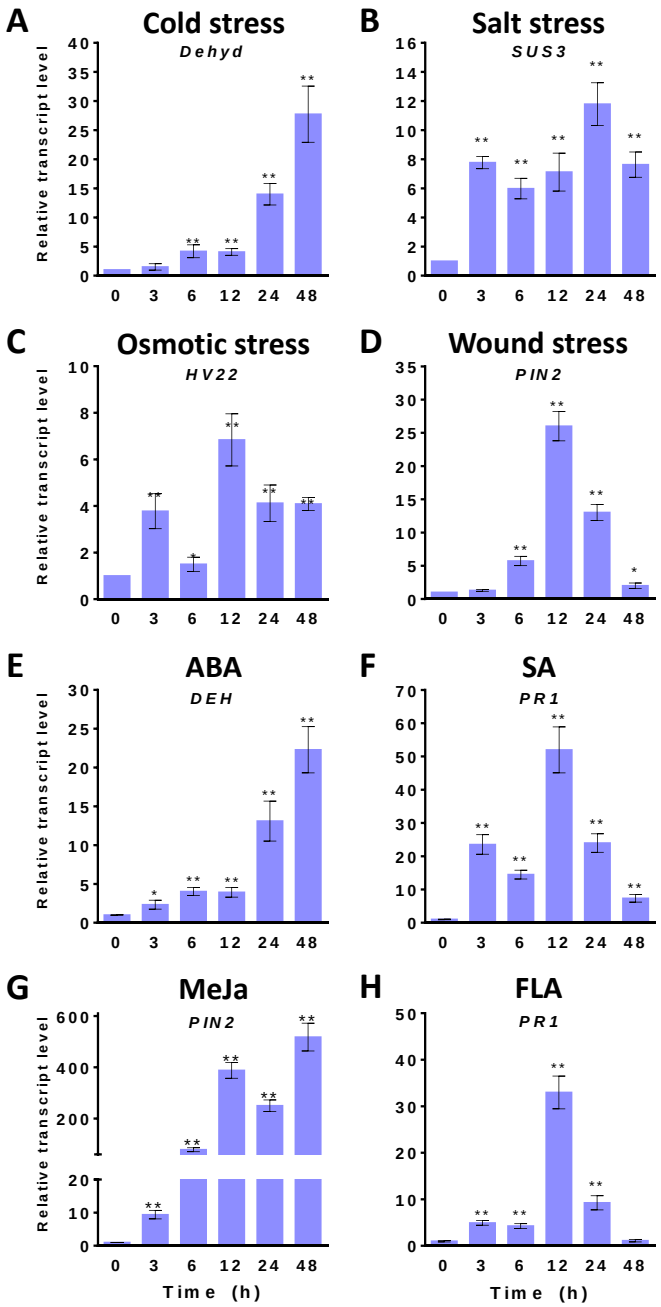

Figure S2 Expression of different responsive marker genes for different stress treatments in tomato seedlings. Marker genes in response to: ABA, *DEH*; cold, *Dehyd*; osmotic, *HVA22*; salt, *SUS3*; SA and flagellin 22, *PR1*; wound and MeJ, *PIN2*. The transcript levels were determined by RT-qPCR using RNA samples from tomato seedlings exposed to different treatments (ABA, osmotic stress, salt stress, cold, wound, SA, MeJA, and flagellin 22). Samples were collected at the indicated time points (3, 6, 12, 24,

and 48 h) from the start of each treatment (0 h). Data are expressed as normalized quantity values calculated using two independent housekeeping genes (*PP2Acs* and *EF1a*) (Ballester et al., 2013) and relative to non-treated seedlings at each time point, which is assumed to be one. Values are means ± SD (*n*= 6). Asterisks show the values that are significantly different (*p< 0.05, **p< 0.01) compared to those at time 0 h.

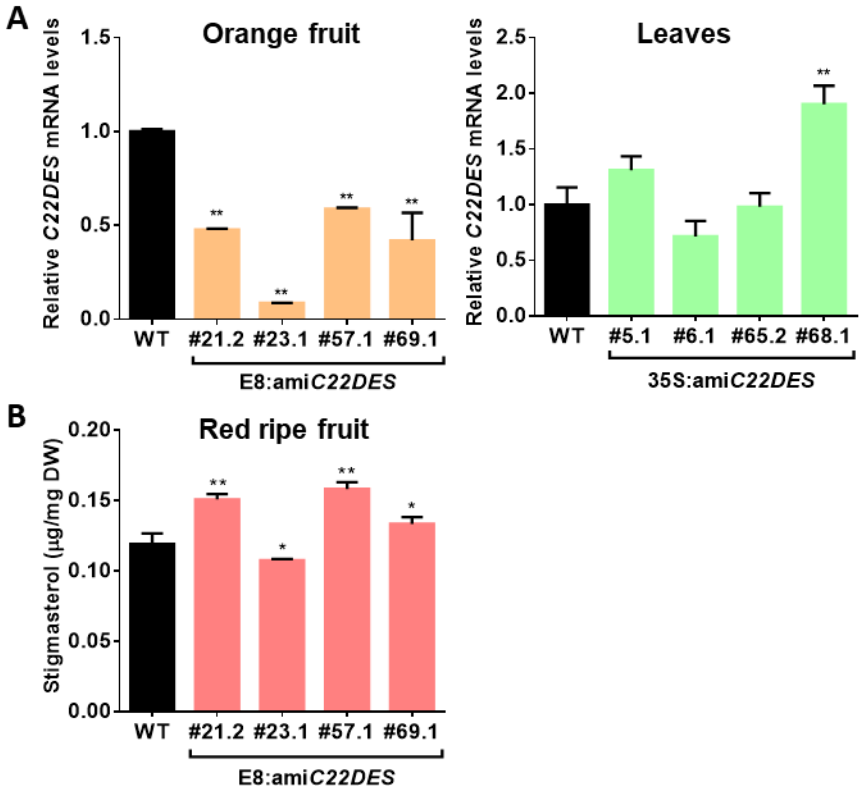

Figure S3 Analysis of *C22DES* transcript levels and sterol composition in T0 transgenic *C22DES* silenced lines. (A) *C22DES* transcript levels were measured in leaves in the constitutive *C22DES* silencing lines (*35S:amiC22DES*), and in orange fruits in the fruit-specific *C22DES* silencing lines (*E8:amiC22DES*). Values are means ± SD (*n*= 3) from 3 technical replicates. **(B)** Stigmasterol content [µg/mg dry weight (DW)] from membrane sterol fraction (FS, SG, and ASG) from red ripe fruits. Values are means ± SD from 3 technical replicates. Asterisks show the values that are significantly different (one-way ANOVA with Dunnett's multiple comparisons test, *p<0.05, **p<0.01) compared to WT. DW, dry weight.

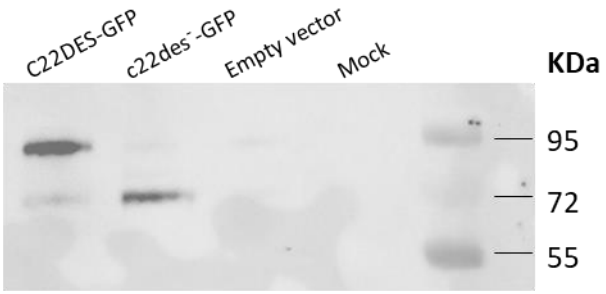

Figure S4 Immunoblot analysis of total protein extracts from agroinfiltrated *N. benthamiana* leaves transiently expressing the indicated chimeric proteins. Lane 1, C22DES-GFP (≈87.24 KDa); lane 2, C22des⁻ -GFP (≈64.68KDa); lane3, empty vector; Lane 4, mock. The molecular mass on protein standards is shown on the right.

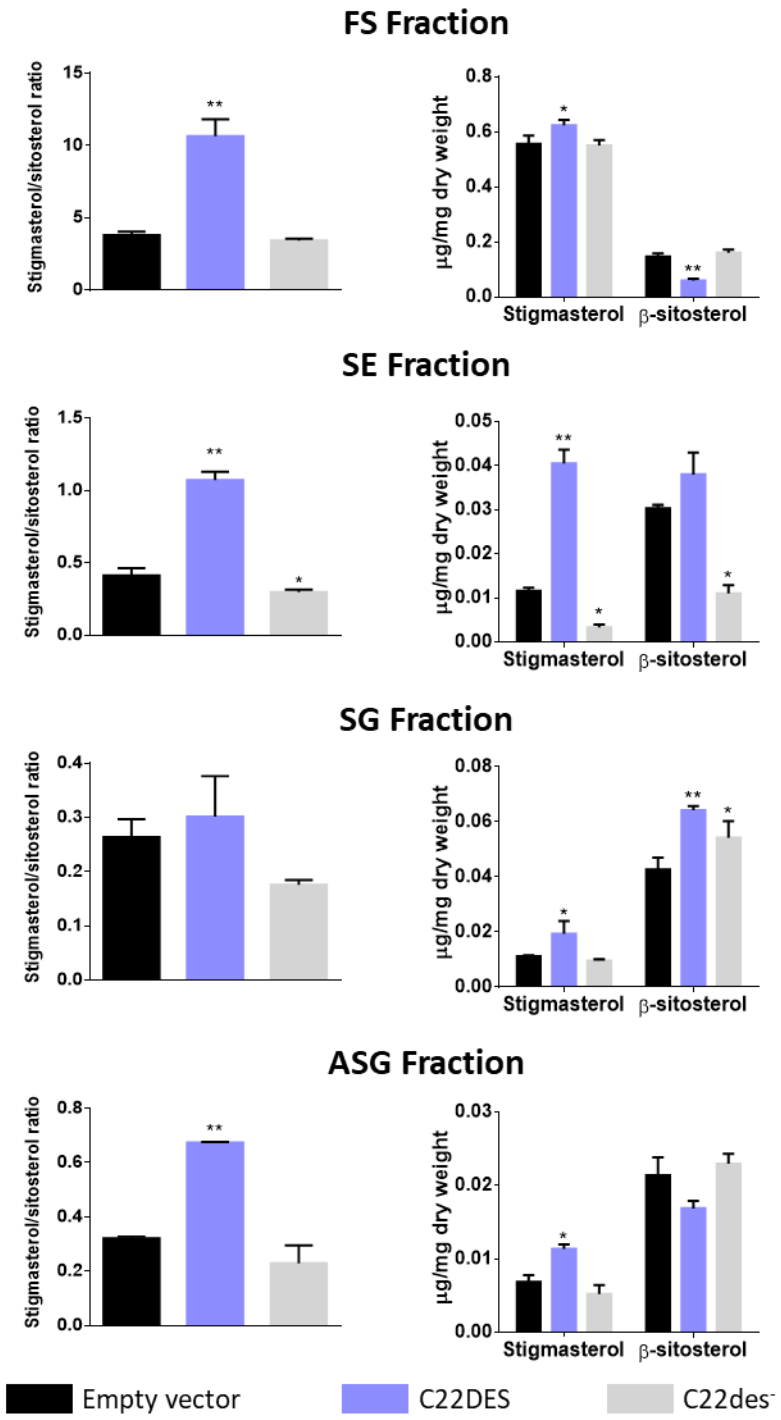

Figure S5 Analysis of sterol composition. The left column shows the ratio of stigmasterol to β-sitosterol in each sterol fraction from *N. benthamiana* leaves expressing C22DES-GFP and C22des⁻-

GFP. The right column shows the stigmasterol and β-sitosterol specific composition in each sterol fraction. Values are means ± SD of two biological replicates (*n*=2). Asterisks indicate significant differences among means relative to those in leaf samples expressing the empty vector (one-way ANOVA with Dunnett's multiple comparisons test, *p<0.05, **p<0.01).

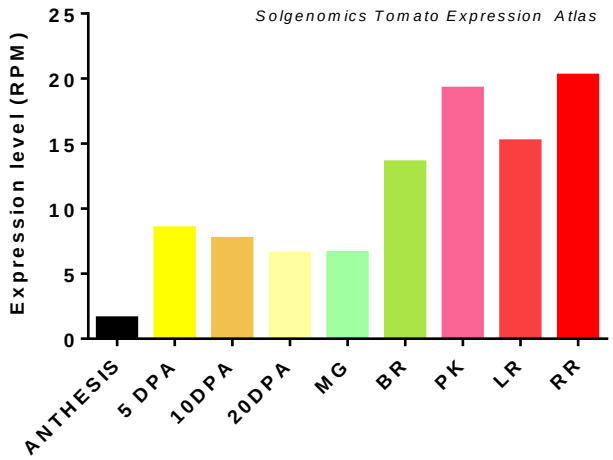

Figure S6 Transcript levels of *C22DES* in seeds at different developmental stages. Expression data were retrieved from the Tomato eFP Browser database (http://bar.utoronto.ca/efp_tomato/cgi-bin/efpWeb.cgi). Graph shows the transcript levels of C22DES in seeds at 5 days post-anthesis (DPA), 10 DPA, 20 DPA, seeds from mature green fruits, from breaker fruits, from pink fruits, from light red fruits and from red ripe fruits.

		Leaves		
			35S:C22DES	
		WT	12.2	31.1
FS	Cholesterol	2.23 ± 0.18	1.25 ± 0.15	1.57 ± 0.04
	Campesterol	0.67 ± 0.16	0.31 ± 0.08	0.25 ± 0.01
	Stigmasterol	11.51 ± 2.16	*nd*	8.16 ± 0.90
	β-sitosterol	3.92 ± 0.85	6.13 ± 0.23	3.03 ± 0.44
SE	Cholesterol	10.75 ± 2.66	12.03 ± 1.83	11.62 ± 0.47
	Campesterol	4.96 ± 0.73	4.66 ± 0.54	9.86 ± 1.60
	Stigmasterol	3.68 ± 0.41	*nd*	3.67 ± 0.11
	β-sitosterol	12.79 ± 1.64	21.84 ± 1.73	11.18 ± 0.67
	Cycloarthenol	23.59 ± 3	20.72 ± 1.23	27.40 ± 8.94
	24-Ethylidenelophenol	1.86 ± 0.38	2.88 ± 0.35	3.05 ± 0.67
SG	Cholesterol	4.71 ± 0.32	3.43 ± 0.81	3.27 ± 0.02
	Campesterol	4.21 ± 1.52	0.87 ± 0.03	2.16 ± 0.77
	Stigmasterol	8.05 ± 0.07	*nd*	4.80 ± 0.22
	β-sitosterol	10.34 ± 1.78	13.02 ± 3.27	5.92 ± 0.61
ASG	Cholesterol	11.43 ± 0.28	8.60 ± 1.83	9.83 ± 0.31
	Campesterol	3.20 ± 0.48	1.97 ± 0.47	3.50 ± 0.43
	Stigmasterol	29.87 ± 2.01	*nd*	24.14 ± 1.47
	β-sitosterol	24.46 ± 0.06	42.88 ± 9.27	19.30 ± 1.56

Table S1 Free and conjugated sterol compositions in leaves of WT and *C22DES* overexpressing lines. Data are the means ± SD of three technical replicates. Values are given in µg/100mg dry weight. *nd.,* not detected. FS, free sterols; SE, steryl esters; SG, steryl glycosides; ASG, acyl-steryl glycosides.

		Red ripe fruits			
			35S:C22DES		*E8:C22DES*
		WT	12.2	31.1	60.1
FS	Cholesterol	0.19 ± 0.04	0.15 ± 0.002	0.12 ± 0.002	0.14 ± 0.01
	Campesterol	0.84 ± 0.05	0.71 ± 0.03	0.67 ± 0.03	1.05 ± 0.01
	Stigmasterol	6.19 ± 0.27	*nd*	2.70 ± 0.19	0.20 ± 0.01
	β-sitosterol	1.35 ± 0.20	6.13 ± 0.37	2.46 ± 0.27	6.51 ± 0.32
SE	Cholesterol	1.00 ± 0.39	1.00 ± 0.03	0.97 ± 0.09	0.77 ± 0.01
	Campesterol	2.93 ± 0.45	2.45 ± 0.10	4. 44 ± 0.15	3.04 ± 0.09
	Stigmasterol	2.90 ± 0.33	*nd*	1.96 ± 0.23	*nd*
	β-sitosterol	6.65 ± 0.74	18.26 ± 1.03	15.04 ± 1.67	14.49 ± 1.4
	Cycloarthenol	1.44 ± 0.19	1.64 ± 0.06	2.60 ± 0.12	1.84 ± 0.005
SG	Cholesterol	0.42 ± 0.04	0.51 ± 0.19	0.29 ± 0.03	0.19 ± 0.01
	Campesterol	1.62 ± 0.04	1.54 ± 0.34	1.43 ± 0.28	1.89 ± 0.45
	Stigmasterol	8.55 ± 0.56	*nd*	3.03 ± 0.16	*nd*
	β-sitosterol	4.58 ± 0.39	11.30 ± 0.57	7.27 ± 0.65	9.5 ± 0.72
ASG	Cholesterol	0.53 ± 0.02	0.84 ± 0.05	0.66 ± 0.01	0.61 ± 0.03
	Campesterol	1.53 ± 0.10	1.99 ± 0.11	1.97 ± 0.10	2.14 ± 0.31
	Stigmasterol	7.66 ± 1.6	*nd*	3.78 ± 0.15	0.38 ± 0.05
	β-sitosterol	4.07 ± 0.43	14.08 ± 0.98	7.37 ± 0.25	12.01 ± 0.85

Table S2 Free and conjugated sterol compositions in red fruits of WT and *35S:C22DES* and *E8:C22DES* overexpressing lines. Data are the means ± SD of three technical replicates. Values are given in µg/100mg dry weight. *nd.,* not detected. FS, free sterols; SE, steryl esters; SG, steryl glycosides; ASG, acyl-steryl glycosides.

		Seeds			
			35S:C22DES		*E8:C22DES*
		WT	12.2	31.1	60.1
FS	Cholesterol	1.85 ± 0.09	2.70 ± 0.12	2.03 ± 0.04	2.68 ± 0.18
	Campesterol	1.29 ± 0.06	1.43 ± 0.12	1.39 ± 0.02	2.08 ± 0.07
	Stigmasterol	3.75 ± 0.25	19.47 ± 0.36	4.14 ± 0.05	3.61 ± 0.13
	β-sitosterol	24.48 ± 1.14	12.07 ± 0.68	25.13 ± 0.14	35.98 ± 0.55
SE	Cholesterol	16.41 ± 1.05	35.77 ± 2.05	23.45 ± 0.98	23.50 ± 3.06
	Campesterol	3.72 ± 0.52	5.49 ± 1.27	2.88 ± 0.30	3.67 ± 0.74
	Stigmasterol	0.96 ± 0.16	7.96 ± 1.10	1.26 ± 0.09	2.49 ± 0.21
	β-sitosterol	23.14 ± 0.36	9.15 ± 0.19	31.38 ± 3.53	49.88 ± 11.70
	Cycloarthenol	1.90 ± 0.34	2.34 ± 0.25	2.67 ± 0.49	4.91 ± 2.64
	24-Ethylidenelophenol	0.45 ± 0.10	0.39 ± 0.13	0.59 ± 0.14	2.43 ± 0.40
SG	Cholesterol	1.07 ± 0.18	1.17 ± 0.05	1.08 ± 0.01	0.49 ± 0.01
	Campesterol	1.88 ± 0.35	2.29 ± 0.02	1.64 ± 0.07	0.84 ± 0.15
	Stigmasterol	4.34 ± 0.51	6.00 ± 0.19	4.21 ± 0.12	0.77 ± 0.13
	β-sitosterol	29.52 ± 1.71	28.64 ± 2.31	32.88 ± 1.73	16.34 ± 2.44
ASG	Cholesterol	0.62 ± 0.01	0.43 ± 0.12	0.50 ± 0.14	0.98 ± 0.01
	Campesterol	0.78 ± 0.01	0.46 ± 0.19	0.41 ± 0.02	0.78 ± 0.24
	Stigmasterol	1.35 ± 0.16	1.00 ± 0.02	0.76 ± 0.31	0.87 ± 0.05
	β-sitosterol	3.78 ± 0.52	3.40 ± 0.48	3.59 ± 0.04	4.94 ± 0.38

Table S3 Free and conjugated sterol compositions in seeds of WT and *35S:C22DES* and *E8:C22DES* overexpressing lines. Data are the means ± SD of three technical replicates. Values are given in µg/100mg dry weight. FS, free sterols; SE, steryl esters; SG, steryl glycosides; ASG, acyl-steryl glycosides.

		Sample		
		Empty vector	C22DES-GFP	C22des^{-}-GFP
FS	Stigmasterol	0.556 ± 0.030	0.623 ± 0.019	0.550 ± 0.020
	β-sitosterol	0.147 ± 0.011	0.059 ± 0.007	0.161 ± 0.011
SE	Stigmasterol	0.012 ± 0.001	0.041 ± 0.003	0.003 ± 0.0007
	β-sitosterol	0.030 ± 0.001	0.038 ± 0.005	0.011 ± 0.002
SG	Stigmasterol	0.0112 ± 0.0004	0.0194 ± 0.0046	0.0095 ± 0.0006
	β-sitosterol	0.0428 ± 0.0042	0.0642 ± 0.0002	0.0542 ± 0.0060
ASG	Stigmasterol	0.0069 ± 0.0009	0.0114 ± 0.0006	0.0052 ± 0.0012
	β-sitosterol	0.0214 ± 0.0024	0.0169 ± 0.0010	0.030 ± 0.0013

Table S4 Stigmasterol and β-sitosterol specific composition in each sterol fraction. Values are expressed as mean µg sterol (recovered from steryl lipid) per mg of dry weight ± SD of two independent biological replicates (*n*=2).

Use	Nº	Name	Primer sequence
sgRNA1	#1	C22.1 Fw	*attg* GAAAGCGTCAGGGCGGACAT
	#2	C22.1 Rv	*aaac* ATGTCCGCCCTGACGCTTTC
sgRNA2	#3	C22.2 Fw	ATTGCGCTGACGGCGGAAATGCTC
	#4	C22.2 Rv	AAACGAGCATTTCCGCCGTCAGCG
Genotyping	#5	Actin Fw	CCTTCCACATGCCATTCTCC
	#6	Actin Rv	CCACGCTCGGTCAGGATCT
	#7	nptII Fw	GACAGGTCGGTCTTGACAAAAAG
	#8	nptII Rv	GAACAAGATGGATTGCACGC
	#9	pKGW Kan Fw	GGAGCATTTTTGACAAGAAATATTTGC
	#10	E8 Fw	TACAACCTCCATGCCACTTG
	#11	amiC22DES Rv	CATGTGTAATATGCGTCCGAGCGTG
	#12	amiC22DES Fw	CACGCTCGGACGCATATTACACATG
	#13	tNOS Rv	TGGGTACCCGATCTAGTAACATAG
	#14	C22DES Rv	GTCGGCGAAGGTCTTTATGT
	#15	C22DES Fw	GAGAAAGTTCGGTCGGATGTAG
	#16	CRISPR Fw	ACAGTCTTTCACCTCTCTTTGG
	#17	CRISPR Rv	GGCCTGCTTCTCTTCTTTCA
	#18	C22.1 genotyping Fw	CCTGGCCCAACTCTTGTATT
	#19	C22.1 genotyping Rv	CCCGGTAAATCAACAGGAAGT
	#20	C22.2 genotyping Fw	GTTGACACCCTTTCGGTTTG
	#21	C22.2 genotyping Rv	CTCTTGTCTCTCCTCCATGAAC
qPCR Genotyping	#22	Lat52 qPCR Fw	AGACCACGAGAACGATATTTGC
	#23	Lat52 qPCR Rv	GCCTTTTCATATCCAGACACAC
	#24	nptII qPCR Fw	GCTATCAGGACATAGCGTTGG
	#25	nptII qPCR Rv	GATACCGTAAAGCACGAGGAAG
Cloning	#26	attb1 C22DES Fw	**GGGGACAAGTTTGTACAAAAAAGCAGGCT**TCATGGCATCCATTTGGGGTTTGTTATC
	#27	attb2-C22DES Rv	**GGGGACCACTTTGTACAAGAAAGCTGGGT**CTCGTGTGCACCTGTGTGCAAG
	#28	attb2 c22des- Rv	**GGGGACCACTTTGTACAAGAAAGCTGGGTC**TTTCCCTGAGATTTCCGCCGTCAGCG
RT-qPCR	#29	PP2A Fw	CGATGTGTGATCTCCTATGGTC
	#30	PP2A Rv	AAGCTGATGGGCTCTAGAAATC
	#31	CAC Fw	CCTCCGTTGTGATGTAACTGG
	#32	CAC Rv	ATTGGTGGAAAGTAACATCATCG
	#33	C22-qPCR Fw	TCCACTCAACTGACCTCTCT
	#34	C22-qPCR Rv	GTCGGCGAAGGTCTTTATGT
Botrytis gDNA quantification	#35	Sl-ACT Fw	CCAGGTATTGCTGATAGAATGAG
	#36	Sl-ACT Rv	GAGCCTCCAATCCAGACAC
	#37	Bc-β-TUB Fw	GTTACTTGACATGCTCTGCCATT
	#38	Bc-β-TUB Rv	CACGGCTACAGAAAGTTAGTTTCTACAA

Table S5 Primers used in this work. ATTB recombination sites are shown in **bold**, and the ATG start codons are underlined. Sequence in red represents non-hybridizing coil.

Construction	Amplified region	Primers
35S:amiC22DES	nptII:35S:amiC22DES	#9, #11
E8:amiC22DES	E8:amiC22DES	#10, #11
35S:amiC22DES, E8:amiC22DES	amiC22DES:tNOS	#12, #13
35S:C22DES	nptII:35S:C22DES	#9, #14
E8:C22DES	E8:C22DES	#10, #14
35S:C22DES, E8:C22DES	C22DES:tNOS	#15, #13

Table S6 Specific pairs of primers used for PCR amplification to genotype the transgenic lines.

					Antibiotic selection	
Construct	**Template**	**Primers**	**Vector**	**Cloning method**	**Bacteria**	**Plant**
35S:C22DES	cDNA	-	pKGW	Gateway®	Sp	Kan
35S:amiC22DES	-	-	pKGW	Gateway®	Sp	Kan
E8:C22DES	cDNA	-	pKGW	Gateway®	Sp	Kan
E8:amiC22DES	-	-	pKGW	Gateway®	Sp	Kan
35S:C22DES-GFP	35S:C22DES	13, 14	pEarleyGate103	Gateway®	Kan	PPT
35S:c22des⁻-GFP	35S:C22DES	13, 15	pEarleyGate103	Gateway®	Kan	PPT
Cas9/C22.1	sgRNA1	1, 2	pDE-Cas9-Kan^R	Gateway®	Sp	Kan
Cas9/C22.2	sgRNA2	3, 4	pDE-Cas9-Kan^R	Gateway®	Sp	Kan

Table S7 Constructs and cloning details

CONCLUSIONS

CONCLUSIONS

1. The sterol C22 desaturase (C22DES) is a membrane-bound enzyme localized in the endoplasmic reticulum (ER), in agreement with the subcellular localization of most CYP family proteins.
2. Tomato C22DES is an ER-membrane integral protein having a single transmembrane α-helix at the N-terminal end (TMH1). Two other regions of still unknown function are predicted to interact with the ER-membrane: a proline-kink region (PK) close to TMH1, extending from residues 38 to 58, and a region extending from residues 227 to 233 located at the end of a predicted amphipathic α-helix.
3. The TMH1 sequence is sufficient for the targeting and retention of tomato C22DES in the ER-membrane. However, the globular domain can also be targeted and retained in the ER-membrane in the absence of TMH1, suggesting the existence of a complex mechanism for the interaction of this enzyme with the ER-membrane.
4. TMH1 is required for C22DES activity *in vivo*. This region contains a highly conserved CRAC motif and is highly enriched in threonine and serine residues which may play a relevant role in the recognition and accessibility of the β-sitosterol present in the membrane to the catalytic site of the enzyme.
5. The molecular mechanism(s) underlying the interaction of C22DES with the major cellular β-sitosterol pool present in the PM is currently unknown, but it may involve the interaction of the ER with the PM at specific contact sites.
6. *C22DES* gene is differentially expressed during tomato fruit development and after exposure to different abiotic stresses including cold, saline and osmotic stresses. These data indicate the involvement of this gene in developmental processes and stress responses in tomato plants.
7. The sterol analysis of transgenic tomato plants with altered expression levels of *C22DES* gene do not show a correlation between the level of *C22DES* expression and the stigmasterol:β-sitosterol ratios, suggesting the existence of post-transcriptional regulatory mechanisms controlling C22DES activity.
8. Stigmasterol is not crucial for completing the life cycle of tomato plants under controlled conditions since a CRISPR-Cas9 *C22DES* knock-out tomato mutant

(*C22des*$^{-}$) that is unable to synthesize stigmasterol is able to complete both vegetative and reproductive stages under greenhouse conditions.

9. The inactivation of C22DES in the *C22des*$^{-}$ mutant and its concomitant depletion of stigmasterol lead to the unbalance of the sterol composition in different tomato plant organs (leaves and red ripe fruits), suggesting the existence of a precise sensing mechanism which maintains proper sterol composition.
10. The lack of stigmasterol results in reduced plant size, due to a reduction in cell division and not in cell elongation, and delayed development.
11. The absence of stigmasterol causes severe defects in embryo development, which are probably due to alterations in the physical properties of plasma membrane that may cause the mislocalization of proteins involved in cell polarity.
12. The *C22des*$^{-}$ mutant shows delayed and reduced rate of seed germination as well as defects in cotyledon establishment which may be related to defects on testa rupture possibly due to problems in the embryo growth.
13. The lack of stigmasterol in tomato fruits increases the susceptibility to *Botrytis cinerea* infection.

GENERAL DISCUSSION

GENERAL DISCUSSION

Plant sterols and their biosynthesis have been the focus of many studies during the last decades which resulted in the elucidation of the whole biosynthetic pathway and the identification of the enzymes involved (Benveniste, 2004; Sonawane *et al.*, 2016). Many of these studies have relied on the use of mutants affected in genes encoding enzymes catalyzing early or intermediate steps of the pathway and, therefore, the sterol profile of the mutant plants was usually affected in an unpredictable way (Schaller, 2003). However, in particular cases, such as the *SMT2/3* mutant, impaired in the function of the gene encoding the enzyme acting at the branch point leading the synthesis of ethyl-sterols (*see* General Introduction, Figure 6), only the level of two sterols (β-sitosterol and stigmasterol) was specifically altered (Carland *et al.*, 2002; Carland, Fujioka and Nelson, 2010). Due to this fact, and apart from the specific function of campesterol as the precursor of brassinosteroids, there is very little information about the biological relevance of other single sterol species. In the present work, we have undertaken the study of the role of stigmasterol (the end product of the 24-ethyl sterol branch) in plants by primarily focusing on the characterization of C22DES, the enzyme involved in its biosynthesis.

Although *C22DES* gene was identified and the resulting protein characterized at the biochemical level in Arabidopsis and tomato more than one decade ago (Morikawa *et al.*, 2006), no other relevant data about the functional and structural characterization of this enzyme have been reported. Here we have described the role of the N-terminal TMH1 sequence in the targeting and association of C22DES with the ER-membrane (*see* Chapter I, Figures 5, 7), although the mechanisms underlying the retention of the enzyme in this cellular compartment remains to be elucidated. The modeling of the tertiary structure of C22DES in association with cell membranes predicts two other membrane contact regions in addition to TMH1. One corresponds to the PK motif located close to TMH1 domain and the other to a motif located in the globular domain near the N-terminal end of a long amphipathic alpha-helix (*see* Chapter I, Figure 4). As shown in this work, the PK motif by itself is not sufficient for targeting and retention in the ER (*see* Chapter I, Figure 5). However, nothing is known on this respect about the other membrane-contact motif present in the globular domain. It is likely that these contact membrane motifs could have a role in mediating interactions with other ER membrane proteins. Further studies

may be required to elucidate this issue. Among them, the systematic deletion of the two membrane contact motifs present in the globular domain, together with the deletion of TMH1, could be a strategy to unveil the existence of a retention mechanism of C22DES in the ER based on protein-protein interactions. In this respect, it has been described that some soluble proteins are able to localize in the ER through the interaction with integral membrane-proteins, as in the case of the mouse ERdj4 protein (Lai *et al.*, 2012).

Regarding the reported involvement of TMH1 in enzyme activity, the low conservation level of this region among the C22DES of the different plant species is striking. It is likely that the TMH1 region could play a role in substrate recognition due to the presence of a highly conserved cholesterol recognition/interaction amino acid consensus (CRAC) motif within this domain (*see* Chapter I, Figure 9A). Mutational analysis of the central tyrosine of this CRAC motif would be of great interest to elucidate whether these residues could actually be involved in β-sitosterol binding and, in this way, be essential for C22DES activity. This kind of approach has been successful for the functional characterization of the CRAC motifs described in several cholesterol-binding proteins (Bhakta *et al.*, 2011; Gál *et al.*, 2015). Apart from the CRAC motif, there are also other common characteristics such as the high density of hydroxylated residues (threonine and serine) as well as the presence of at least one proline residue in this region. These common amino acids might be considered as an interesting target for punctual mutations to analyze their contribution to the substrate specificity or even to the correct positioning of the protein in the membranes, respectively. The domain swapping is another strategy that could be considered to assess that the TMH1 regions of the C22DES of distant species share the same function.

As previously discussed in the Chapter I, there are additional CRAC and CARC motifs (*see* Chapter I, Figure 9B) that might be crucial for the retrieving of β-sitosterol from other cell membrane compartments different than the ER, including the PM. This is an interesting point that has not been fully elucidated in this work, but represents a subject of study for further investigations. The study of selective mutations of these motifs within the whole protein context could provide relevant information about the mechanism of action of the C22DES on the different β-sitosterol pools present in the cells.

Furthermore, all these mutant variants of the protein that have been proposed to check the substrate binding ability could be also tested for the complementation of the *C22des*$^{-}$ mutant plants, since they represent the most reliable genetic background to prove the C22DES enzyme activity.

Taking advantage of the *C22des*$^{-}$ mutant, in which the lack of stigmasterol has been demonstrated (*see* Chapter II, Table 1), we have been able to suggest the involvement of this metabolite in different plant processes, such as embryo development (*see* Chapter II, Figure 10), cell division (*see* Chapter II, Table 2), and the response and resistance to biotic stress (*see* Chapter II, Figure 11).

Further investigations might be required to confirm all our proposed roles for the stigmasterol and also for those functions that have been suggested in previous studies, such as the involvement on salinity resistance (Hashem *et al.*, 2011) or chilling injury (Whitaker, 1991). In this respect, preliminary data have been obtained in our laboratory (Minlong Chen, Treball Fin de Grau, UB, 2019). In this work, the *C22des*$^{-}$ mutant plants have been exposed to salt and cold stresses in addition to the *Botrytis cinerea* infection of their fruits and leaves, to analyze their differential responses in comparison with WT plants. Despite the observed induction of *C22DES* gene expression after different abiotic stresses including salt, osmotic and cold stresses (*see* Chapter II, Figure 2), the lack of stigmasterol in *C22des*$^{-}$ plants seemed not to increase their susceptibility in salt or cold stresses (Minlong Chen, Treball Fin de Grau, UB, 2019). These results raise the question of why the *C22DES* gene gets induced by different abiotic stresses if stigmasterol has been shown not to be essential for the plant resistance to them. In addition to the *C22DES* transcript levels, it would be also interesting to measure the stigmasterol content after those treatments in order to verify that the induction of the gene expression was actually translated into an increment of the enzyme activity.

However, in the case of *B. cinerea* infection (both in leaves and fruits), in agreement with the results obtained in this thesis, Minlong Chen also described a higher susceptibility of the *C22des*$^{-}$ mutant, reinforcing the hypothesis of stigmasterol to be important in the resistance to biotic stress.

After the present work, there are more available information about the mechanism of action of C22DES, and also about the possible roles of the stigmasterol in tomato plants. The complete understanding of these issues might help us in the improvement of different plant traits such as germination and stress resistance, given the putative role of stigmasterol in these characteristics.

GENERAL REFERENCES

GENERAL REFERENCES

Aboobucker, S. I. and Suza, W. P. (2019) 'Why Do Plants Convert Sitosterol to Stigmasterol?', *Frontiers in Plant Science*, 10(March), pp. 1–8. doi: 10.3389/fpls.2019.00354.

Arnqvist, L. *et al.* (2008) 'Overexpression of CYP710A1 and CYP710A4 in transgenic Arabidopsis plants increases the level of stigmasterol at the expense of sitosterol', *Planta*, 227(2), pp. 309–317. doi: 10.1007/s00425-007-0618-8.

Baranski, R. *et al.* (2016) *Improving Color Sources by Plant Breeding and Cultivation*, *Handbook on Natural Pigments in Food and Beverages*. Elsevier Ltd. doi: 10.1016/B978-0-08-100371-8.00019-1.

Barry, C. S. and Giovannoni, J. J. (2007) 'Ethylene and Fruit Ripening', *Journal of Plant Growth Regulation*, 26, pp. 143–159. doi: 10.1007/s00344-007-9002-y.

Benveniste, P. (2002) *Sterol Metabolism*, *The Arabidopsis Book*. doi: 10.1199/tab.0004.

Benveniste, P. (2004) 'Biosynthesis and Accumulation of Sterols', *Annual Review of Plant Biology*, 55(1), pp. 429–457. doi: 10.1146/annurev.arplant.55.031903.141616.

Bhakta, S. J. *et al.* (2011) 'Mutagenesis of tyrosine and di-leucine motifs in the HIV-1 envelope cytoplasmic domain results in a loss of Env-mediated fusion and infectivity', *Retrovirology*. BioMed Central Ltd, 8(37), pp. 1–17. doi: 10.1186/1742-4690-8-37.

Carland, F., Fujioka, S. and Nelson, T. (2010) 'The Sterol Methyltransferases SMT1, SMT2, and SMT3 Influence Arabidopsis Development through Nonbrassinosteroid Products', *Plant Physiology*, 153(2), pp. 741–756. doi: 10.1104/pp.109.152587.

Carland, F. M. *et al.* (2002) 'The Identification of CVP1 Reveals a Role for Sterols in Vascular Patterning', *The Plant Cell*, 14(9), pp. 2045–2058. doi: 10.1105/tpc.003939.

Chen, W. *et al.* (2014) 'Fungal Cytochrome P450 Monooxygenases : Their Distribution, Structure, Functions, Family Expansion, and Evolutionary Origin', *Genome Biology and Evolution*, 6(7), pp. 1620–1634. doi: 10.1093/gbe/evu132.

Choi, N. H. *et al.* (2017) 'Antifungal activity of sterols and dipsacus saponins isolated from Dipsacus asper roots against phytopathogenic fungi', *Pesticide Biochemistry and Physiology*. Elsevier B.V., 141, pp. 103–108. doi: 10.1016/j.pestbp.2016.12.006.

Ferrer, A. *et al.* (2017) 'Emerging roles for conjugated sterols in plants', *Progress in*

Lipid Research. Elsevier, 67, pp. 27–37. doi: 10.1016/j.plipres.2017.06.002.

Gál, Z. *et al.* (2015) 'Mutations of the central tyrosines of putative cholesterol recognition amino acid consensus (CRAC) sequences modify folding, activity, and sterol-sensing of the human ABCG2 multidrug transporter', *Biochimica et Biophysica Acta*. Elsevier B.V., 1848(2), pp. 477–487. doi: 10.1016/j.bbamem.2014.11.006.

Grosjean, K. *et al.* (2015) 'Differential Effect of Plant Lipids on Membrane Organization: hot features and specificities of phytosphingolipids and phytosterols', *Journal of Biological Chemistry*, 290, pp. 5810–5825. doi: 10.1074/jbc.m114.598805.

Gutensohn, M. and Dudareva, N. (2016) *Tomato Fruits — A Platform for Metabolic Engineering of Terpenes*. 1st edn, *Methods in Enzymology*. 1st edn. Elsevier Inc. doi: 10.1016/bs.mie.2016.03.012.

Hartmann, M.-A. (1998) 'Plant sterols and the membrane environment', *Trends in Plant Science*, 3(5), pp. 170–175. Available at: http://www.cell.com/trends/plant-science/pdf/S1360-1385(98)01233-3.pdf.

Hashem, H. A. *et al.* (2011) 'Stigmasterol seed treatment alleviates the drastic effect of NaCl and improves quality and yield in flax plants', *Australian Journal of Crop Science*, 5(13), pp. 1858–1867.

Hemmerlin, A., Harwood, J. L. and Bach, T. J. (2012) 'A raison d'être for two distinct pathways in the early steps of plant isoprenoid biosynthesis?', *Progress in Lipid Research*, 51, pp. 95–148. doi: 10.1016/j.plipres.2011.12.001.

Jang, J.-C. *et al.* (2000) 'A critical role of sterols in embryonic patterning and meristem programming revealed by the fackel mutants of Arabidopsis thaliana', *Genes and Development*, 14(12), pp. 1485–1497.

Kimura, S. and Sinha, N. (2008) 'Tomato (Solanum lycopersicum): A Model Fruit-Bearing Crop', *Cold Spring Harbor Protocols*, 3(11), pp. 1–9. doi: 10.1101/pdb.emo105.

Klee, H. J. and Giovannoni, J. J. (2011) 'Genetics and Control of Tomato Fruit Ripening and Quality Attributes', *Annual Review of Genetics*, 45, pp. 41–59. doi: 10.1146/annurev-genet-110410-132507.

Lai, C. W. *et al.* (2012) 'ERdj4 Protein Is a Soluble Endoplasmic Reticulum (ER) DnaJ Family Protein That Interacts with ER-associated Degradation Machinery', *The Journal of Biological Chemistry*, 287(11), pp. 7969–7978. doi: 10.1074/jbc.M111.311290.

Lara, J. A. *et al.* (2018) 'Identification and Characterization of Sterol Acyltransferases Responsible for Steryl Ester Biosynthesis in Tomato', *Frontiers in Plant Science*, 9(588), pp. 1–18. doi: 10.3389/fpls.2018.00588.

McMurchie, E. J., B., M. W. and Eaks, I. L. (1972) 'Treatment of Fruit with Propylene gives Information about the Biogenesis of Ethylene', *Nature*, 237, pp. 235–236.

Morikawa, T. *et al.* (2006) 'Cytochrome P450 CYP710A Encodes the Sterol C-22 Desaturase in Arabidopsis and Tomato', *The Plant Cell*, 18(4), pp. 1008–1022. doi: 10.1105/tpc.105.036012.

Morikawa, T. *et al.* (2009) 'CYP710A genes encoding sterol C22-desaturase in Physcomitrella patens as molecular evidence for the evolutionary conservation of a sterol biosynthetic pathway in plants', *Planta*, 229(6), pp. 1311–1322. doi: 10.1007/s00425-009-0916-4.

Nelson, D. R. (2018) 'Cytochrome P450 diversity in the tree of life', *BBA - Proteins and Proteomics*. Elsevier, 1866(1), pp. 141–154. doi: 10.1016/j.bbapap.2017.05.003.

OECD (2017) 'Tomato (Solanum lycopersicum)', *Safety Assessment of Transgenic Organisms in the Environment: OECD Consensus Documents*, 7(September 2016), pp. 69–105.

Ohta, D. and Mizutani, M. (2013) *Isoprenoid Synthesis in Plants and Microorganisms: New Concepts and Experimental Approaches*. doi: 10.1007/978-1-4614-4063-5.

Peralta, I. E. and Spooner, D. M. (2006) *Genetic Improvements of Solanaceous Crops*.

Pulido, P., Perello, C. and Rodriguez-Concepcion, M. (2012) 'New Insights into Plant Isoprenoid Metabolism', *Molecular Plant*. Â© The Authors. All rights reserved., 5(5), pp. 964–967. doi: 10.1093/mp/sss088.

Ramírez-Estrada, K. *et al.* (2017) 'Tomato UDP-Glucose Sterol Glycosyltransferases : A Family of Developmental and Stress Regulated Genes that Encode Cytosolic and Membrane-Associated Forms of the Enzyme', *Frontiers in Plant Science*, 8(June), pp. 1–21. doi: 10.3389/fpls.2017.00984.

Rodríguez-Concepción, M. and Boronat, A. (2002) 'Elucidation of the Methylerythritol Phosphate Pathway for Isoprenoid Biosynthesis in Bacteria and Plastids . A Metabolic Milestone Achieved through Genomics', *Plant Physiology*, 130, pp. 1079–1089. doi: 10.1104/pp.007138.ISOPRENOID.

Rodríguez-Concepción, M. and Boronat, A. (2015) 'Breaking new ground in the regulation of the early steps of plant isoprenoid biosynthesis', *Current Opinion in*

Plant Biology, 25, pp. 17–22. doi: 10.1016/j.pbi.2015.04.001.

Sattelmacher, B. (2001) 'The apoplast and its significance for plant mineral nutrition', *New Phytologist*, 149(22), pp. 167–192.

Schaller, H. (2003) 'The role of sterols in plant growth and development', *Progress in Lipid Research*, 42, pp. 163–175. Available at: http://www.sciencedirect.com/science/article/pii/S0163782702000474%5Cnpapers2://publication/uuid/E01C48C7-E57A-4FAD-9057-1279540D4315.

Schrick, K. *et al.* (2000) 'FACKEL is a sterol C-14 reductase required for organized cell division and expansion in Arabidopsis embryogenesis', *Genes and Development*, 14, pp. 1471–1484.

Schrick, K. *et al.* (2004) 'A link between sterol biosynthesis, the cell wall, and cellulose in Arabidopsis', *Plant Journal*, 38(2), pp. 227–243. doi: 10.1111/j.1365-313X.2004.02039.x.

Senthil-Kumar, M., Wang, K. and Mysore, K. S. (2013) 'AtCYP710A1 gene-mediated stigmasterol production plays a role in imparting temperature stress tolerance in Arabidopsis thaliana', *Plant Signaling and Behavior*, 8(2), pp. 1–5. doi: 10.4161/psb.23142.

Sonawane, P. D. *et al.* (2016) 'Plant cholesterol biosynthetic pathway overlaps with phytosterol metabolism', *Nature Plants*. Nature Publishing Group, 3(16205), pp. 1–13. doi: 10.1038/nplants.2016.205.

Tholl, D. (2015) 'Biosynthesis and Biological Functions of Terpenoids in Plants', *Advances in Biochemical Engineering/ Biotechnology*, 148, pp. 63–106. doi: 10.1007/10.

Trivedi, M. *et al.* (2016) *Ecofriendly Pest Management for Food Security*. doi: 10.1016/B978-0-12-803265-7.00023-3.

Valitova, J. N., Sulkarnayeva, A. G. and Minibayeva, F. V (2016) 'Plant Sterols: Diversity, Biosynthesis, and Physiological Functions', *Biochemistry (Moscow)*, 81(8), pp. 819–834.

Vickers, C. E. *et al.* (2014) 'Metabolic engineering of volatile isoprenoids in plants and microbes', *Plant, Cell and Environment*, 37, pp. 1753–1775. doi: 10.1111/pce.12316.

Vranová, E., Coman, D. and Gruissem, W. (2013) 'Network Analysis of the MVA and MEP Pathways for Isoprenoid Synthesis', *Annual Review of Plant Biology*, 64, pp. 665–700. doi: 10.1146/annurev-arplant-050312-120116.

Wang, K. *et al.* (2012) 'Phytosterols Play a Key Role in Plant Innate Immunity against Bacterial Pathogens by Regulating Nutrient Efflux into the Apoplast', *Plant Physiology*, 158(4), pp. 1789–1802. doi: 10.1104/pp.111.189217.

Whitaker, B. D. (1988) 'Changes in the steryl lipid content and composition of tomato fruit during ripening', *Phytochemistry*, 27(11), pp. 3411–3416.

Whitaker, B. D. (1991) 'Changes in lipids of tomato fruit stored at chilling and non-chilling temperatures', *Phytochemistry*, 30(3), pp. 757–761.

Willemsen, V. *et al.* (2003) 'Cell Polarity and PIN Protein Positioning in Arabidopsis Require', *The Plant Cell*, 15, pp. 612–625. doi: 10.1105/tpc.008433.1999.

UNIVERSITAT DE BARCELONA